Spring 5-4-2022

Mechanisms Of Telomere Maintenance In Trypanosoma Brucei

M A G G. Rabbani
Cleveland State University

MECHANISMS OF TELOMERE MAINTENANCE IN *TRYPANOSOMA BRUCEI*

M A G RABBANI

Bachelor of Science in Biochemistry and Molecular Biology

University of Dhaka

July 2011

Master of Science in Biochemistry and Molecular Biology

University of Dhaka

Dec 2012

Submitted in partial fulfillment of requirements for the degree

DOCTOR OF PHILOSOPHY IN REGULATORY BIOLOGY

at the

CLEVELAND STATE UNIVERSITY

May 2022

We hereby approved this dissertation

for

M A G Rabbani

Candidate for the Doctor of Philosophy in Regulatory Biology

Department of Biological, Geological, and Environmental Sciences

and

CLEVELAND STATE UNIVERSITY

College of Graduate studies by

---Date: ----------------------
Bibo Li, Ph.D. BGES, Cleveland State University
Major Advisor

---Date: ----------------------
Girish Shukla, Ph.D. BGES, Cleveland State University
Advisory Committee Member

---Date: ----------------------
Aaron F Severson, Ph.D. BGES, Cleveland State University
Advisory Committee Member

---Date: ----------------------
Keith McCrae, MD Lerner Research Institute, Cleveland Clinic
Advisory Committee Member

---Date: ----------------------
G. Valentin Börner, Ph.D. BGES, Cleveland State University
Internal Examiner

---Date: ----------------------
Kurt Runge, Ph.D. Lerner Research Institute, Cleveland Clinic
External Examiner

Date of Defense: May 4, 2022

DEDICATION

I dedicate my thesis to my parents, my loving family, and everyone who has always supported me along the way.

ACKNOWLEDGMENTS

MECHANISMS OF TELOMERE MAINTENANCE IN *TRYPANOSOMA BRUCEI*

M A G RABBANI

ABSTRACT

Telomeres are a nucleoprotein structure at the end of the chromosome and are essential for genome integrity and chromosome stability. Telomere lengths are primarily maintained by a telomerase-mediated pathway but can be maintained by a homologous recombination-mediated pathway. However, detailed mechanisms of telomere maintenance are still unclear in many eukaryotes, including an important human pathogen, *Trypanosoma brucei*. Telomeres can be elongated by telomerase in *T. brucei*, a causative agent of fatal sleeping sickness in humans and nagana in cattle. *T. brucei* evades host immune response by regularly switching its major surface antigen, variant surface glycoprotein (VSG), a process known as antigenic variation. The telomere structure and telomere proteins play critical roles in *T. brucei* pathogenesis. In mammalian, yeast, and plant cells, ssDNA binding proteins with OB-fold domains play important roles in coordinating telomere G- and C-strand syntheses. However, no such protein has been described in *T. brucei* to be specifically associated with the telomere. We identified POLIE, an A-type DNA polymerase, as a crucial telomere complex component in *T. brucei* and essential in maintaining telomere integrity in *T. brucei*. Depletion of POLIE in *T. brucei* leads to an increased amount of DNA damage at telomere/subtelomere, increased frequency of gene conversion-mediated VSG switching, and an increased amount of the telomeric circles (T-circles), suggesting a potential role of POLIE in suppressing DNA recombination at the telomere and the subtelomere. However, I find that telomeric and subtelomeric DNA recombination is unlikely to be mediated by the increased telomeric R-

loop level as the telomeric repeat-containing RNA (TERRA) level is significantly lower in POLIE-depleted cells. The telomere G-rich 3'overhangs are dramatically elongated in POLIE-depleted cells, indicating a potential role of POLIE to coordinate telomere G- and C-strand syntheses and suggesting that the long telomere 3' overhang can induce more telomeric and subtelomeric recombination. In addition, I find that POLIE inhibits telomerase-dependent telomere G-strand extension, identifying POLIE as the first telomere protein that potentially suppresses telomerase in *T. brucei*. Moreover, depletion of POLIE greatly increases the amount of telomeric C-circles which can be derived from replication stress in the telomere C-strand. Importantly, the elongated telomere 3' overhang and elevated telomeric C-circle level phenotypes are independent of the telomerase, which suggests that POLIE may promote the telomere C-strand synthesis. Therefore, we identified that POLIE plays a major role in suppressing telomere recombination, coordinating telomerase-mediated telomere G-strand extension, and telomere C-strand synthesis, and maintaining telomere integrity in *T. brucei*.

TABLE OF CONTENTS

LIST OF TABLES

LIST OF FIGURES

CHAPTER I

INTRODUCTION

1.1 *Trypanosoma brucei* and Human African Trypanosomiasis (HAT)

Trypanosoma brucei is a eukaryotic unicellular parasite that belongs to the Kinetoplastea class. It causes African trypanosomiasis or sleeping sickness in humans and animal trypanosomiasis or nagana in cattle. The nagana name in the animal is derived from "N'gana" which means "powerless/useless', meaning the animal is unfit for work. This vector-borne disease is limited to sub-Saharan Africa and is fatal without treatment. *T. brucei* is a heteroxenous pathogen which means it requires at least two hosts to complete its full life cycle. It reproduces extracellularly in the mammalian host and is transmitted by the Tsetse fly (*Glossina spp.*). African trypanosomiasis affected the cultural and economic growth of central Africa throughout its history (Steverding, 2008). Few drugs were developed but most of these drugs are cautiously used due to their high toxicity.

There are three subspecies of *T. brucei, T. brucei gambiense, T. brucei rhodesiense,* and *T. brucei brucei*, all of which are morphologically alike. Among these subspecies, *T. brucei gambiense* and *T. brucei rhodesiense* cause sleeping sickness in humans, whereas *T. brucei brucei* causes nagana in livestock and other African hoofed animals (Steverding,

2008). *T. brucei brucei* is unable to infect humans because it is susceptible to trypanosome lytic factor (TLF) present in the human blood (Thomson *et al.,* 2009). *T. brucei rhodesiense* neutralizes TLF by expressing a serum resistance-associated protein (SRA) (De Greef *et al.,* 1989) whereas *T. brucei gambiense* evolved to reduce the expression of TLF receptor which contributes to TLF resistance (Kieft *et al.,* 2010). *T. brucei gambiense* is more prevalent in central and west Africa and causes a chronic form of the disease, while *T. brucei rhodesiense* is more prevalent in Southern and Eastern Africa and causes an acute form of the disease (Steverding, 2008).

T. *brucei* is estimated to have diverged from mammals more than 500 million years ago (Schulz *et al.,* 2016; Li, 2021). Phylogenetic analyses based on rRNA genes suggest that, about 300 million years ago, *T. brucei* diverged from other trypanosomes (Haag *et al.,* 1998). At that time, early insects which evolved before *T. brucei* may have served as a host (Steverding, 2008). However, when tsetse flies evolved around 35 million years ago, they finally served as a vector to carry the pathogen to mammals through a blood meal (Steverding 2008).

One of the earliest records of nagana-like symptoms in cattle was described in Kahun Papyriin in around the 2nd millennium BC in ancient Egypt (Griffith, 1898). The earliest record of sleeping sickness in humans was described by Ibn Khaldun (1332–1406) who published a case report that the Emperor of Mali, Sultan Mari Jata died from a disease whose symptom was similar to sleeping sickness, a frequent disease in that region (Williams, 1996; Steverding 2008). Those affected individuals rarely awake, and sickness continues until the patients die (Steverding 2008).

John Aktins, a naval surgeon, first described neurological symptoms of the disease in the patient which developed at the late phase of infection (Cox, 2004). Later, in 1803, Thomas Winterbottom, an English physician reported the early phase of the disease with swollen lymph glands around the neck (Cox, 2004). David Livingston, a Scottish explorer first described in 1852 that, the bite of tsetse flies causes trypanosomiasis in animals (Winkle *et al.*, 2005). In 1902, Joseph Everett Dutton, an English physician identified the pathogen in European patients and termed the pathogen *Trypanosoma gambiense* (now *T. brucei gambiense*) (Dutton, 1902).

There are two stages of disease pathogenesis of sleeping sickness. The first phase symptoms include enlargement of the spleen and liver, headache, fever, and swollen lymph nodes. In the next phase, the parasite travels through the blood-brain barrier (BBB) and infiltrates the CNS to cause neuro-psychological disorders including speech disorders, paralysis of the extremities, and disruption of the circadian rhythm, the features of sleeping sickness in humans (Blum *et al.*, 2012). In the 20th century, there were several epidemics caused by *T. brucei* in Africa. The largest one happened mainly in Uganda and Kenya between 1896-and 1906 which cost about 800,000 lives (de Raadt, 2005, Hide, 1999). Several scientific missions aimed to find a cure for African trypanosomiasis at that time to minimize the devastation caused by the epidemic (Winkle *et al.*, 2005, de Raadt, 2005). The first drug, sodium arsenite, was identified in 1902 which inhibited the growth of *T. brucei* in infected laboratory animals (Cox, 2004). In 1904, the arsenical drug atoxyl was shown to cure animal trypanosomiasis in the laboratory which was less toxic than any other arsenical compound at that time (Winkle *et al.*, 2005). However, Robert Koch, a German

physician, later identified that atoxyl causes atrophy of the optic nerve which ultimately leads to blindness in the patient (Winkle *et al.,* 2005).

In 1915, Jacobs and Heidelberger discovered an organo-arsenical tryparsamide which was the first drug to treat late-stage disease (Vickerman, 1997). Another drug Suramin, which was often used with organo-arsenical tryparsamide, was discovered in 1916 by Wilhelm Roehl in a collaborative project with Bayer pharmaceutical (Winkle *et al.,* 2005; Simarro *et al.,* 2008). Suramin is still in use to treat the first stage of infections caused by *T. b. rhodesiense* infections (Winkle *et al.,* 2005; Simarro *et al.,* 2008). Suramin inhibits various enzymes including enzymes in the glycolytic pathway and thymidine kinase to inhibit the rapid proliferation of *T. brucei* (Wang, 1995). However, the limitation of Suramin treatment is that it cannot pass through the blood-brain barrier to inhibit the parasite growth in CNS (Wang, 1995). With the help of both drugs and the implementation of strategic decisions such as the introduction of special service units and mobile teams, host reservoir control and vector control effectively reduced the infection rate (Steverding 2008). In 1937, Baker pharmaceutical company and Ewins, an English chemist co-developed pentamidine to treat the first stage of disease caused by *T. b. gambiense* (Bray *et al.,* 2003; Simarro *et al.,* 2008). Although the mechanism of action of pentamidine is poorly understood, it is believed to interfere with the nucleic acid metabolism in *T. brucei.* Pentamidine is not effective against the second stage of the disease and has toxic side effects (Bacchi, 2009). In 1939, the invention of DDT as an insecticide helped to eradicate tsetse flies from its endemic areas (Winkle *et al.,* 2005, de Raadt, 2005). In 1949, Ernst Friedheim, a Swiss pathologist, invented arsenical melarsoprol to treat the second stage of *T. b. rhodesiense* infection which is still the only effective drug against the pathogen

4

(Steverding 2008). Melarsoprol diminishes energy for trypanosome growth by interfering with ATP production and inhibiting the S-H group found in many enzymes (Bacchi, 2009). Melarsoprol is the most toxic HAT drug with a high failure rate due to its nonspecific activity. Since the 1950s, there were several drugs introduced by different companies to treat both sleeping sickness and nagana (Steverding, 2008).

Decolonization of Africa, economic collapse, and political instability in the mid-1960 led to the disruption of disease control and surveillance in many African countries, which caused a sharp increase in sleeping sickness (Steverding 2008). But existing drugs and newly evolving drugs such as eflornithine (DL-α-di fluoromethyl ornithine, DFMO) reduced the suffering in treatment. Eflornithine, although originally discovered in 1990 as a treatment for cancer, was found to be effective against *T. b. gambiense* infection and had a better toxicity profile than available melarsoprol (Meyskens and Gerner, 1999). DFMO inhibits ornithine decarboxylase, a rate-limiting enzyme in the polyamine synthetic pathway (Bacchi, 2009).

With time, an increase in surveillance leads to the reduction of new cases number gradually (Steverding, 2008). By 2006, the number of cases was estimated to be around 50,000-70,000 per year (WHO, 2006), which further reduced to below 10000 cases per year by 2009 (Kennedy and Rodgers, 2019). By 2016 the number of confirmed cases came down to approximately 2,184 cases a year (Kennedy and Rodgers, 2019) although the actual number remain underestimated due to the lack of detection method to detect the early-stage infection (Welburn and Maudlin, 2012).

The diagnosis of HAT is complex as the clinical presentation varies depending on the pathogen type and stage of the disease. The major contributor to this diversity is the

host-parasite interactions and the genetic background of parasite and host (Morrison, 2011). The choice of drug for treatment depends on the infection stage. The later stage treatment requires a drug that is more toxic to the patient. Although HAT is still fatal without treatment, the disease is still considered one of the most neglected tropical diseases in the current times (Buguet *et al.,* 2014). Recently, a combination treatment of Eflornithine and Nifurtimox was found to be cost-effective and efficient (Simarro *et al.,* 2008; Alirol *et al.,* 2013). The treatment of HAT requires special administration and special training due to diversity in subspecies type, disease stage-specific action, nature of the drug, toxicity, resistance development, and careful follow-up (Alirol *et al.,* 2013). Further research is required to design a therapeutic strategy that would be safer for the host but effective against any subspecies type and stage of the disease.

1.2 *T. brucei* Life Cycle

Humans and insects are the two hosts required to complete the lifecycle of *T. brucei* (Fig. 1). The tsetse fly (*Glossina spp.*) is the vector for both *T. brucei rhodesiense* and *T. brucei gambiense*. The pathogen enters the midgut of the fly when the tsetse fly takes a blood meal from an infected host. In the anterior midgut of the fly, the parasite undergoes biochemical and morphological changes to form long slender parasitic forms (Aksoy, 2003). The parasite then rapidly multiplies in the posterior midgut and expresses surface protein procyclin to protect the pathogen from hydrolytic enzymes present in the midgut of the fly (Gruszynski *et al.,* 2006). Then the pathogen travels to salivary glands through the digestive and respiratory tract to develop into epimastigotes form. In the salivary gland of the fly, the pathogen differentiates into the short stumpy metacyclic form which is an infective form. The metacyclic form expresses metacyclic VSGs (mVSGs) as their surface

6

protein (Graham and Barry, 1995). The flies gain the ability to infect ~ 21 days after feeding

and retain infection ability for the rest of their life (Atouguia and Kennedy, 2000).

The metacyclic form of the pathogen enters the mammalian host from the tsetse fly

when the fly bites the host for a blood meal (Kennedy, 2004). Several thousands of

metacyclic trypanosomes can be transmitted in a single bite. Then the parasite transforms

into an infectious dividing bloodstream form that resides in the lymph nodes, spleen, and

bloodstream of the host. At this form, *T. brucei* starts to express monoallelic bloodstream

VSGs from its *VSG* gene pool (>2500 *VSG* genes and pseudogenes) and regularly switch

to express a different VSG to escape from the host immune response in a mechanism called

antigenic variation. *T. brucei gambiense* primarily invades the central nervous system of

the host to cause chronic infections and sleeping sickness whereas *T. brucei rhodesiense*

can invade almost all organs to cause acute infections and rapid death. The disease is fatal

if left untreated (Kennedy, 2004). The infected host also serves as a reservoir for tsetse flies

to further spread the disease. The life cycle of the *T. brucei* in its mammalian host and the

insect host is summarized in Fig. 1 (CDC, 2021).
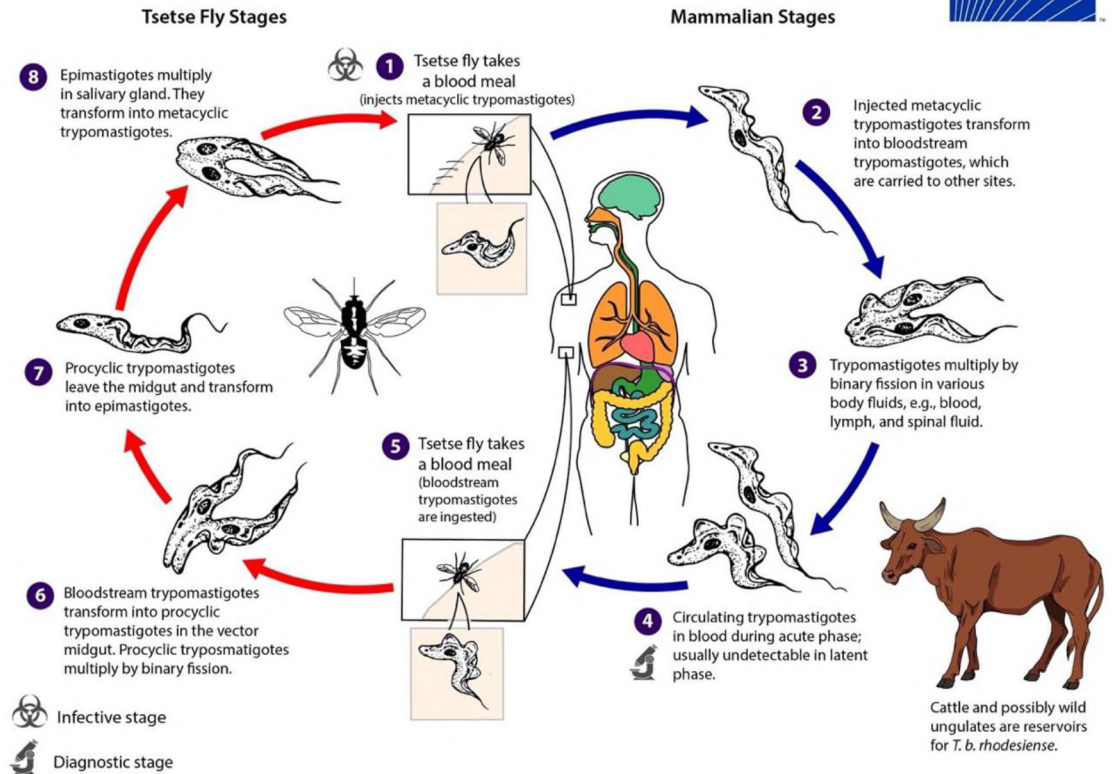
Fig. 1: *T. brucei rhodesiense* **and** *T. brucei gambiense* **life cycle** (CDC, 2021). The life cycle of *T. brucei* starts when the Tsetse fly takes a blood meal from the host. Injected trypomastigotes transform into infective bloodstream form which multiplies in the host. When a Tsetse fly takes another blood meal, the circulating bloodstream form develops into procyclic trypomastigotes which can be transferred back to a host with another blood meal.

1.3 Genome Organization

The *T. brucei* haploid genome size is about ~35 Mb. Its DNA is enclosed in a nucleus of ~2.5 μm in diameter (Daniels *et al.,* 2010). One of the previous studies predicted about 10000 genes in the *T. brucei* genome (Berriman *et al.,* 2005). Recent studies estimated more than 2500 *variant surface glycoprotein* (*VSG*) genes and pseudogenes in the *T. brucei* genome (Navarro and Cross, 1996, Berriman *et al.,* 2005, Cross *et al.,* 2014, Li, 2021). Based on their sizes, the *T. brucei* chromosomes are divided into three classes. There are 11 pairs of megabase chromosomes (1–5.2 Mb) (El-Sayed, 1997; Donelson,

8

2002; Melville *et al.,* 1998), 5 intermediate chromosomes (200-900 kb), and ~100 minichromosomes (30-150 kb) (Donelson, 2002; El-Sayed, 1997; Donelson, 2002). All of these chromosomes end with telomeric TTAGGG repeats. The immediate region upstream of the telomere in some megabase and intermediate chromosomes contains bloodstream expression sites (BESs), which are responsible for the expression of VSGs (El-Sayed, 1997). *VSGs* are expressed from about 15 BESs (Navarro and Cross, 1996).

Minichromosomes contain additional silent *VSG* genes (64–67 VSGs on ~96 minichromosomes), which increase the number of *VSGs* genes in the *VSG* pool (Alsford *et al.,* 2001; Cross *et al.,* 2014). These minichromosomes were shown to segregate and replicate without any aberration for greater than 360 generations and more than five years of culture, which implies their stability in the genome of *T. brucei* (Alsford *et al.,* 2001). There are approximately 900 *VSG* pseudogenes in the genome of *T. brucei* (Cestari and Stuart, 2018). *VSG* gene constitutes a large portion of the pseudogenes (Berriman *et al.,* 2005) but the mechanism of activation of these *VSG* pseudogenes is yet not fully understood (Alsford *et al.,* 2001, Berriman *et al.,* 2005).

1.4 The Telomere and Subtelomere Structure

Telomeres are a nucleoprotein complex composed of repetitive DNA and associated proteins which protect the chromosome ends (Blackburn, 1991). Telomeres are important for maintaining chromosome stability and genome integrity (Lim and Cech, 2021; de Lange, 2018). Telomeres are shortened after each round of cell duplication as conventional DNA polymerases cannot fully replicate the ends of the chromosome; a phenomenon termed as end replication problem (Blackburn, 2001, Feng *et al.,* 2017; Olovnikov, 1973; Ohki *et al.,* 2001). This telomere shortening mechanism ultimately leads

to cellular senescence if telomere elongation mechanisms are absent or defective (Blackburn, 2001). In most eukaryotic cells, there is a correlation between the life span of cells to their telomere length. Eukaryotic telomeres usually contain TG-rich double-stranded DNA that terminates in a 3' single-stranded G-rich overhang structure (Podlevsky *et al.,* 2008; Bonetti *et al.,* 2014; de Lange, 2005).

Mammalian telomeres consist of the Shelterin protein complex and 2-15 kilobases of duplex 5'-TTAGGG-3':3'-AATCCC-5' repeated sequence which terminates in ~15-300 nt of 3' overhang (Fig. 2) (Lim and Cech, 2021). The 3' overhang can form a T-loop structure by invading the double-stranded telomere DNA section of the same telomere (Bruce, 1895). The T-loop structure helps to stabilize telomeres by protecting them from unwanted nucleolytic degradation, and components of DNA damage repair machinery (de Lange, 2018). Hence, the telomere 3' G-rich overhang is essential for chromosome end protection and preservation of telomere structure. The 3' overhang structure generation is tightly regulated by several telomere proteins and takes several steps to process (Bonetti *et al.,* 2014; Bonnell *et al.,* 2021). In most eukaryotes, the 3' overhang structure act as a substrate for the telomerase, a specialized reverse transcriptase, which elongates the 3' overhang by adding G-rich repeats to the single-stranded 3′ termini (Greider and Blackburn, 1987; Greider and Blackburn, 1989; Blackburn and Collins, 2011; Schmidt and Cech, 2015, Feng *et al.,* 2017). After elongation by telomerase, a DNA polymerase covert a part of the elongated overhang to double-stranded DNA (Feng *et al.,* 2017). Hence, the collective action of the DNA polymerase and telomerase is required to counterbalance the shortening of telomere in proliferating cells (Feng *et al.,* 2017; Olovnikov, 1973; Ohki *et al.,* 2001).
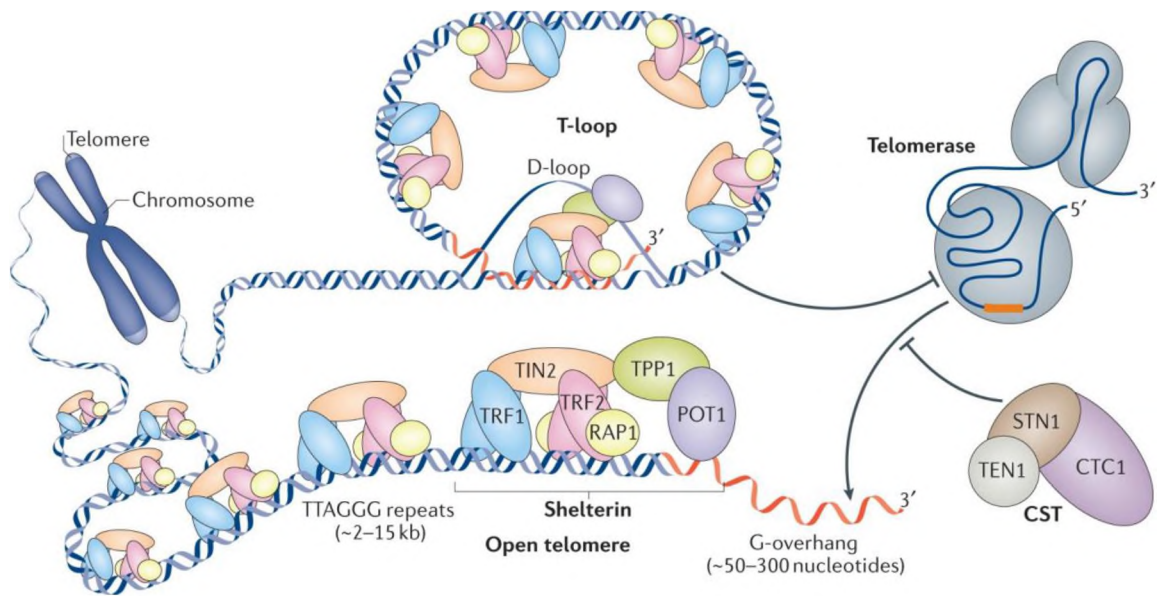
Fig 2: Structure of mammalian telomere at the end of the chromosome (Figure reproduced from Lim and Cech, 2021). Telomere and the individual component of the human Shelterin complex are shown.

The Shelterin complex is a multimeric protein complex that plays a key role in telomere end protection and telomere length maintenance in a wide array of organisms (de Lange, 2005). The human Shelterin complex component includes RAP1, POT1, TPP1, TRF1, TRF2, and TIN2. The Shelterin complex facilitates telomere replication and averts the triggering of ATM/ATR-mediated DNA damage response at the DNA terminus (Arnoult and Karlseder, 2015, Hockemeyer and Collins, 2015, Martinez and Blasco, 2015). TRF1 and TRF2 are the dsDNA telomeric repeats binding proteins (Broccoli *et al.,* 1997) while POT1 binds the single-stranded 3' overhang structure at the end of the chromosome (Feng *et al.,* 2017). TPP1 dimerizes with single-stranded DNA binding protein POT1 and acts as a linker to connect TRF1/2 to POT1 via another Shelterin complex protein TIN2 (Feng *et al.,* 2017). Similar to humans, the fission yeast *Schizosaccharomyces pombe* also forms a Shelterin-like complex (Moser and Nakamura 2009). The Shelterin-like complex in *S. pombe* is composed of Rap1, Pot1, Taz1, Ccq1, Tpz1, and Poz1 (Moser and Nakamura

2009). *S. pombe* Rap1 is a homolog of mammalian RAP1 with analogous telomere and non-telomeric function (Cooper *et al.*, 1997). Taz1 is a double-stranded telomeric repeat binding protein with structural and functional resemblances to mammalian TRF1 and TRF2 (Cooper *et al.*, 1997). The *S. pombe* equivalent of mammalian single-stranded 3' overhang-binding proteins POT1 and TPP1 are Pot1 and Tpz1, respectively (Miyoshi *et al.*, 2008). Poz1 is structurally and functionally similar to mammalian TIN2 which connects single-stranded 3' overhang-binding proteins to double-stranded telomeric repeats binding protein Rap1 (Miyoshi *et al.*, 2008; Harland *et al.*, 2014). The is no mammalian homolog of Ccq1 which plays a key role in telomerase recruitment to telomeres (Moser *et al.*, 2011). In budding yeast, *Saccharomyces cerevisiae*, the CST complex is associated with the telomeric overhang (Martín *et al.*, 2007) and performs a function similar to the Shelterin complex in mammals (Price *et al.*, 2010). In *S. pombe* Pot1 as well Stn1 and Ten1 associate with the telomeric ssDNA overhang, but Stn1 and Ten1 do not interact with Pot1, rather works as a two separate complex (Martín *et al.*, 2007). In humans, POT1 and TPP1 are associated with telomeric ssDNA overhang (Martín *et al.*, 2007). Shelterin and the CST-like proteins have been identified in the plant as well (Procházková *et al.*, 2016).

Several telomere-associated proteins were identified in *T. brucei* (Fig. 3). The functions of these telomere-associated proteins are surprising because, besides their function in telomere maintenance, telomere-associated proteins regulate antigenic variation, a key mechanism to evading the immune response of the host (Duraisingh and Horn, 2016). Similar to other eukaryotic organisms, *T. brucei* telomere is primarily synthesized and maintained by telomerase (Gupta *et al.*, 2013; Sandhu *et al.*, 2013; Dreesen *et al.*, 2005). Additionally, telomeres in *T. brucei* telomeres were shown to form a T-loop

structure (Munoz-Jordan *et al.,* 2001), despite having a much shorter G-rich 3' overhang compared to mammals (Sandhu and Li, 2011; Sandhu and Li, 2017). *Tb*TRF plays a key role in maintaining the telomere 3' overhang structure in *T. brucei* (Li *et al.,* 2005).

     T. brucei telomere structure and telomere proteins are unique in the aspect that, apart from maintaining genome stability and cell proliferation, telomere structure and telomere proteins are also crucial for regulating the VSG switching rate and monoallelic *VSG* expression (Li *et al.,* 2005; Yang *et al.,* 2009; Hovel-Miner *et al.,* 2012; Pandya *et al.,* 2013; Benmerzouga *et al.,* 2013; Jehi *et al.,* 2014a; Jehi *et al.,* 2014b; Nanavaty *et al.,* 2017; Li and Zhao, 2017; Saha *et al.,* 2019; Afrin *et al.,* 2020; Saha *et al.,* 2021; Li, 2021). The VSG switching rate is also affected by telomere length (Hovel-Miner *et al.,* 2012). Genes located near telomeres are silenced by the telomeric chromatin structure, a phenomenon known as the telomere position effect (TPE) (Gottschling *et al.,* 1990). In budding yeast, TPE depends on the distance of the gene from the telomere and the length of the telomere (Gottschling *et al.,* 1990). *Tb*RAP1 was shown to silences VSG by a TPE-like mechanism in *T. brucei* (Yang *et al.,* 2009). Additionally, depletion of *Tb*RAP1 causes derepression of all silent BES-linked genes at the subtelomere (Yang *et al.,* 2009). Since most of the telomeric proteins in *T. brucei* are essential, targeting telomeric protein is a promising therapeutic area to explore for the treatment of sleeping sickness (Li, 2012).
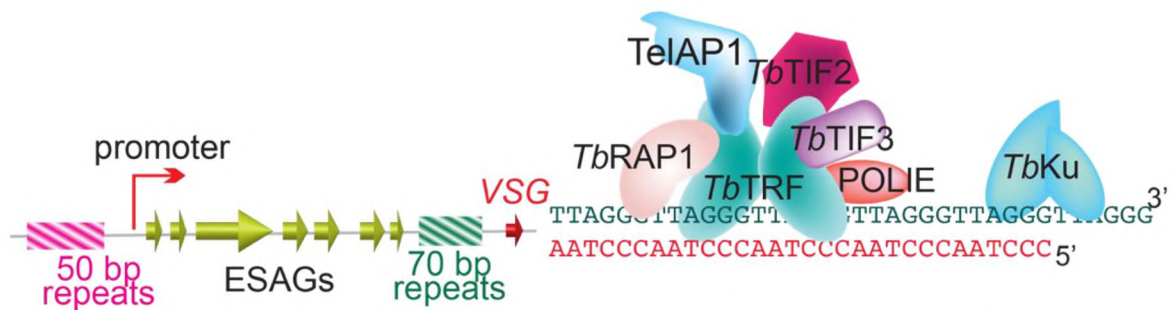
Fig. 3: Schematic diagram of *T. brucei* Telomere DNA structures. *Tb*TRF and *Tb*RAP1 bind to double-stranded telomere DNA, and TelAP1 interact with both *Tb*TRF and *Tb*RAP1 (Reis *et al.,* 2018). *Tb*RAP1, *Tb*TIF2, *Tb*TIF3, and POLIE interact with *Tb*TRF.

1.5 VSG and Antigenic Variation

While it is proliferating in the mammalian host, *T. brucei* express, VSG, the major surface antigen, and the type of expressed VSG is routinely changed to evade the host immune response (Fig 4). VSGs are about 58 kDa glycoprotein with enormous sequence diversity which facilitates the pathogen to escape antibody-mediated pathogen clearance from the host blood (Metcalf *et al.,* 1987, Manna *et al.,* 2014). About 10 million copies of a single type of VSG cover the entire surface of the parasite (Kennedy, 2004). The C-terminal hydrophobic region of VSG is secured to the plasma membrane by a glycosylphosphatidylinositol (GPI) anchor and the N-terminal hydrophilic region of VSG faces towards extracellular space (Carrington *et al.,* 1991; Dubois *et al.,* 2005; Donelson, 2002). The GPI anchor of VSG contains a galactose side chain and a dimyristoyl-phosphatidyl-inositol moiety (Hong and Kinoshita, 2009). GPI is attached to the VSG in the endoplasmic reticulum (ER) by a GPI transamidase so that it can be transported to the cell surface (Hong and Kinoshita, 2009, Kruzel *et al.,* 2017). In *T. brucei,* GPI anchors alone function as a forward trafficking signal to transport VSG from the ER to the plasma membrane (Kruzel *et al.,* 2017).

After a new VSG switching, the pathogen simultaneously presents both pre-and post-switch VSGs on their surface. The pathogen must replace the pre-switch VSG with the post-switch VSGs as soon as possible as the pre-switch VSGs remain susceptible to the host immune response. The pre-switch VSGs may persist several days for a full replacement with the new VSGs (Seyfang *et al.,* 1990). The turnover of the preexisting VSG is mediated by the action of proteases such as a GPI-specific phospholipase (GPI-PLC) and zinc metalloprotease activity (MSP-B) so that old VSG can be replaced with a new VSG. The complete replacement of the pre-existing VSG takes about 48hr (Dubois *et al.,* 2005).

The C-terminal region is usually conserved in different VSGs while the N-terminal region is usually highly variable (Carrington *et al.,* 1991). VSGs are highly immunogenic, and the immune system rapidly raises antibodies against them for immune clearance. However, T. *brucei* regularly switches VSG for immune evasion and long-term survival in the host (Aresta-Branco *et al.,* 2019). Millions of rod-like VSGs form a continuous layer on the parasite cell surface, which alleviates the host immune response by masking other invariant surface molecules of *T. brucei* (Morrison *et al.,* 2009).
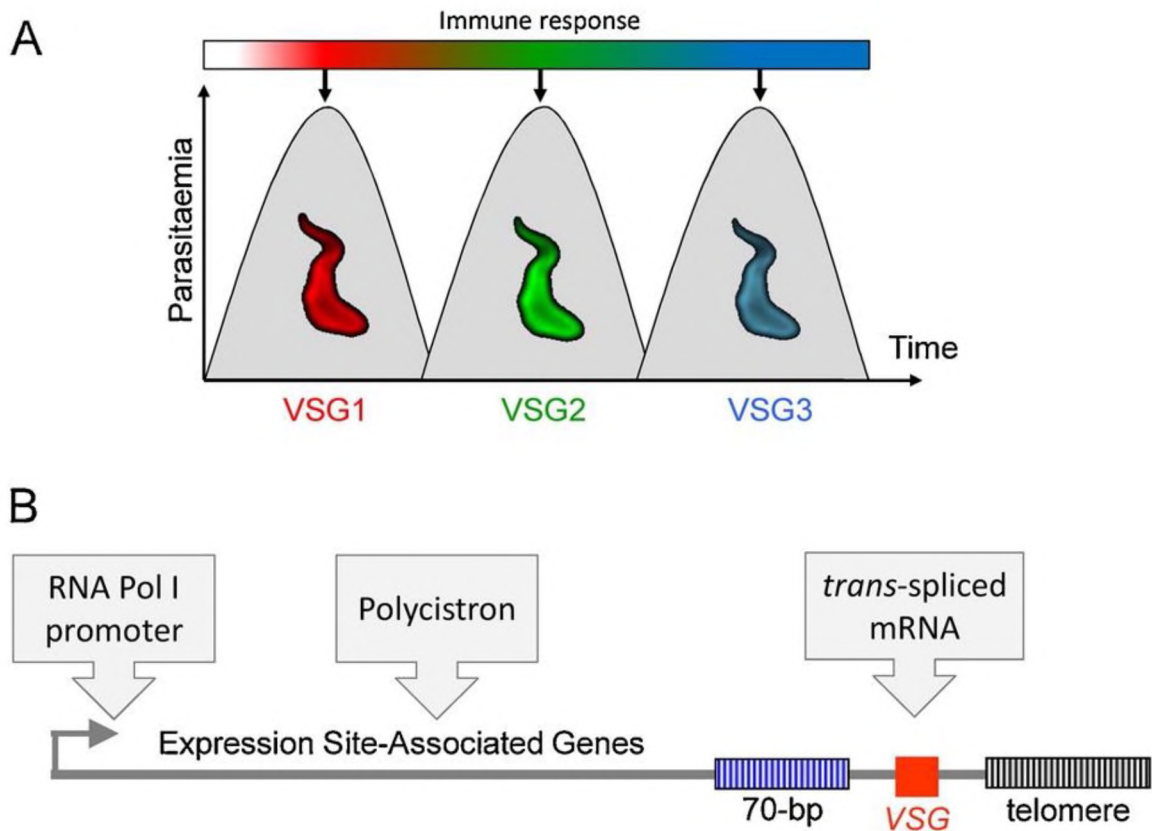
Fig. 4. *T. brucei* antigenic variation. (A) Antigenic variation occurs through continuous switching of VSG. Consecutive immune responses lead to waves of parasitemia. (B) Structure of a VSG expression site (ES) containing a single *VSG* gene flanked by distinct repetitive sequences. The cassette has several unusual features (marked on the arrowed box) (Figure reproduced from Horn, 2014).

VSG is monoallelically expressed in the bloodstream form of *T. Brucei*. That means, at a time, only one *VSG* is expressed from one ES (Hertz-Fowler *et al.,* 2014). *VSG* gene arrays can be found in megabase chromosomes at subtelomeric regions, and individual *VSGs* can be found at minichromosome subtelomeres (Fig. 6). The active *VSG* is expressed from one of the ~15 subtelomeric bloodstream VSG expression sites (BES) (Navarro and Cross, 1996), and the rest *VSG* genes remain transcriptionally silent (Donelson, 2002) (Fig. 5). Each VSG ES contains a sub-telomeric *VSG* gene, several *expression sites associated genes (ESAGs)*, and an upstream 70 bp repeat sequence (Alexandre *et al.,* 1988). The alpha amanitin-resistant RNA Pol-I drives the transcription of VSG ES and the promoter is

located approximately 45 kb upstream of the *VSG* gene locus (Pays *et al.*, 1989). In the metacyclic stage, *T. brucei* also expresses metacyclic VSG (mVSG), although mVSG is transcribed monocistronically (Alarcon *et al.*, 1994) and the promoter of *mVSG* is activated when the parasite resides in the salivary gland of the tsetse fly (Fig. 6) (Graham and Barry, 1995).
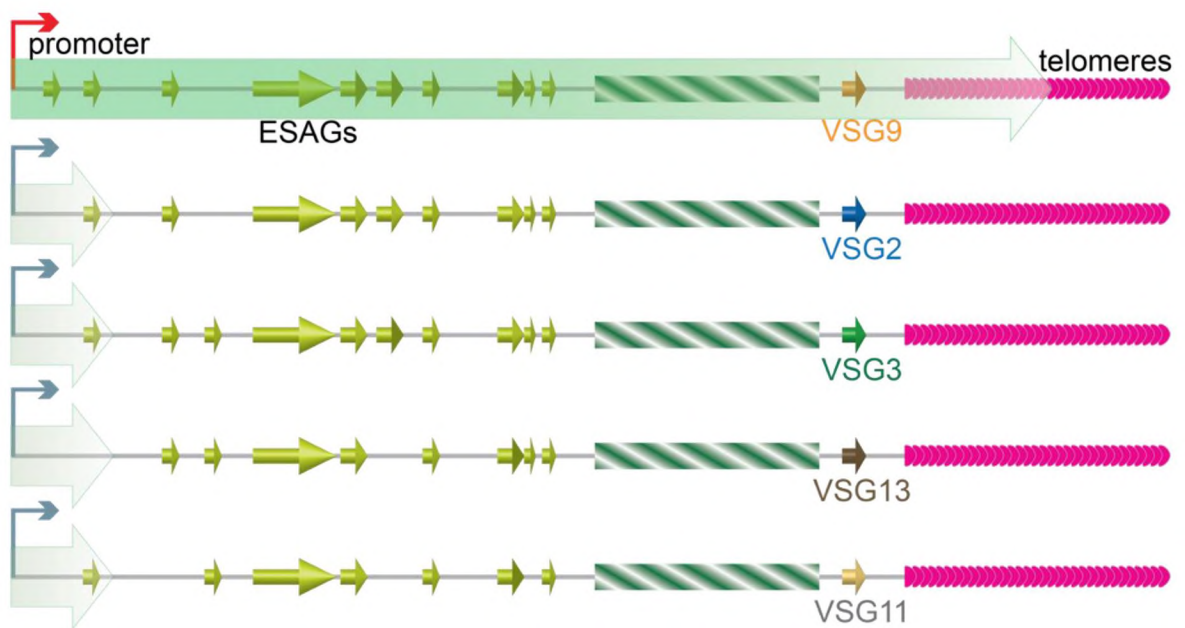
Fig. 5: Monoallelic *VSG* expression. *VSG* is expressed from a larger pool of *VSG* genes in a monoallelic fashion from the active ES only. Each VSG gene encodes for an antigenically distinct coat protein.

The molecular basis of antigenic variation is derived from a very large *VSG* gene pool and VSG is periodically switched to a new VSG from the pool to evade the host immune response (Fig. 5) (Donelson, 2002, Cross, 1975). There is a low-frequency recombination-based mechanism, in which a previously silent VSG can recombine to replace the originally active VSG, which in turn activates the expression of a new VSG to escape from the host immune response (Kennedy, 2004). This mechanism prolongs the endurance of the pathogen in the host circulatory system (Rudenko *et al.*, 1998) and

produces a wave of parasitemia to cause sleeping sickness (Barry, 1997) (Fig. 4A). VSG switching can be mediated by *in-situ* switches, cross-over, gene conversion, and a combination of ES loss and *in situ* (Fig. 6). In the *in-situ*, the originally active BES is silenced, and a previously silent BES is expressed without any DNA rearrangements. In the cross-over switch, the originally active VSG is exchanged with a silent VSG to activate it with a loss of genetic information from the VSG ES (Rudenko *et al.,* 1996). In gene conversion (GC), the donor VSG is duplicated, and the original VSG is lost in the process (Robinson *et al.,* 1999).

VSG monoallelic expression and VSG switching are tightly regulated by several mechanisms, making evolutionally developed antigenic variation as one of the most complex mechanisms to escape the host immune response (Taylor and Rudenko, 2006).
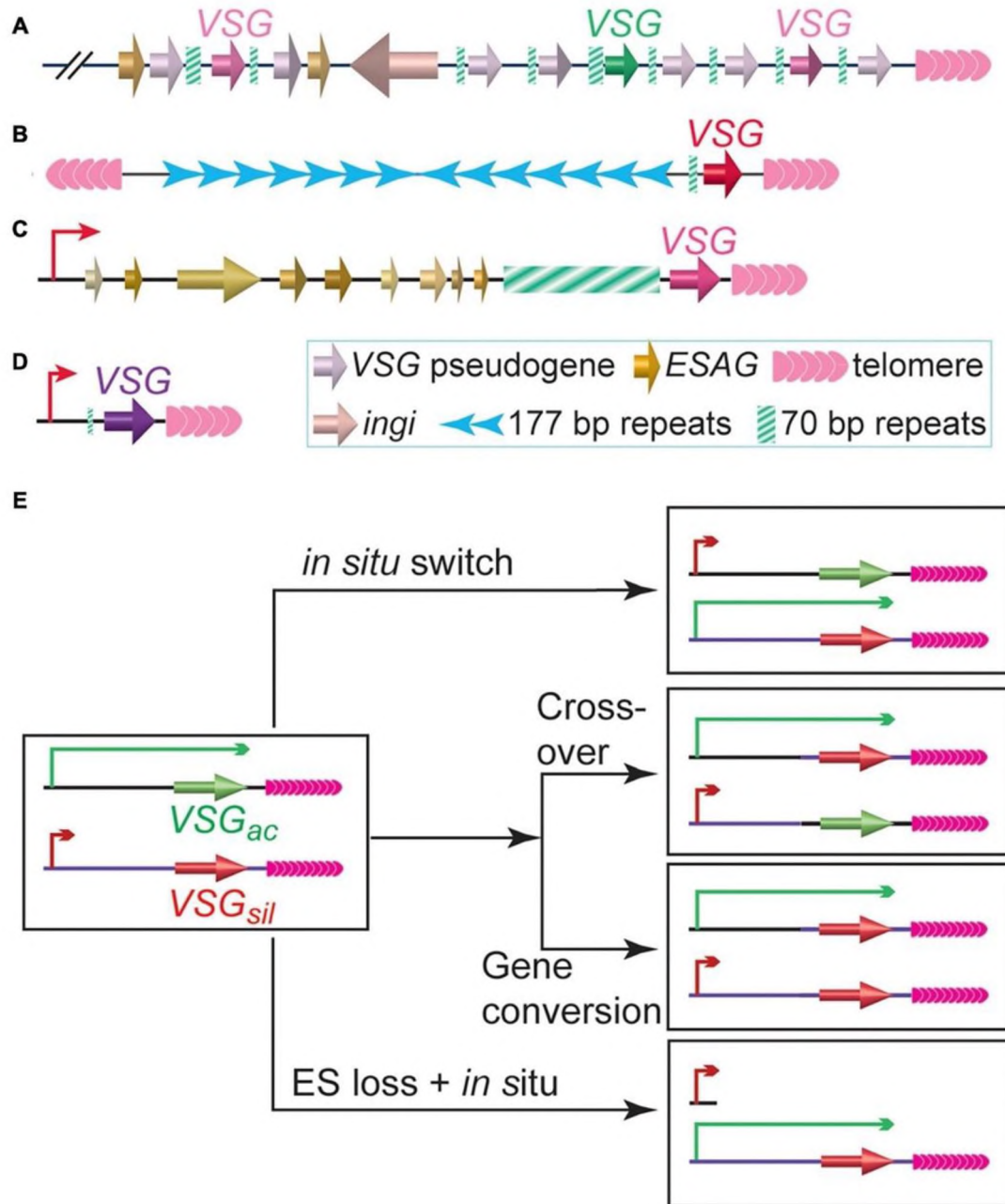
Fig. 6: *T. brucei VSG* **gene pool and mechanisms of VSG switching** (Figure reproduced from Li, 2021). (A) Schematic representation of subtelomeric *VSG* gene array in megabase chromosome. (B) The structure of a *VSG* gene located at the subtelomere of a minichromosome. (C) A representative VSG BES (D) A representative metacyclic VSG ES. (E) Schematic representation of major VSG switching pathways *T. Brucei* use to evade host immuno response. The originally active *VSG* was denoted as *VSGac* and the originally silent *VSG* was denoted as *VSGsil*. The silent ES promoter is represented by a short red arrow and the active ES promoter is represented by a long green arrow.

BES is located adjacent to the telomeres from which active VSG is singularly transcribed. A silent VSG can be activated by recombination-mediated switching which replaces the originally active *VSG* gene with a silent gene that leads to activation of the originally silent *VSG* gene (McCulloch *et al.*, 2015).

VSG transcription is controlled by several telomere-associated proteins in a way that only one BES is transcribed from the *VSG* gene pool and these proteins affect recombination-mediated VSG switching for the survival of the pathogen in the host (Duraisingh and Horn, 2016). For example, *Tb*RAP1 (*T. brucei* repressor activator protein 1) may be required for monoallelic *VSG* expression as transient depletion of *Tb*RAP1 derepresses all silent BES (Yang *et al.*, 2009). Furthermore, *Tb*TRF, the telomere duplex DNA binding factor, suppresses homologous recombination-mediated VSG switching (Jehi *et al.*, 2014a). The *Tb*TIF2 (*T. brucei* TRF interacting factor 2) may also act as a negative regulator of VSG switching in association with *Tb*TRF but by a mechanism independent of *Tb*TRF (Jehi *et al.*, 2014b, Jehi *et al.*, 2016). A recent study identified that the replication of actively transcribed BES happens in the early S-phase, but replication of all silent BES happens later (Devlin *et al.*, 2016). The factors that direct the early replication of transcribed BES or replication of all silent BES compared to the rest of the genome are still unidentified (Tiengwe *et al.*, 2012, Benmerzouga *et al.*, 2013, Kim, 2019). A previous study identified POLIE as a putative *T. brucei* translesion polymerase, although the translesion polymerase activity of POLIE has not been verified yet (Reis *et al.*, 2018). The study purified POLIE by coimmunoprecipitation with *Tb*TRF, and with a telomeric repeat-containing oligonucleotide (Reis *et al.*, 2018). It was shown that POLIE is closely related to four mitochondrial-targeted DNA polymerases but seems to be localized to the

periphery of the nucleus in *T. brucei* and that RNAi-mediated depletion of POLIE results in slowed growth without a specific cell cycle arrest, accumulation of DNA damage, and chromosome segregation defects (Leal *et al.,* 2020). The study also documents substantial deregulation of telomeric *VSG* genes after POLIE depletion, which suggests at least one putative translesion DNA polymerase can contribute to antigenic variation (Leal *et al.,* 2020).

1.6 DNA Polymerase and Genome Duplication

Accurate duplication of genomic DNA is indispensable for organism survival. Precise duplication of genomic DNA depends on two processes, replication of the genome, and necessary repair of DNA damage (Cotterill and Kearsey, 2009). DNA polymerases are involved in both genome replication as well as repair of DNA lesions. Based on sequence and structural homologies, there are four different families of eukaryotic DNA polymerase, A, B, X, and Y. Nuclear DNA is replicated by B family DNA polymerases while the mitochondrial DAN is replicated by A family DNA polymerases (Raia *et al.,* 2019).

Translesion DNA polymerases span all families of DNA polymerases and are involved in replication to bypass DNA damage. Replicative DNA polymerases are high-fidelity polymerases with a very low error rate (Kunkel, 2004). Replicative DNA polymerases can efficiently select the appropriate nucleotide for incorporation into the newly synthesized DNA by its polymerase activity and remove incorrectly inserted nucleotides by its proofreading activity (Leal *et al.,* 2020). Furthermore, post-replicative repair decreases overall error rates by removing damaged or mispaired bases (Sale, 2013).

1.7 Translesion Polymerase and POLIE

Cells developed a wide array of DNA repair mechanisms that can effectively identify and eliminate DNA lesions from the DNA template during replication. Yet few forms of DNA lesions can persist in the genome which may lead to fork stalling during replication and affect organism survival (Iyama and Wilson, 2013, Gao *et al.,* 2019). Cells from different organisms express a wide array of translesion DNA polymerases to ensure efficient duplication of the genome. When replicative DNA polymerases encounter a lesion in the template strand, translesion DNA Polymerases are recruited to bypass DNA damage to allow genome duplication (Powers and Washington, 2018, Vaisman and Woodgate, 2017, Goodman and Woodgate, 2013). Translesion synthesis bypasses this lesion by incorporating nucleotides in the newly synthesized DNA strand (Sale, 2013). Translesion DNA polymerases are recruited to the damaged DNA by proliferating cell nuclear antigen, PCNA (Fig. 7) (Andersen *et al.,* 2008). The PCNA complex encompasses DNA and helps to recruit replicative DNA Polymerases, increasing the processivity for repairing DNA damage (Zhuang and Ai, 2010). Additionally, PCNA interacts with translesion DNA polymerases through its PIP box motif (Boehm *et al.,* 2016). It was shown previously that at least some Translesion DNA polymerases can form a complex with other proteins at stalled replication forks (Wojtaszek *et al.,* 2016). Replication fork stalling can cause a longer appearance of single-stranded DNA, which can be identified by the RPA (replication protein A) heterotrimer. The binding of RPA stimulates RAD18/RAD6 complex to mono-ubiquitinate PCNA, which assists the exchange of replicative polymerases with Translesion polymerases to circumvent DNA lesions in replication (Mailand *et al.,* 2016).
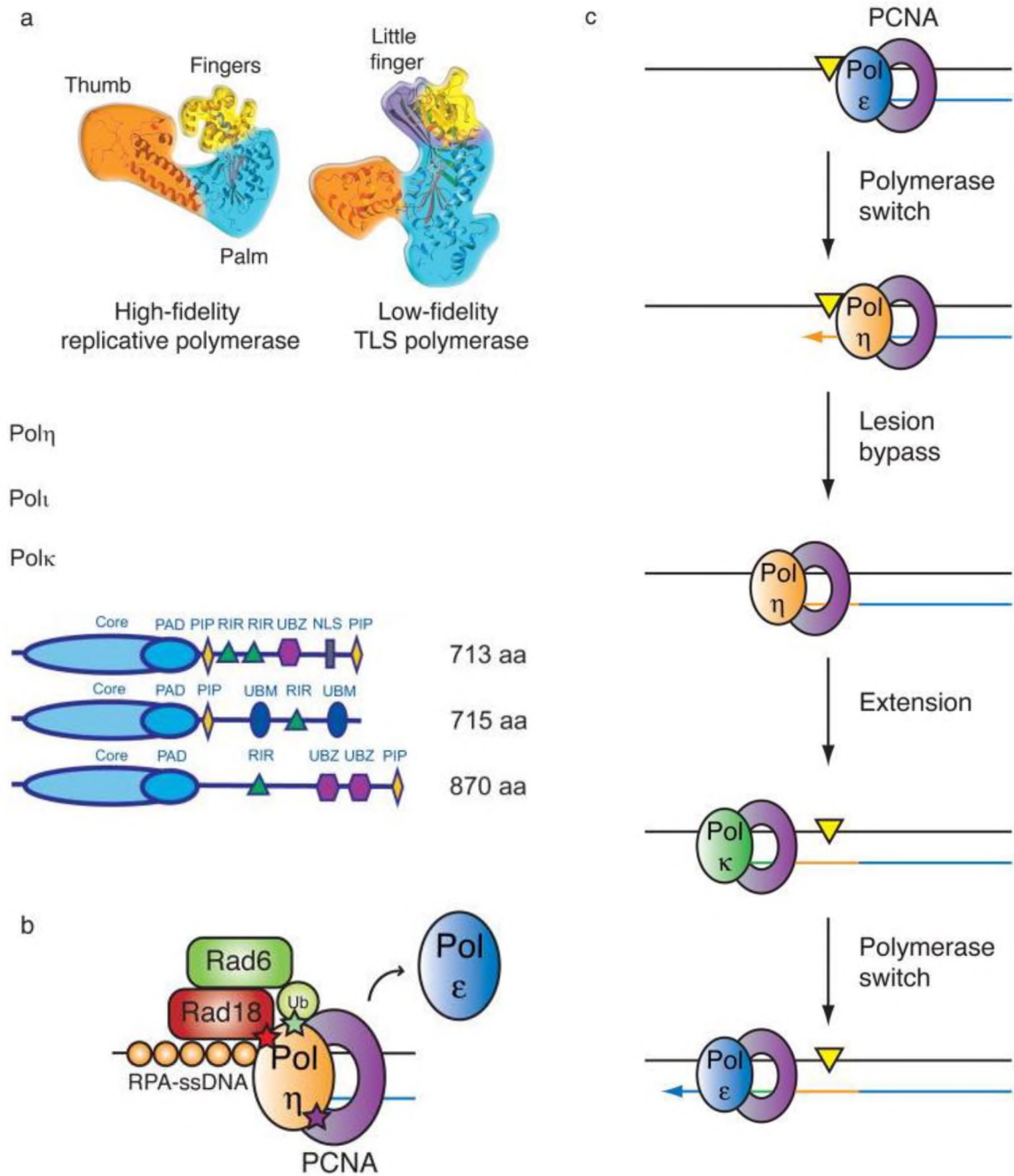
Fig. 7: Schematic representation of translesion synthesis (figure reproduced from Chang and Cimprich, 2009, Pustovalova *et al.,* 2016). (a) Structure of replicative DNA polymerase and translesion DNA polymerase. Translesion DNA polymerases, such as Polη, Polι, and Polκ contain a core polymerase domain with palm, finger, and thumb domains, a polymerase associated domain (PAD), a ubiquitin-binding zinc finger (UBZ) domain, PCNA interacting domain (PIP), REV1 interacting region (RIR), and a nuclear localization signal domain (NLS). (b) Model of polymerase switching at lesions. (c) At the stalled fork, translesion DNA polymerase (tan) is recruited to slide clamp PCNA and bypass the lesion. Then another (green) or same translesion DNA polymerase extends the "patch" and switches to replicative DNA polymerase (blue) to restore DNA synthesis.

23

Translesion activities in *T. brucei* are not well documented. The only studied translesion DNA polymerases are two primase-polymerase-like proteins called PPL1 and PPL2 in *T. brucei* (Rudd *et al.,* 2016). In an *in vitro* experiment, these polymerases were shown to incorporate nucleotides opposite to thymine dimers in DNA templates. Furthermore, PPL2 depletion leads to a severe cell cycle defect after completion of most nuclear DNA synthesis and initiation of the DNA damage response (Rudd *et al.,* 2016). The substrate of PPL2 in the *T. brucei* genome is yet unknown but translesion polymerase was shown to form a complex with other telomere-binding proteins in *T. brucei* (Reis *et al.,* 2018).

1.8 Telomere Replication and C-Strand Fill-in

Although the duplex region of telomere is replicated by conventional DNA polymerase, several other proteins play important roles in accurate, efficient telomere replication and in maintaining organism-specific length homeostasis. Cells carrying linear chromosomes must find a way to prevent progressive telomere shortening due to the end replication problem, as conventional DNA polymerases cannot prime the 3'end of the DNA in a lagging strand. During replication, only the leading strand can be continuously synthesized in the 5' to 3' direction. The lagging strand is replicated in small Okazaki fragments where each fragment requires a primer. The end replication problem is driven by the fact that a small stretch of the parental DNA in the lagging strand at the chromosome end cannot be primed with RNA primer by the DNA polymerase α/primase complex and that region is lost in the newly replicated DNA. Hence telomere DNA is shortened after each round of DNA replication due to the inability of conventional polymerase to fully replicate telomere DNA. Telomerase, a specialized reverse transcriptase, is the enzyme that

solves the end replication problem by elongating the G-rich strand of the telomere. While telomerase is mostly inactive in human somatic cells but active in highly dividing cells such as germ cells (Ishikawa, 2013). About 90% of clinical primary tumors maintain their telomere length (Ishikawa, 2013). Hence, inactivating telomerase is an attractive therapeutic model to treat cancer.

Human telomerase is an RNA-protein complex with two major components, telomerase RNA (TER, product of the *TERC* gene) and telomerase reverse transcriptase (TERT). Human TERT is expressed only in telomerase-positive cells and TERT expression indicates the telomerase activity of cells (Avilion *et al.,* 1996). Telomerase uses a 3' overhang to add telomeric sequences to the G-rich strand using an RNA component as a template. Since telomerase only elongates the G-rich strand of the telomere, the C-rich strand needs to be extended to maintain telomere length. In human, budding yeast, and plant, the CST complex (CTC1-STN1-TEN1) play important role in the synthesis of complementary C-strand by fill-in (Song *et al.,* 2008; Ishikawa, 2013; Ge *et al.,* 2020). However, the homolog/ortholog of the CST complex has not been identified in *T. brucei.* This suggests that *T. brucei* may use a CST-independent mechanism to maintain G-overhang. Telomerase-mediated telomere synthesis is the principal mechanism of telomere maintenance in *T. brucei* (Dreesen *et al.,* 2005; Sandhu *et al.,* 2013; Gupta *et al.,* 2013).

Telomere replication in humans is extensively studied. Human telomeres replication is a multi-step process that involves not only the conventional DNA replication machinery but also telomerase, telomere proteins, and various other accessory factors (Feng *et al.,* 2017). Human telomeric dsDNA is replicated by the conventional DNA replication machinery, which is aided by TRF1, TRF2, CST, and multiple helicases

(Martinez and Blasco, 2015; Wang *et al.,* 2012). In the S phase, DNA replication by conventional DNA polymerases generates a blunt-ended product in the leading strand telomere synthesis while in the lagging strand telomere synthesis, the removal of the 5' RNA primer generates a short 3' overhang. In mammalian cells, the 5' end of the leading strand synthesis product is first resected by Apollo, a 5' to 3' exonuclease (Wu *et al.,* 2010), then resected further by Exo1 (Keijzers *et al.,* 2016; Wu *et al.,* 2012) which leads to the generation of telomere 3' overhangs on the leading strand (Chow *et al.,* 2012; Wu *et al.,* 2012).

On the other hand, the lagging strand telomere synthesis generates telomere 3' overhangs after the removal of the RNA primer and sub-terminal position of the last Okazaki fragment (Chow *et al.,* 2012). Exo1 also resects the 5' ends of lagging strand to generate longer telomere 3' overhangs (Keijzers *et al.,* 2016; Wu *et al.,* 2012). Afterward, the 3' overhang is elongated by telomerase to generate telomere G-strand (Blackburn and Collins, 2011). Telomerase extension happens immediately after the replication of duplex telomere DNA and the generation of a 3' overhang (Feng *et al.,* 2017). In humans, TPP1 stabilizes the association of telomerase to the telomeres which allows telomerase to extend the G-strands by ~60 nt (Hockemeyer and Collins, 2015; Zhao *et al.,* 2009; Schmidt *et al.,* 2016; Sexton *et al.,* 2014). The TEL patch of TPP1 is involved in the recruitment of telomerase to the telomeres and promotes DNA synthesis with high processivity (Nandakumar *et al.,* 2012). The final maturation of the 3' overhang only happens after S/G2 when a DNA polymerase, such as DNA polymerase alpha-primase in mammals, synthesizes a complementary C-strand DNA in a process termed as C-strand fill-in (Zhao

et al., 2009; Wei and Price, 2003). CST complex recruits DNA polymerase alpha-primase to the lagging strand to facilitate C-strand fill-in at telomeres (Rice and Skordalakes. 2016).
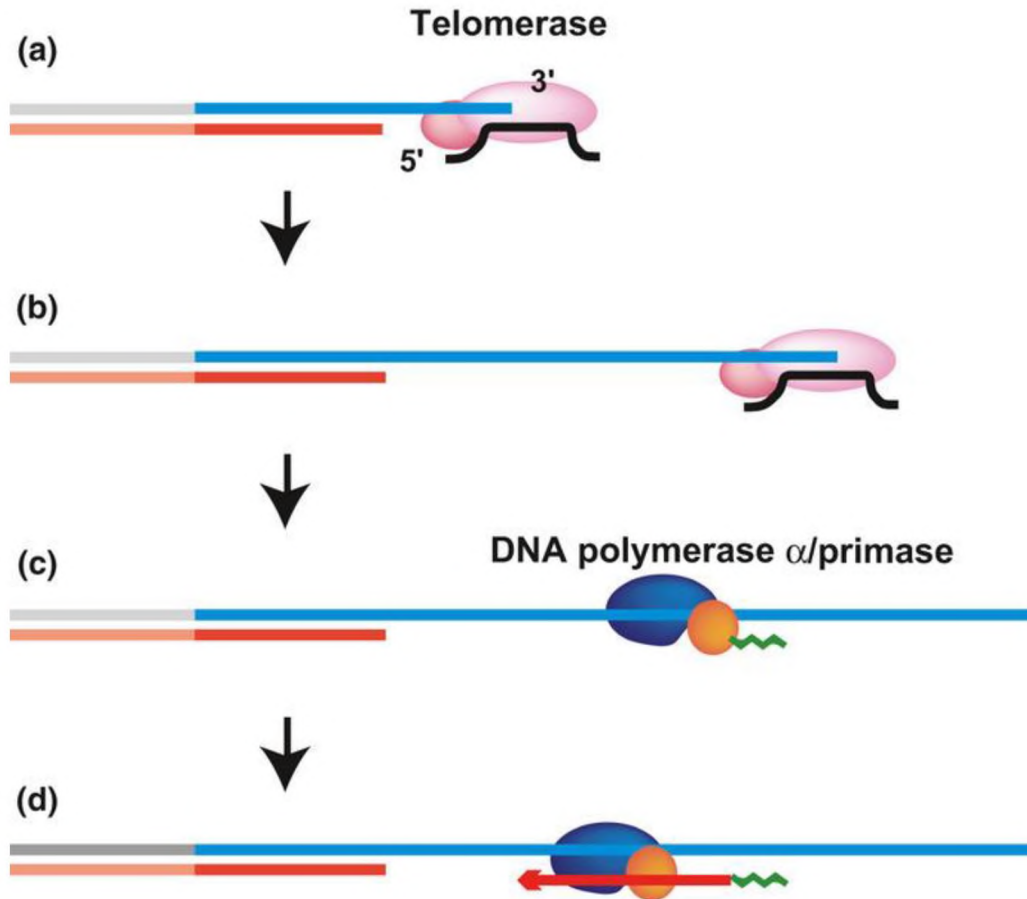
Fig. 8: Schematic representation of C-strand fill-in (Ishikawa, 2013). C-strand fill-in occurs after telomerase extends the telomere. In humans, DNA polymerase α/primase involve in the C-strand fill-in reaction.

T. brucei telomere 3' overhangs are very short (~12 nts) (Sandhu and Li, 2017; Li *et al.,* 2005), suggesting that the telomere C-strand fill-in is well coordinated with the G-strand extension. However, the OB fold-containing telomere-specific ssDNA binding factors appear to be absent in the *T. brucei* genome, and so far, no telomerase regulators have been identified. Rather, a zinc finger-containing protein UMSBP2 that is important for mitochondrial DNA replication can bind the G-rich telomere ssDNA (Milman *et al.,*

2007; Klebanov-Akopyan *et al.,* 2018). Depletion of UMSBP2 leads to a decreased G-rich but an increased C-rich ssDNA signal level and an increased amount of telomeric circles (Klebanov-Akopyan *et al.,* 2018). In this study, I explored whether POLIE plays a potential role to maintain telomere 3' overhangs length in *T. brucei*, similar to OB fold-containing telomere-specific ssDNA binding factors that function in maintaining human 3' overhangs length.

CHAPTER II

MATERIAL AND METHOD

2.1 *T. brucei* Strain

Each *T. brucei* strain used in this study is listed in Table 1. Only bloodstream form (BF) strains used in this study which is derived from VSG2-expressing Lister 427 cells. This strain is known as Single Marker (SM) which expresses a Tet repressor and a T7 polymerase (Wirtz *et al.*, 1999). All BF cells were cultured in HMI-9 media containing 10% FBS with proper antibiotics for selection.

The HSTB261 strain is derived from SM and specifically designed for assaying VSG switching (Kim and Cross, 2010), which we renamed as the S strain for easier reference (Jehi *et al.*, 2014b). HSTB261 contains a *blasticidin resistance* gene (*BSD*) immediately downstream of the active ES promoter and a *puromycin resistance* gene (*PURO*) fused with the Herpes simplex virus *thymidine kinase* (*PURO-TK*). SM, TIF$^{2+F2H/+}$ (Jehi *et al.*, 2014b), and the S cells were used for conditional expression of the POLIE double-stranded RNA (dsRNA) for downregulation of POLIE. Briefly individual cells were transfected with pSK-POLIE-myc13-Hyg-tar to tag one endogenous allele of POLIE with a C-terminal 13 x myc tag. Correctly targeted clones were confirmed by PCR and western blotting. POLIE single knockout cells were generated by replacing the *POLIE*

allele with the *Blasticidin resistance gene* using a targeting construct. Correctly targeted

clones were confirmed by PCR.

Table 1: List of *T. brucei* strains used in this study

Strain	Life cycle stage & Description of genotype
POLIE$^{+myc/+}$	BF; One allele of *POLIE* is C-terminally tagged with 13 x myc
POLIE$^{+/-}$	BF; One allele of *POLIE* is deleted
POLIE$^{+myc/-}$	BF; One allele of *POLIE* is C-terminally tagged with 13 x myc and the other is deleted
POLIE$^{+myc/+}$ *TIF2*$^{+F2H/+}$	BF; One allele of *POLIE* is C-terminally tagged with 13 x myc; One allele of *TIF2* is C-terminally tagged with F2H
POLIE$^{+myc/+}$ TRF RNAi	BF; One allele of *POLIE* is C-terminally tagged with 13 x myc; The Tet-inducible TRF RNAi expressing construct is integrated into an rDNA spacer
POLIE$^{+myc/+}$ RNAi	BF; One allele of *POLIE* is C-terminally tagged with 13 x myc; The Tet-inducible POLIE RNAi expressing construct is integrated into an rDNA spacer
S (Kim and Cross, 2010)	BF; In the active *VSG2*-containing ES, a *BSD* marker is inserted immediately downstream of the ES promoter, and a *PUR-TK* marker is inserted immediately upstream of the *VSG2* gene (Fig. S3A)
S/ev (Jehi *et al.*, 2014b)	BF; The active ES has the *BSD* and *PUR-TK* markers; The empty RNAi construct is integrated into an rDNA spacer
S/IEi	BF; The active ES has the *BSD* and *PUR-TK* markers; The Tet-inducible POLIE RNAi expressing construct is integrated into an rDNA spacer
POLIE$^{+myc/+}$ S/IEi	BF; The active ES has the *BSD* and *PUR-TK* markers; The Tet-inducible POLIE RNAi expressing construct is integrated into an rDNA spacer; One allele of *POLIE* is C-terminally tagged with 13 x myc
S/IEi + ecPOLIE-myc	BF; The active ES has the *BSD* and *PUR-TK* markers; The Tet-inducible POLIE RNAi expressing construct is integrated into an rDNA spacer; An inducible ectopic *POLIE-myc* expressing construct is integrated into an rDNA spacer
TR$^{-/-}$ (Sandhu *et al.*, 2013)	BF; Both *TR* alleles are deleted
TR$^{-/-}$ POLIE RNAi	BF; Both *TR* alleles are deleted; The Tet-inducible POLIE RNAi expressing construct is integrated into an rDNA spacer

POLIE$^{+myc/+}$ cells were transfected with pZJMβ-TRF (Li *et al.*, 2005) and pZJMβ-

POLIE to generate *POLIE*$^{+myc/+}$ TRF RNAi and *POLIE*$^{+myc/+}$ RNAi, respectively. pZJMβ-

TRF or pZJMβ-POLIE was linearized with NotI before transfection and correctly targeted clones were confirmed by western blot. Surviving clones were screened for doxycycline sensitivity; only clones exhibiting strong depletion of TbTRF/POLIE were used for further studies.

The S cells were transfected with pZJMβ-POLIE to generate S/IEi followed by transfection with pSK-POLIE-myc13-Hyg-tar to generate $POLIE^{+myc/+}$ S/IEi. Clones were tested for doxycycline sensitivity and only clones exhibiting depletion of POLIE were used for VSG Switching studies. S/IEi cells were also transfected with pLew100v5-POLIE-myc to generate S/IEi + ecPOLIEmyc. TR$^{-/-}$ cells (Sandhu et $al.,$ 2013) were transfected with pZJMβ-POLIE to generate TR$^{-/-}$ POLIE RNAi. SM and $POLIE^{+myc/+}$ cells were transfected with pSK-POLIE-ko-BSD to generate $POLIE^{+/-}$ and $POLIE^{+myc/-}$. All transfections were done using an AMAXA Nucleofector (Lonza, Inc.) in Basic Parasites Buffer 1 using program X-001 according to manufacture protocol.

2.2 $T.$ $Brucei$ Plasmids Construct

To generate pSK-F2HTRF-Pur-tar, a 500 bp genomic DNA fragment upstream of the TRF gene, the $Puromycin$ $resistance$ gene (PUR), the α/β tubulin intergenic sequence, the F2H tag, and a 500 bp fragment of the TRF gene (Encoding its N-terminus) are inserted into pBluescript SK in this order.

To generate pSK-POLIE-myc13-Hyg-tar, a 400 bp $POLIE$ gene fragment (encoding its C-terminus), a 13 x myc tag, the α/β tubulin intergenic sequence, the $Hygromycin$ $resistance$ gene (HYG), and a 500 bp genomic DNA fragment downstream of the $POLIE$ gene were inserted into pBluescript SK.

To generate pZJMβ-POLIE RNAi, a 470 bp DNA fragment at the N-terminus of

POLIE ORF and a 520 bp DNA fragment at the C-terminus of POLIE ORF were inserted into pZJMβ.

To generate pSKPOLIE-ko-BSD, the *Blasticidin-resistance* gene (*BSD*) flanked by genomic DNA fragments upstream and downstream of the *POLIE* gene, respectively, were inserted into pBluescript SK.

To generate pLew100v5-POLIE-myc, the DNA fragment encoding the full-length POLIE and a C-terminal 13 x myc tag were inserted into pLew100v5.

2.3 Growth Analysis

To measure the growth of individual strains, the experimental cells were grown with control cells and the growth rates were compared. Cells were counted at 24Hr intervals and population doublings were calculated. Population doubling = log2 (total number of cells, n/total number of cells, (n-1)) + PD (n-1), where n is the day when cells were counted, and n-1 is the immediate day preceding it.

2.4 UV and Cisplatin Sensitivity Assay

The sensitivity of $POLIE^{+myc/+}$ RNAi cell lines towards DNA-damaging agents such as UV and Cisplatin were tested. Briefly, $POLIE^{+myc/+}$ RNAi cells were incubated with and without doxycycline for 12 hrs, then diluted to a concentration of 1.5 x 10^6 cells/ml. For assessing UV irradiation effects, the RNAi cell was induced with dox for 12 hrs. The induced and non-induced cells were diluted to a concentration of 1.5 x 10^6/ml and were exposed to 0, 50, or 100 J m^{-2} of UV using the Stratalinker® Crosslinker (Stratagene). For Cisplatin (Sigma) sensitivity assays, the RNAi cells were induced with dox for 12 hrs, treated with 0 and 20 μM Cisplatin, and incubated for 1Hr in the incubator. In each case, treated and untreated control cell cultures were washed to remove doxycycline and diluted

daily to a concentration of 0.1 x 10^6/ml. Cell growth was monitored every 24hr with necessary dilutions and the survival was calculated as a percentage of untreated controls.

2.5 Chromatin Immunoprecipitation

200 million cells were harvested and crosslinked with 1% formaldehyde for 20 minutes at room temperature. *T. brucei* BF cells were lysed and sonicated at a volume of 330 uL using a Bioruptor300 for 4 cycles with high output for 30 sec on/off per cycle. Lysates were incubated using Dynabeads® Protein G with or without specific antibodies to immunoprecipitate protein-DNA complexes. 50 uL lysate was collected as the input. The rest of 280 ul of lysate was divided into 3 equal fractions and each was subjected to immunoprecipitation using Dynabeads® Protein G conjugated with IgG, anti-TRF (1261), and Anti-Myc (9e10) antibody. Before IP, beads were washed and equilibrated following the manufacturer's protocol. Immunoprecipitated DNA was reverse cross-linked and purified using the Qiaquick spin PCR purification Kit (Qiagen). The final sample was dissolved in 50 uL of ddH2O. The sample was analyzed by slot blot using a telomere-specific TTAGGG repeat containing a radioactive probe. As a control for pull-down specificity, blots were hybridized with a tubulin probe.

2.6 Western Blot

Cells growing at exponential phase (~1.5X10^6/ml) were lysed in 2x Laemmli buffer (0.1 M Tris-Cl-pH 6.8, 6% SDS, 20% glycerol, 0.004% bromophenol blue) and boiled at 100°C for 10 min to collect total cell lysate. Samples were separated on a Tris-Glycine polyacrylamide gel at 100 V for ~2 hrs. After separation, proteins were transferred onto 0.45 μm nitrocellulose membrane (GE healthcare life sciences) by electrophoresis at 100 V for 90 min at 4°C. The membrane was blocked with 10% milk/ 0.5% Tween 20/ 1x PBS

(phosphate buffer saline) at room temperature for ~1 hour. The membrane was rinsed twice for ~5 minutes each using 0.1% milk/0.1% Tween 20/1x PBS. The membrane was hybridized overnight in a plastic bag using an appropriate primary antibody and dilution, in 5% milk/0.1% Tween 20/1x PBS. The next day, the membrane was washed three times for ~5 minutes using 0.1% milk/0.1% Tween 20/1x PBS and hybridized with an appropriate secondary antibody in 5% milk/0.1% Tween 20/1x PBS at room temperature for one hour. Subsequently, the membrane was washed 4 times, each for ~5 minutes, using 0.1% milk/0.1% Tween 20/1x PBS. Finally, the membrane was washed for 5 minutes using 1x PBS. The membrane was rinsed with water and incubated with Amersham ECL Western blotting reagent (GE Healthcare Life Sciences) for ~2 minutes. The blot was imaged with Odyssey Fc (LI-COR Biosciences). In POLIE-RNAi cells, 13 x myc-POLIE was detected using the 9E10 monoclonal antibody against Myc. As a loading control, beta-tubulin antibody TAT-1 was used (gift from Dr. Keith Gull) (Yang *et al.,* 2009).

2.7 VSG Switching Assay

The VSG switching frequency was determined in switching cells (HSTB261) where POLIE was transiently knocked down by RNAi. HSTB261- POLIE-RNAi cells were maintained in the presence of blasticidin and puromycin until the start of the assay to homogenize the cell population (that expresses VSG2). Then 1100 cells were incubated with doxycycline to induce POLIE RNAi for 30 hrs in the absence of blasticidin and puromycin so that cells were then allowed to switch. Doxycycline was washed off and cells were grown in the absence of doxycycline until cell density reaches ~1.5-1.7 million cells/ml (10.5 population doublings) before they were harvested. Switchers were enriched

by passing cells through a VSG2 Ab-conjugated MACS column and collecting the flow through.

To determine plating efficiency, cells were plated at 1 cell/well in 3 x 96-well plates without ganciclovir (GCV) selection. Switchers were selected by 5 μg/ml GCV after they were diluted and distributed in 1 million cells/6 x 96-well plates. GCV-resistant switchers were further verified by western dot-blot analysis using a VSG2 Ab (ΔCRD) to determine the switching frequency. The VSG switching rate was calculated by dividing the number of switchers (GCV resistant and VSG2- cell) by the total number of plated cells and was further normalized by the plating efficiency. To determine the switching mechanisms, switchers were analyzed for their sensitivity to 5 μg/ml and 100 μg/ml blasticidin and 2 μg/ml puromycin. The presence of the *BSD* and *VSG2* genes was determined by PCR using genomic DNA isolated from the switchers.

2.8 Telomere DNA Isolation

Genomic DNA was isolated using PCIA extraction followed by DNA strand fishing. Briefly, 200 million BF cells were washed 1X TDB (80 mM NaCl, 5 mM KCl, 1 mM MgSO4, 2 mM NaH$_2$PO$_4$, 20 mM Na$_2$HPO$_4$ and 20 mM glucose at pH 7.4) and resuspended in 1 ml of TNE (10 mM Tris pH 7.4, 10 mM EDTA, 100 mM NaCl). 1 ml of TNES/proteinase K (10 mM Tris pH 7.4, 100 mM NaCl, 10 mM EDTA, 1% SDS + 100 μg/ml proteinase K (Roche)) was added, and samples were incubated overnight at 37°C. DNA was extracted using 2 ml of phenol-chloroform-isoamyl alcohol. DNA was precipitated with 2M NaAc pH 5.5 and an equal volume of isopropanol and gently spooled out. The DNA was resuspended in 300 ul TNE+100 μg/ml RNase. After incubation for 2 hrs and 30 min with RNase at 37°C, 300 ul of TNES/proteinase K was added and reaction

samples were incubated for 1 hour at 37°C. The DNA was extracted and precipitated as mentioned above and resuspended in 100 ul of $T_{10}E_{0.1}$ (10 mM Tris pH 7.5/0.1 mM EDTA).

2.9 Southern Blot Analysis of Telomeric DNA

5-10 μg of genomic DNA was digested overnight at 37°C by AluI and MboI. The DNA concentration after digestion was measured using Qubit (Thermofisher). 500 ng of digested DNA was separated in a 0.7% agarose gel in 0.5 x TAE with 20x20 cm dimensions with an appropriate DNA marker. The gel was first run for 1 hour at 30 volts followed by overnight at 50 volts, in a total of ~1,000-1,100 Vhrs. The EtBr-stained gel was scanned using Typhoon FLA 9140 (GE healthcare life sciences) by placing a ruler next to it. The gel was depurinated for 30 min with depurination buffer (0.25 M HCl), denatured 2 times 30 min each with denaturation buffer (1.5 M NaCl, 0.5 M NaOH), neutralized 2 times 30 min each with neutralization buffer (1 M Tris pH 7.4. 1.5 M NaCl) and blotted onto a Hybond nylon membrane (GE Healthcare Life Sciences) by capillary blotting in 20XSSC (3 M NaCl, 0.3 M sodium citrate) overnight. The blot was UV cross-linked (Stratalinker UV crosslinker) pre-hybridized with Church Mix (1% BSA, 0.5 M NaPi pH 7.2, 7% SDS, 4 mM EDTA pH 8.0) and hybridized with the appropriate radiolabeled probe at 65 °C overnight. The blot was washed three times in 15-minute washing intervals with Church Wash (40 mM NaPi-pH 7.2, 1 mM EDTA pH-8.0, and 1% w/v SDS) at 65 °C, wrapped, and exposed to a phosphorimager.

2.10 Telomere 3' Overhang Assay (Native In-Gel Hybridization)

Genomic DNA from the bloodstream form *T. brucei* cells was treated with or without Exo I (NEB) and digested with MboI and AluI. An equal amount of ExoI treated and non-treated DNA was separated by agarose gel electrophoresis. The DNA-containing

agarose gel was dried for 4 hrs at room temperature and hybridized overnight with an end-labeled $(CCCTAA)_4$ or $(TTAGGG)_4$ probe at $50°C$ in Church Mix (1% BSA, 0.5 M NaPi pH 7.2, 7% SDS, 4 mM EDTA pH 8.0). The hybridized gel was washed three times for 30 minutes each with 4xSSC (0.6 M NaCl and 0.06 M sodium citrate) at $50°C$ followed by a final wash in 4xSSC with 0.1% SDS for 30 minutes at $50°C$ and exposed to a phosphorimager for 24 – 72 hrs. The gel was then denatured 2 times 30 min each with denaturation buffer (1.5 M NaCl, 0.5 M NaOH), neutralized 2 times 30 min each with neutralization buffer (1 M Tris pH 7.4. 1.5 M NaCl), and hybridized with the same oligo probe at $55°C$ in Church Mix (1% BSA, 0.5 M NaPi pH 7.2, 7% SDS, 4 mM EDTA pH 8.0). The gel was washed three times for 30 minutes each with 4xSSC (0.6 M NaCl and 0.06 M sodium citrate) at $50°C$ followed by a final wash in 4xSSC with 0.1%SDS for 30 minutes at $55°C$, followed by exposure to a phosphorimager for 2-4 hrs. The hybridization signals were quantified using ImageQuant. Telomere 3' overhang signal levels were quantified by dividing the amount of native hybridization signals by the amount of post-denaturation hybridization signals.

2.11 Pulsed-Field Gel Electrophoresis

DNA plugs were prepared according to Li *et al.* (Li *et al.*, 2005). 150 million cells were centrifuged at 2000rpm for 10min, and the cell pellet was washed with 1 x TDB (80 mM NaCl, 5 mM KCl, 1 mM MgSO4, 2 mM NaH$_2$PO$_4$, 20 mM Na$_2$HPO$_4$, and 20 mM glucose at pH 7.4). Cells were resuspended in L buffer (0.02 M NaCl, 0.01 M Tris-HCl pH 7.6) at a concentration of 5×10^8 cells/ml. Cells were incubated at $42-50°C$ for 10 minutes and an equal volume of 1.6% low-melting-point (LMP) agarose in L buffer (already melted and equilibrated at $50°C$) was added to cells (to a final concentration of 2.5×10^8 cells/ml).

Approximately 85 μl of this solution (2×10^7 cells) was loaded into each well of disposable plug-preparing molds. The DNA plugs were kept at RT for 10 minutes to solidify and transferred into a 15ml tube containing 2 ml of L buffer, 1% Sarkosyl, and 1 mg/ml Proteinase K. Samples were incubated at 50°C for 48 hrs and washed 2 times at 10 minutes each with L buffer. The Proteinase K treatment was repeated for another 48 hrs and washed again as above. The plugs were stored at 4°C in L buffer until running (but not more than a week).

The undigested *T. brucei* chromosomes in the DNA plugs were separated by a Pulsed Field Gel Electrophoresis (PFGE) apparatus (CHEF-DR II, Bio-Rad) according to Jehi *et al.* (Jehi *et al.*, 2014b). 200 ml of a 1.2 % agarose gel was prepared in 0.5 x TBE (40 mM Tris-Cl pH 8.3, 4 mM boric acid, 1 mM EDTA) and kept at 42°C in water to cool down. The plugs were attached to the comb with 1.6% melted LMP agarose and placed on a 1.2 % agarose gel. The agarose gel was run on PFGE apparatus with prechilled 3 L 0.5 x TBE. Running parameters are initial pulse: 1500s, ending pulse: 700s, voltage: 2.5 V/cm for 120 hrs at 12°C. The gel was stained for 1 hour in 0.5 x TBE with 1 μg/ml EtBr and washed for 2 times 30 minutes each with ddH$_2$O before imaging.

After imaging, the ethidium bromide-stained gel was dried for 8 hrs at room temperature. The dried gel was pre-hybridized at 50°C in 35 ml Church Mix (1% BSA, 0.5 M NaPi pH 7.2, 7% SDS, 4 mM EDTA pH 8.0) for at least 1 hr and hybridized overnight at 50 °C with end-labeled probe in 35 ml Church Mix (1% BSA, 0.5 M NaPi pH 7.2, 7% SDS, 4 mM EDTA pH 8.0). The (CCCTAA)$_4$ probe was used to detect the telomeric G-strand DNA and the (TTAGGG)$_4$ probe was used to detect the telomeric C-strand DNA. The hybridized gel was washed in 4 x SSC three times for 30 minutes at 50°C. The gel was

washed again in 0.1% SDS in 4 x SSC once for 30 minutes at 50°C. The washed gel was exposed to a phosphorimager screen overnight. After scanning of the phosphorimager, the gel was denatured 2 times 30 min each with denaturation buffer (1.5 M NaCl, 0.5 M NaOH), neutralized 2 times 30 min each with neutralization buffer (1 M Tris pH 7.4. 1.5 M NaCl), hybridized again with the same probe in Church Mix (1% BSA, 0.5 M NaPi pH 7.2, 7% SDS, 4 mM EDTA pH 8.0) at 55°C. The gel was washed at 55°C as above and exposed to the phosphorimager for 4 hrs. The signals were quantified with ImageQuant. Telomere 3' overhang signal levels were calculated by dividing the amount of signals obtained before denaturation by the amount of those obtained after denaturation. The change in the telomere 3' overhang level was quantified by normalizing 3' overhang levels to WT level.

2.12 EDU-Labeling

Exponentially growing bloodstream form *T. brucei* cells (0.7-0.9 x 10^6 cells/ml) were incubated with 150 µM 5-ethynyl-2'-deoxyuridine (EdU) (Click Chemistry Tools) for 3 hrs at 37 °C. Cells were harvested by centrifugation at 1,500 g for 5 min and the genomic DNA was isolated using strand fishing described in section 2.8. DNA was sonicated to 400-1000 bp fragments. Newly synthesized EdU-labeled DNA fragments were conjugated with desthiobiotin in native or denatured conditions (4M Urea) using the click chemistry reagent (2 mM desthiobiotin-Azide, 100 mM/500 mM CuSO4/THPTA, 50 mM Na-Ascorbate, 100 mM HEPES pH 7, and 10% DMSO). The desthiobiotin conjugated DNA was pulled down using streptavidin beads (ThermoFisher) and eluted from the beads using 25 mM D-biotin. The eluted DNA was dot-blotted onto a Hybond N nylon membrane (GE Healthcare) and UV-crosslinked and hybridized with telomere and tubulin probes at

65°C. The blot was exposed to a phosphorimager and the signals were quantified using ImageQuant.

2.13 Two-Dimensional Gel Electrophoresis

Genomic DNA from $POLIE^{+myc/+}$ RNAi uninduced and induced cells (24 hrs) were digested with MboI/AluI. 5 μg of digested DNA was separated on 2-dimensional (2D) gel electrophoresis according to a protocol from Cohen and Mechali (Cohen and Méchali, 2002). DNAs were separated in the first dimension in a 0.4% agarose 1 x TBE gel without EtBr for 18 hrs at 40 volts at room temperature. Subsequently, the gel was incubated in 1 x TBE with 0.3 μg/ml EtBr for 20 minutes followed by washing 3 times 10 min each with 1 x TBE. DNAs were then excised from the gel, transferred to a second 1.1% agarose gel with 1 x TBE with 0.3 μg/ml EtBr, and electrophoresed for 5 hrs at 150 volts at 4°C. DNA was transferred to a Hybond N nylon membrane (GE Healthcare) by blotting and subsequently hybridized with a telomere probe.

2.14 The Telomeric C-Circle (and G-Circle) Assay

The φ29 DNA polymerase-mediated rolling-circle assay was performed according to Henson *et al* (Henson *et al.*, 2009) with minor modifications. 8 μg of AluI, MboI digested genomic DNA from BF *T. Brucei* was digested by λ Exonuclease and Exonuclease I to remove dsDNA. 20 ng of the resulting DNA was incubated with 7.5 U φ29 DNA polymerase (NEB) in reaction buffer [1 μg/μl BSA, 0.05% Tween 20, 0.5 mM dATP, 0.5 mM dGTP (or 0.5 mM dCTP for detecting G-circles) and 0.5 mM dTTP, 1 x φ29 Buffer] at 30°C for 8 hrs, then φ29 was heat-inactivated at 65 °C for 20 min. The reaction products were slot blotted onto a Hybond N nylon membrane (GE Healthcare) followed by hybridization at 50°C with end-labeled (CCCTAA)$_4$ to detect C-circles or (TTAGGG)$_4$ to

detect G-circles. The blot was exposed to a phosphorimager and the signals were quantified with ImageQuant.

2.15 TERRA RNA Isolation

Total RNA was isolated from *T. brucei* cells using RNA STAT-60 (TEL-TEST, Inc). Briefly, 200 million cells at the log growth phase (1.2 – 1.5 million/ml) were harvested by centrifugation at 1.5 krpm, 4°C for 10 minutes. The pellet was resuspended and evenly homogenized in 1 ml of RNA STAT-60 reagent at room temperature for 5 min. After incubation, 200 µl of chloroform was added to the tube and mixed vigorously by vortexing for 15 sec. The sample was incubated for another 5 minutes at room temperature and centrifuged at 13.2k rpm for 15 minutes at 4°C to collect the aqueous phase. 600 µl of isopropanol was added to the aqueous phase and mixed thoroughly. Samples were stored at -80°C for at least 1 hour. Samples were centrifuged at 13.2k rpm for 30 min at 4°C. The pellet was washed twice with 1 ml of 70% EtOH and centrifuged at 13.2k rpm for 10 mins at 4°C. The RNA was air-dried and dissolved in 50 µl of RNase-free ddH2O. The RNA sample was treated with 10U of DNAse I enzyme (Thermo Fisher) for 45 mins at 37°C to remove telomeric DNA from the RNA sample. The RNA was mixed with 900 µl of RNA STAT-60 and the isolation process was repeated 2 times and the final RNA was dissolved in 20 µl of RNase-free water for subsequent use in northern or slot blot.

2.16 Northern Blot Analysis

TERRA was separated in a 1.5% agarose gel prepared with formaldehyde in 1 x MOPS buffer (0.4 M MOPS, 0.1 M NaOAc, and 0.01 M EDTA). Briefly, 10 µg of RNA was mixed with the premix buffer (1.5 µl 10 x MOPS, 2.6 µl 37% formaldehyde, 7.5 µl Formamide, 3 µl 5 x loading buffer (1mM EDTA pH-8.0, 0.25% (w/v) bromophenol blue,

0.25% (w/v) xylene cyanol, 50% glycerol) and Ethidium bromide) in a volume of ~20 μl. 5 μg of RNA marker was also mixed with the premix. Samples were heated at 65°C for 10 minutes and immediately loaded onto the gel. The gel was run at ~5V/cm using 1 x MOPS buffer. The EtBr-stained gel was washed in ddH2O for one hour and scanned using a Typhoon FLA 9140. The gel was blotted onto a nylon hybond membrane (GE healthcare life sciences) overnight in 20 x SSC (3 M NaCl, 0.3 M sodium citrate), UV cross-linked and prehybridized at 55°C for one hour using the CHURCH mix (1% BSA, 0.5 M NaPi pH 7.2, 7% SDS, 4 mM EDTA pH 8.0). To detect the TERRA transcript, The blot was hybridized with an end-labeled $(CCCTAA)_4$ or $(TTAGGG)_4$ probe at 55°C overnight, and the blot was washed twice for 15 minutes each at 65°C using 0.1 x SSC (15 mM NaCl, 1.5 mM sodium citrate)/0.1% SDS followed by exposure to a phosphorimager screen overnight. Tubulin was used as a loading control. To detect the tubulin, hybridization was performed overnight at 55°C using a tubulin probe. The blot was washed three times for 15 min each at 55°C using the CHURCH wash (40 mM NaPi-pH 7.2, 1 mM EDTA pH-8.0, and 1% w/v SDS), wrapped, and exposed overnight to a Phosphorimager screen (GE healthcare life sciences).

2.17 Probe Preparation

To make a telomere or tubulin probe, 100 ng of this DNA fragment was mixed with 5 ng of random hexamer in a volume of 39 μl. The mixture was incubated at 100°C for 5 minutes and immediately chilled on ice. 5 μl of 10 x nucleotide mixture (dATP, dGTP, dTTP) without dCTP, 1 μl Klenow polymerase (New England Biolabs) and 5 μl of 32P-alpha-dCTP (3000 Ci/mmol) were added to the reaction. The reaction was incubated at room temperature for 90 minutes and stopped by adding 50 μl of TNES (10 mM Tris pH7.4,

10 mM EDTA, 100 mM NaCl, 1%SDS) buffer. The probe was purified over a sepharose G-50 column and eluted using TNES buffer. The probe was heated at 100°C for 5 minutes and added to 10-25 ml of CHURCH mix (1% BSA, 0.5 M NaPi pH 7.2, 7% SDS, 4 mM EDTA pH 8.0). This mixture was filtered using a 0.22 μm syringe filter and added directly onto the blot. End labeling of oligonucleotide probe was done for telomere in-gel hybridization. Briefly, 50 ng of TELC4 oligo ((CCCTAA)4) or TELG4 oligo ((TTAGGG)4) was mixed with 32P-gamma-ATP, Kinase buffer, and Polynucleotide kinase (New England Biolabs). The reaction was incubated at 37°C for 45 min. The reaction was stopped by adding 80 μl of TES (Tris-HCl/EDTA/SDS) buffer to the mixture. The probe was purified using a 3 ml Sepharose G-25 column and elution with TNES buffer. The purified probe was mixed with 25 ml of CHURCH mix (1% BSA, 0.5 M NaPi pH 7.2, 7% SDS, 4 mM EDTA pH 8.0), filtered through a 0.22 μm syringe filter, and added to the blot for hybridization.

2.18 Strand-Specific Telomere Probe Preparation

To synthesize radioactive (CCCTAA)n probe, 100 ng of purified 800 bp TTAGGG repeat dsDNA template were boiled for 5 min at 95°C with a random hexamer. Reaction was performed at room temperature with 5 μl of OLB buffer (0.5 M Tris pH 6.8, 0.1 M MgOAc, 1 mM DTT, 0.5 mg/ml BSA, 60 μM dATP, and 60 μM dTTP), 1 μl of Klenow polymerase (NEB) and 5 μl of radioactive dCTP. The probe was purified with a G-50 Sepharose beads column and immediately used for hybridization. The radioactive (TTAGGG)n probe was similarly synthesized except radioactive dGTP was included in the reaction instead of radioactive dCTP.

CHAPTER III

POLIE REGULATES TELOMERE G-STRAND EXTENSION AND C-STRAND SYNTHESIS IN *TRYPANOSOMA BRUCEI*

3.1 Introduction

Telomeres protect the eukaryotic chromosome ends from unwanted damage repair and DNA recombination. Therefore, telomeres are essential for genome integrity and chromosome stability. Proper telomere length maintenance is a prerequisite for chromosome end protection. Telomere lengths are primarily maintained by telomerase. However, telomere lengths can also be maintained by homologous recombination. Telomere maintenance mechanisms are still unclear in many eukaryotes including *T. brucei*.

T. *brucei* is a protozoan parasite that causes Human African Trypanosomiasis which is fatal without treatment. Telomere and telomeric protein of *T. brucei* play key roles in the pathogenesis of the disease. *T. brucei* regularly switches its major surface antigen, VSG, to effectively evade the host immune response. Such antigenic variation is a key pathogenesis mechanism that enables the parasite to establish a long-term infection. Interestingly, VSG is expressed exclusively from regions adjacent to the telomere in a

strictly monoallelic manner. Telomere proteins and the telomere structure play key roles in antigenic variation and parasite virulence.

Telomeres in *T. brucei* are primarily maintained by telomerase. In vertebrates, yeasts, metazoans and plants, OB fold-containing telomere ssDNA binding proteins such as the POT1/TPP1 complex (Takai *et al.,* 2016; Arnoult *et al.,* 2009; Aramburu *et al.,* 2020; Rajavel *et al.,* 2014, Myler *et al.,* 2021) and the CST complex (vertebrate CTC1/budding yeast CDC13, STN1, and TEN1) (Feng *et al.,* 2018; Gu *et al.,* 2018; Feng *et al.,* 2017; Amir *et al.,* 2020) play critical roles in coordinating the telomere G-strand extension and C-strand fill-in (Lue, 2018; Feng *et al.,* 2017). However, no homolog/ortholog of CST complex or POT1/TPP1 complex has been identified in *T. Brucei* (Li and Zhao, 2021). There were several attempts to identify single-stranded telomere G-overhang binding proteins in *T. Brucei.* Field and Field first attempted to identify the exitance of telomere G-overhang binding proteins in *T. Brucei* (Field and Field, 1996). However, this protein-DNA complex was neither purified nor characterized in this or later study. Cano and his colleagues purified a three-protein complex (complexes C1-C3) that was associated with single-stranded telomeric DNA (Cano *et al.,* 2002). However, mass spectrometry analysis failed to identify the components of these complexes. This implies that *T. brucei* may use a novel pathway using yet unknown single-stranded telomere G-overhang binding proteins to coordinate the telomere G-strand extension and C-strand fill-in.

The human TPP1/POT1 complex binds the telomere 3' overhang through POT1 (Loayza and de Lange, 2003; Lei *et al.,* 2004) and recruits telomerase to the telomere, and stimulates telomerase activity through TPP1 (Nandakumar *et al.,* 2012; Zhong *et al.,* 2012; Sandhu *et al.,* 2021). Mammalian CST is a trimeric complex that has structural similarity

to RPA (Replication Protein A) and like RPA, appears to bind ssDNA via multiple OB-folds (Bryan *et al.,* 2013; Bhattacharjee *et al.,* 2016; Miyake *et al.,* 2009; Surovtseva *et al.,* 2009). The binding of the CST complex on the telomere 3' overhang effectively inhibits telomerase-mediated telomere extension in humans (Chen *et al.,* 2012). Similarly, in budding yeasts, CDC13, the single-stranded telomere DNA binding factor, both positively and negatively regulates telomerase-mediated telomere extension: CDC13 interacts with EST1, a telomerase accessory protein, to help recruit telomerase to the telomere (Wu and Zakian, 2011). However, the binding of the CST complex (CDC13/STN1/TEN1) to the telomere also prevents the access of telomerase to the telomere substrate (Mersaoui and Wellinger, 2019). Furthermore, both vertebrate and yeast CST complexes promote the telomere C-strand fill-in by directly interacting with and recruiting DNA polymerase alpha-primase to the telomere (Fig 6) (Feng *et al.,* 2017; Lue, 2018; Casteel *et al.,* 2009; Huang *et al.,* 2012; Qi and Zakian, 2000). A disruption in CTC1 of CST leads to a decrease in C-strand length (Feng *et al.,* 2017), and several studies identified that CST complex is essential in C-strand fill-in (Huang *et al.,* 2012; Gu *et al.,* 2012; Stewart *et al.,* 2012; Kasbek *et al.,* 2013; Feng *et al.,* 2017; Ganduri and Lue, 2017). Therefore, telomere ssDNA binding factors are major players to coordinate the synthesis of the two telomere strands. No OB fold-containing telomere ssDNA binding proteins have been identified in *T. brucei* (Li and Zhao, 2021). In this project, I studied whether POLIE potentially functions as a human OB fold-containing telomere ssDNA binding protein in maintaining telomere G and C -strands in *T. brucei*.

3.2 Results

3.2.1 POLIE is an intrinsic component of the telomere complex and is essential for survival

POLIE was initially identified through its ability to bind a telomeric sequence-containing oligo (Leal *et al.,* 2020). However, it was not shown whether POLIE is a component of the telomere complex. Our lab previously identified homologs of several Shelterin components that are associated with the telomere but no OB fold-containing telomere-specific ssDNA binding factors in *T. brucei* have been identified (Li *et al.*, 2005; Yang *et al.,* 2009; Jehi *et al.,* 2014b). To identify additional components of the telomere complex, our lab member Maiko Tonini performed an affinity pulled down assay for telomere protein complex using known telomere proteins, TRF (Li *et al.*, 2005) and TIF2 (Jehi *et al.,* 2014b). Additionally, Maiko Tonini isolated the telomere chromatin by Proteomics of Isolated Chromatin segments (PICh) (Dejardin and Kingston, 2009) to identify proteins associated with the telomere chromatin (Rabbani *et al.,* 2022). About 800 proteins protein was identified using every two approaches and 282 proteins were identified in both. Among these, DNA polymerase IE (POLIE, Tb927.11.5550) (Reis *et al.,* 2018; Leal *et al.,* 2020) is one of the most abundant proteins in both experiments along with other telomeric proteins such as TRF, TIF2, RAP1, etc. (Rabbani *et al.,* 2022).

To verify that POLIE is an intrinsic component of the telomere complex, we tagged one endogenous POLIE allele with a C-terminal 13 x myc tag and established BF *T. brucei* *POLIE*$^{+\text{myc}/+}$, *POLIE*$^{+/-}$, and *POLIE*$^{+\text{myc}/-}$ strains (Table 1). These and WT cells grew at similar rates (Fig. 9), indicating that *POLIE*-myc appears to be functional. A slightly reduced growth was observed in POLIE$^{+\text{myc}/-}$ strains than in *POLIE*$^{+\text{myc}/+}$ and *POLIE*$^{+/-}$. We

performed an additional experiment in part 3.6 (Fig. 20) to show that POLIE-13 x myc is indeed functional. Moreover, we used POLIE-13 x myc as a negative control for all experiments to consider the mild effect of the tagged allele.
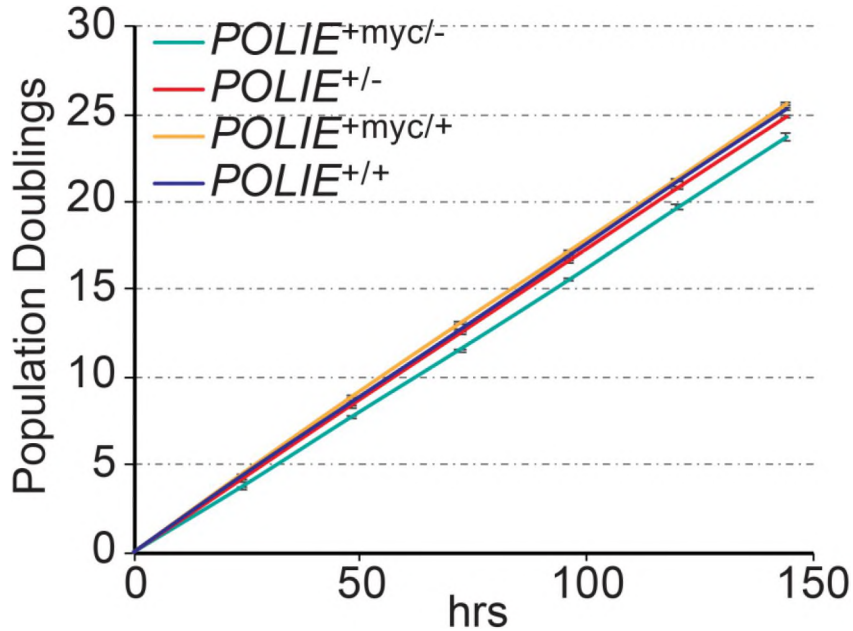
Fig. 9: C-terminal 13 x myc tagged POLIE in BF *T. brucei*. Growth curves of *POLIE*$^{+myc/+}$, *POLIE*$^{+myc/-}$, *POLIE*$^{+/+}$, and *POLIE*$^{+/-}$. Average population doublings were calculated from three independent experiments. Here, error bars represent standard deviation.

In *POLIE*$^{+myc/+}$ *TIF2*+F2H/+ cells, Maiko Tonini performed IP of POLIE-myc using the myc monoclonal antibody 9E10 pulled down TIF2-F2H and TRF (Fig. 10A). Similarly, POLIE-myc and TIF2-F2H were present in the TRF IP (done by Maiko Tonini) (Fig. 10B), confirming that POLIE interacts with TRF and TIF2. In *POLIE*$^{+myc/+}$ cells, Maiko Tonini also performed ChIP using the myc antibody and observed that POLIE-myc is associated with the telomere chromatin (Fig. 10C). Additionally, our lab member, Marjia Afrin performed the Immunofluorescence (IF) analysis in *POLIE*$^{+myc/+}$ cells to show that POLIE-myc is colocalized with TRF, a component of telomere complex (Li *et al*., 2005),

throughout the cell cycle. These observations confirm that POLIE is an intrinsic component of the telomere complex. I, then, further investigated whether the association of POLIE with the telomere chromatin depends on TRF, which has a duplex telomeric DNA binding activity (Li *et al.*, 2005). ChIP was performed in *POLIE*$^{+myc/+}$ TRF RNAi cells (Table 1) before and after induction of TRF RNAi for 24 hrs, and ChIP products were hybridized with telomere and tubulin probes. TRF was successfully depleted from the telomere chromatin (Fig. 10D). However, POLIE remained at the telomere after TRF depletion (Fig. 10E). Therefore, POLIE is localized to the telomere independent of TRF.

A

IP

kD | Input | IgG | myc Ab
150
75 — POLIE-myc, TIF2-F2H
50
37 — TRF

B

IP

kD | Input | IgG | TRF Ab
150 — POLIE-myc
75 — TIF2-F2H
37 — TRF

C

Enrichment (ChIP/Input, %)

- TTAGGG
- tubulin

0.30
0.25
0.20
0.15
0.10
0.05
0.00

$p = 0.002$ $p = 0.009$

IgG   POLIE-myc   TRF

D

$POLIE^{+myc/+}$

TRF RNAi

kD | 0 | 24 hrs + Dox
50 —
37 — TRF
150 —
100 — POLIE-myc
50 — tubulin

E

TTAGGG

Enrichment (ChIP/Input, %)

- -Dox
- +Dox

3.5
3.0
2.5
2.0
1.5
1.0
0.5
0.0

$p = 0.02$ $p = 0.83$

IgG   TRF   POLIE-myc
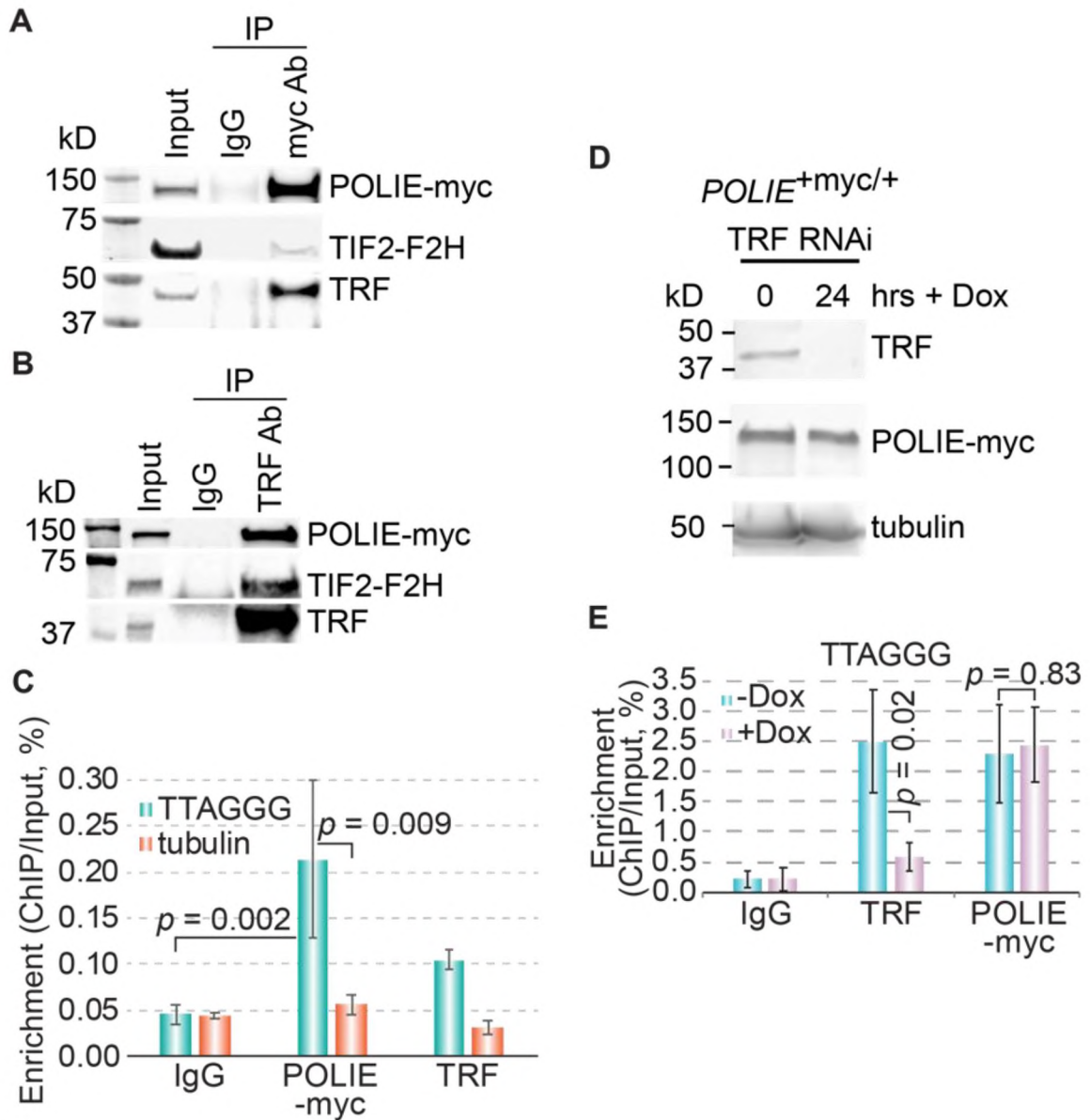
Fig. 10: POLIE is a component of the *T. brucei* telomere complex. IP using the myc antibody 9E10 (MSKCC Antibody & Bioresource Core Facility) **(A)** and a TRF rabbit antibody (Yang *et al.,* 2009) **(B)** or IgG (as a negative control in both) in $POLIE^{+myc/+}$ $TIF2^{+F2H/+}$ cells (done by Maiko Tonini). Western analyses were performed using the myc antibody 9E10, the HA antibody (HA probe, Santa Cruz Biotechnologies), and a TRF chicken antibody (Yang *et al.,* 2009). **(C)** Quantification of ChIP results using the myc antibody 9E10, a TRF rabbit antibody (Yang *et al.,* 2009), and IgG (as a negative control) in $POLIE^{+myc/+}$ cells. Average enrichment (ChIP/Input) was calculated from three to four independent experiments. **(D)** Western blotting showing depletion of TRF in $POLIE^{+myc/+}$ TRF RNAi cells after a 24-hr induction. A TRF rabbit antibody, the myc antibody 9E10, and the tubulin antibody TAT-1 were used. **(E)** Quantification results of POLIE-myc and TRF ChIP in $POLIE^{+myc/+}$ TRF RNAi cells before (-Dox) and after (+Dox) the induction of TRF RNAi. Average enrichment (ChIP/Input) was calculated from three independent

experiments. *P* values of unpaired *t*-tests are shown in (C) and (E). Here, error bars represent standard deviation.

To examine the functions of POLIE, Maiko Tonini introduced the inducible POLIE RNAi construct into the $POLIE^{+myc/+}$ cells to establish the $POLIE^{+myc/+}$ RNAi strain (Table 1). Significant depletion of POLIE-myc (Fig. 11A) was observed upon induction of POLIE RNAi by doxycycline (done by Maiko Tonini) (Rabbani *et al.*, 2022).
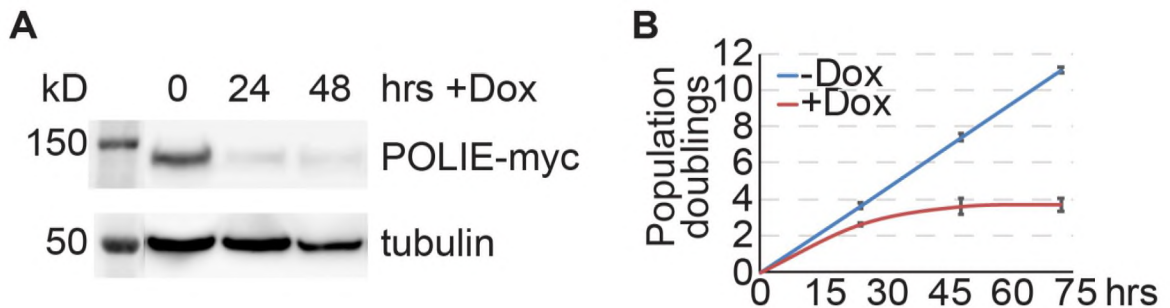
Fig. 11: POLIE is essential for *T. brucei* cell proliferation. (A) Western blotting shows depletion of POLIE-myc in $POLIE^{+myc/+}$ RNAi cells (done by Maiko Tonini). **(B)** Growth curves of $POLIE^{+myc/+}$ RNAi cells without (-Dox) and with (+Dox) the induction of RNAi (done by Maiko Tonini) (Rabbani *et al.*, 2022).

Additionally, Maiko Tonini and I observed significant growth arrest by 24 hrs (Fig. 11B) upon induction of POLIE RNAi by doxycycline, confirming that POLIE is essential for cell proliferation. Overall, we identified POLIE as an intrinsic component of the *T. brucei* telomere complex.

3.2.2 POLIE plays important roles in DNA damage repair

POLIE is an A family DNA polymerase, and its polymerase domain is homologous to the C-terminal DNA polymerase domains of mammalian Polθ and Polν (Leal *et al.*, 2020). Since Polθ and Polν play important roles in DNA damage repair (Wood and Doublié, 2016; Moldovan *et al.*, 2010), I examined whether POLIE is important for DNA damage repair. POLIE-depleted cells were subjected to different DNA damaging agents to

evaluate its role in DNA damage repair. In the POLIE[+myc/+] RNAi cells, RNAi was induced for 12 hrs and irradiated with UV light which causes cyclobutane pyrimidine dimers, or incubated with cisplatin which causes inter-strand crosslinks, and cell growth was monitored (Fig. 12A, B). After UV irradiation, the relative growth (irradiated/un-irradiated) is significantly poorer for POLIE-depleted cells compared to uninduced cells (Fig. 12C). Similarly, cells treated with cisplatin had a poorer relative growth (treated/untreated) in POLIE RNAi-induced cells than in uninduced cells (Fig. 12D).

Fig. 12: POLIE plays important role in DNA damage repair. (A) *POLIE*[+myc/+] RNAi cells incubated with or without doxycycline for 12 hrs were irradiated with and without 50 mJ and 100 mJ UV before cells were washed free of doxycycline. Subsequently, cell growth was monitored. (B) *POLIE*[+myc/+] RNAi cells incubated with or without doxycycline

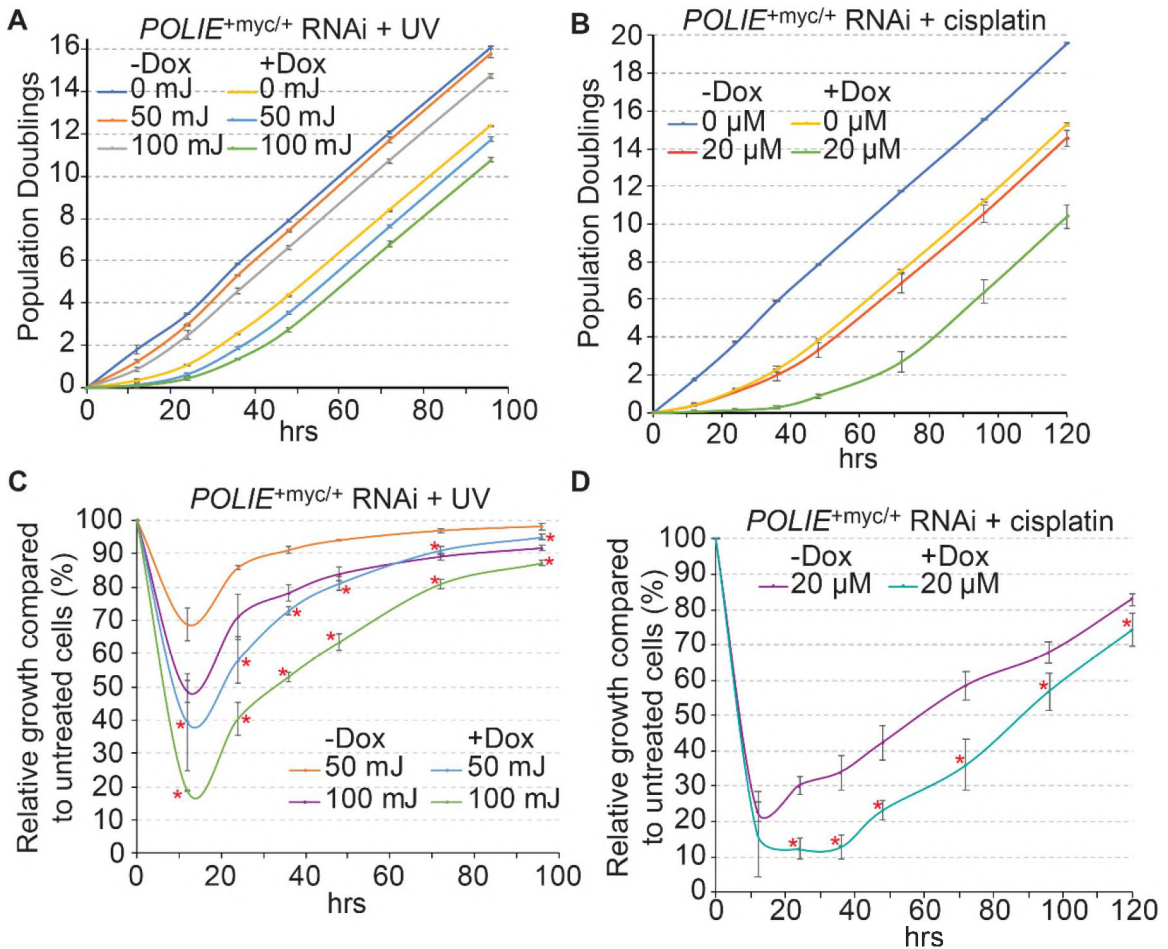for 12 hrs were treated with and without 20 μM cisplatin for 1 hr before cells were washed free of doxycycline and cisplatin. Subsequently, cell growth was monitored. Relative growth (treated/untreated) after UV **(C)** or cisplatin **(D)** was calculated from three independent experiments. Asterisks indicate significant differences between the relative growth of uninduced and induced cells.

Therefore, POLIE appears to play an important role in UV, and cisplatin-induced DNA damage repair in *T. brucei*. In summary, POLIE is an essential protein that is required to maintain telomere integrity.

3.2.3 POLIE suppresses DNA recombination at the subtelomere

DNA double-strand breaks (DSBs) at or near the active *VSG* locus are a potent inducer for VSG switching (Boothroyd *et al.,* 2009; Glover *et al.,* 2013) and DSBs serve as a site for DNA recombination. *T. brucei* has a large *VSG* gene pool with all *VSGs* located in subtelomeric regions (Cross *et al.,* 2014), and VSG is expressed exclusively from subtelomeric expression sites (ESs) in a strictly monoallelic manner (de Lange and Borst, 1982; Cross, 1975). To estimate the VSG switching rate upon POLIE depletion, I introduced the POLIE RNAi construct into a strain that was specifically established for analyzing VSG switching (which we refer to as the S strain) (Kim and Cross, 2010) to create S/IEi (Table 1). Our lab member Marjia performed VSG switching assay in the switching cell line. Because recovering VSG switchers relies on cell proliferation, she only induced POLIE RNAi for 30 hrs followed by removal of doxycycline from the medium by extensive washing.

The S strain has a *puromycin resistance* (*PUR*) gene fused with a *thymidine kinase* (*TK*) gene immediately upstream of the active *VSG* (Fig. 13). Switchers are expected to lose the TK expression and can be selected by *GCV* (Scahill *et al.,* 2008).
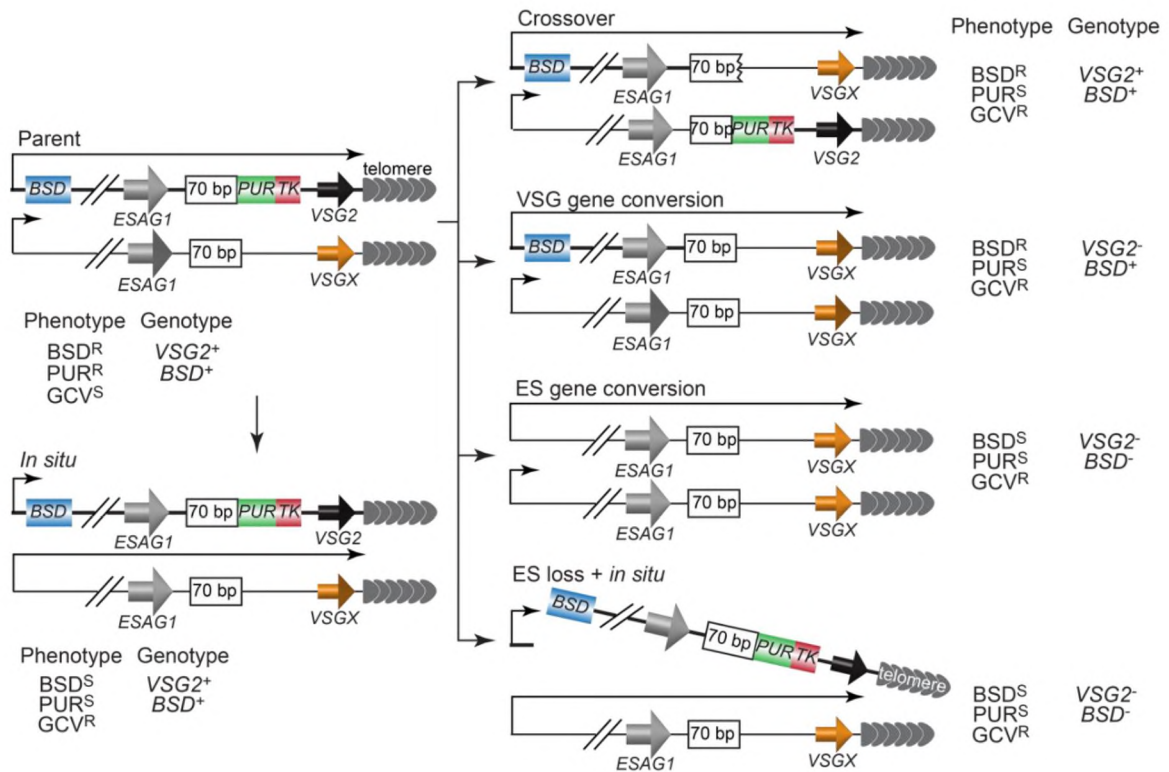
Fig. 13: A schematic diagram of the VSG switching assay. The S strain (parent, top left (Kim and Cross, 2010) contains a *BSD* (*blasticidin resistance*) marker immediately downstream of the active ES promoter (long arrow) and *puromycin resistance* (*PUR*)- *thymidine kinase* (*TK*) fusion gene inserted between the 70 bp repeats and the active *VSG2* gene. Other ESs are silent, and only one silent ES is shown. Loss of TK expression renders *T. brucei* cells resistant to GCV, so VSG switchers can be selected by GCV. In an *in situ* switch, the active ES becomes silenced while a previously silent ES becomes expressed. In crossover events, the active *VSG2* gene and its neighboring DNA sequences change place with a silent *VSG* X (frequently also in an ES). In VSG gene conversion events, a silent *VSG* X is duplicated into the active ES to replace the active *VSG2* gene, which is lost. In ES gene conversion events, a whole silent ES is duplicated to replace the originally active ES, which is lost. In ES loss coupled with an *in situ* switch (ES Loss + *in situ*), the originally active ES is lost and a different ES is expressed. In each scenario, the expected resistant (R) or sensitive (S) phenotypes to 100 µg/ml blasticidin, 2 µg/ml puromycin, 5 µg/ml GCV, and the *VSG2* and *BSD* genotypes (tested by PCR analyses) are listed. +, the gene is present; -, the gene is absent.

I also observed that removal of doxycycline after 30 hrs of induction allowed cells to recover, and these cells were still responsive to doxycycline upon repeated treatment (Fig. 14A). As a control, one endogenous *POLIE* allele was tagged with the C-terminal 13 x myc to establish the *POLIE*[+myc/+] S/IEi strain (Table 1). Western analysis showed depletion of

POLIE-myc upon induction of POLIE RNAi and the recovery of the POLIE-myc protein level after removal of doxycycline (Fig. 14B).
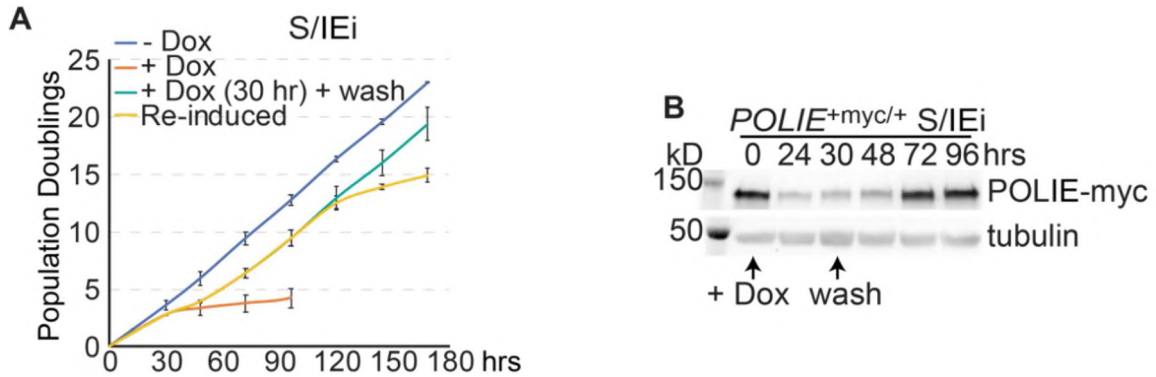
Fig. 14: RNAi-mediated POLIE depletion in switching cell (S/IEi) is reversible. (A) Growth curves of S/IEi cells under several conditions: without induction (-Dox), continued induction (+Dox), a transient induction (+Dox for 30 hrs followed by wash), and re-induction (after a transient 30-hr induction and wash, +Dox at 96 hrs). Average population doublings were calculated from three independent experiments. **(B)** Western blotting showing that inducing POLIE RNAi for 30 hrs resulted in a transient depletion of POLIE-myc in *POLIE*$^{+myc/+}$ S/IEi cells.

Transient depletion of POLIE resulted in an ~3-fold higher VSG switching rate when compared to the S/ev control strain (Fig. 15A), indicating that POLIE suppresses VSG switching. To confirm that this phenotype is specifically due to depletion of POLIE, I established the S/IEi + ecPOLIE-myc strain that carries an ectopic POLIE allele (Table 1). Adding doxycycline induced both POLIE RNAi and the expression of the ectopic POLIE-myc (Fig. 15C). The VSG switching rate in S/IEi + ecPOLIE-myc cells is significantly lower than that in S/IEi cells and similar to that in S/ev cells when all cells were induced by doxycycline for 30 hrs (Fig. 15A), confirming that the more frequent VSG switching phenotype was specifically caused by POLIE depletion. We also determined the VSG switching pathways in all obtained switchers (Fig. 15B; 13). In the S/ev control cells, a small fraction of the switchers arose from *in situ* switch (5%) and crossover (10%), while

VSG gene conversion (43%) and ES gene conversion/ES loss + *in situ* events (42%) were more popular (Fig. 15C; 13). In contrast, in cells depleted of POLIE, *in situ* switcher and crossover events were absent, a small fraction of switchers arose from ES gene conversion/ES loss + *in situ* events (12%), while *VSG* gene conversion became the predominant switching event (88%) (Fig. 15C; 13). Therefore, POLIE suppresses VSG gene conversion to maintain telomere integrity.
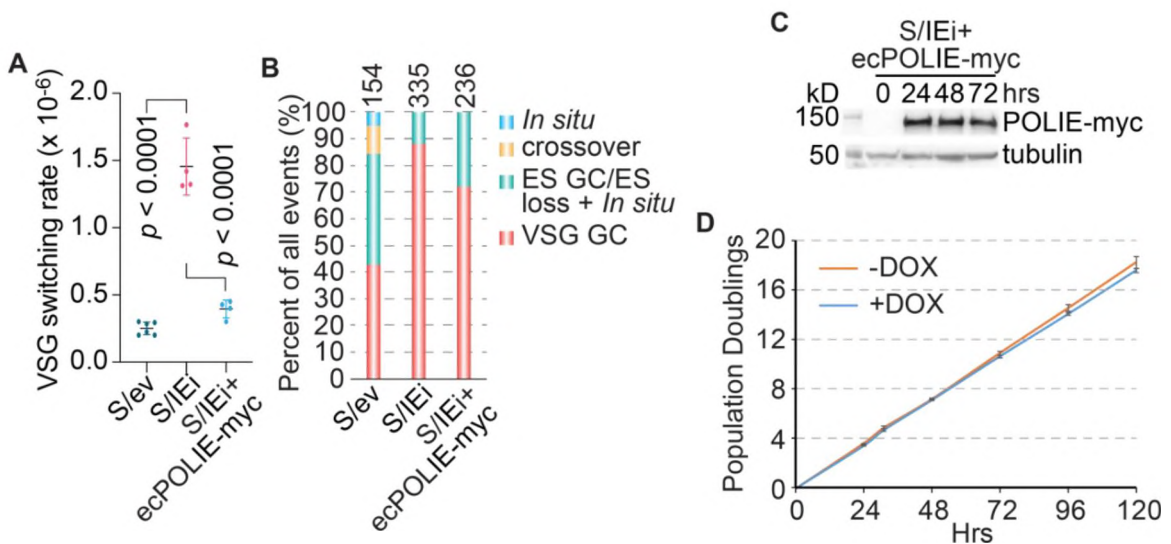
Fig. 15: POLIE suppresses VSG switching. (A) VSG switching rates in the indicated strains (done by Marjia Afrin). **(B)** Percent of various VSG switching mechanisms in the indicated strains. The total number of switchers characterized in each strain is listed on top of each column (done by Marjia Afrin) (Rabbani *et al.,* 2022). **(C)** Western blotting showed that induced ectopic POLIE-myc expression in S/IEi+ecPOLIE-myc cells. **(D)** Growth curves of S/IEi+ecPOLIE-myc cells in the presence (+) or the absence (-) of doxycycline (DOX). Average population doublings were calculated from three independent experiments. *P*-values of unpaired *t*-tests are shown in (A).

These experiments suggest that POLIE suppresses DNA recombination at the subtelomere.

3.2.4 POLIE suppresses DNA recombination at the telomere

I speculated that, in addition to suppressing subtelomere DNA recombination, POLIE may also suppress telomere recombination. Intratelomeric homologous recombination (HR), such as excision of the T-loop structure, can result in extrachromosomal telomeric circles (T-circles) (Tomaska *et al.,* 2009). I performed 2D gel electrophoresis to separate circular from linear DNA molecules followed by southern hybridization with a telomere probe (Fig. 16A).

Fig. 16: Depletion of POLIE leads to an increased amount of T-circles. (A) 2D gel electrophoresis of AluI/MboI digested genomic DNA isolated from *POLIE*$^{+myc/+}$ RNAi cells before (-Dox) and after (+Dox) 24-hr of RNAi induction. Red arrowheads indicate the circular telomere DNA. **(B)** A diagram showing expected migration patterns of linear and circular DNAs in 2D electrophoresis (139). **(C)** Quantification of southern results after 2D electrophoresis. The average T-circle amount (percent of total telomeric DNA) was calculated from six independent experiments.

In uninduced POLIE RNAi cells, there is only a faint signal representing the

telomere sequence-containing circular DNA (Fig. 16, A, B). After depletion of POLIE, the T-circle signal was much stronger (Fig. 16, A, C), suggesting that POLIE suppresses telomere recombination.

3.2.5 Recombination at telomere and subtelomere is not mediated by increased TERRA

The active VSG-adjacent telomere is transcribed by RNA polymerase I into telomeric repeat-containing RNA (TERRA) in *T. brucei* (Nanavaty *et al.,* 2017; Saha *et al.,* 2021). TERRA has a propensity to form the telomeric R loop (TRL) (Toubiana and Selig, 2018), and our lab has shown that an excessive amount of TRL induces more frequent telomere/subtelomere recombination (Nanavaty *et al.*; 2017, Saha *et al.,* 2021). Since POLIE depletion induced a mild VSG derepression (Fig. 15), I tested the hypothesis that increases in recombination at the telomere and subtelomere in POLIE depleted cells caused by an increase in TERRA level.
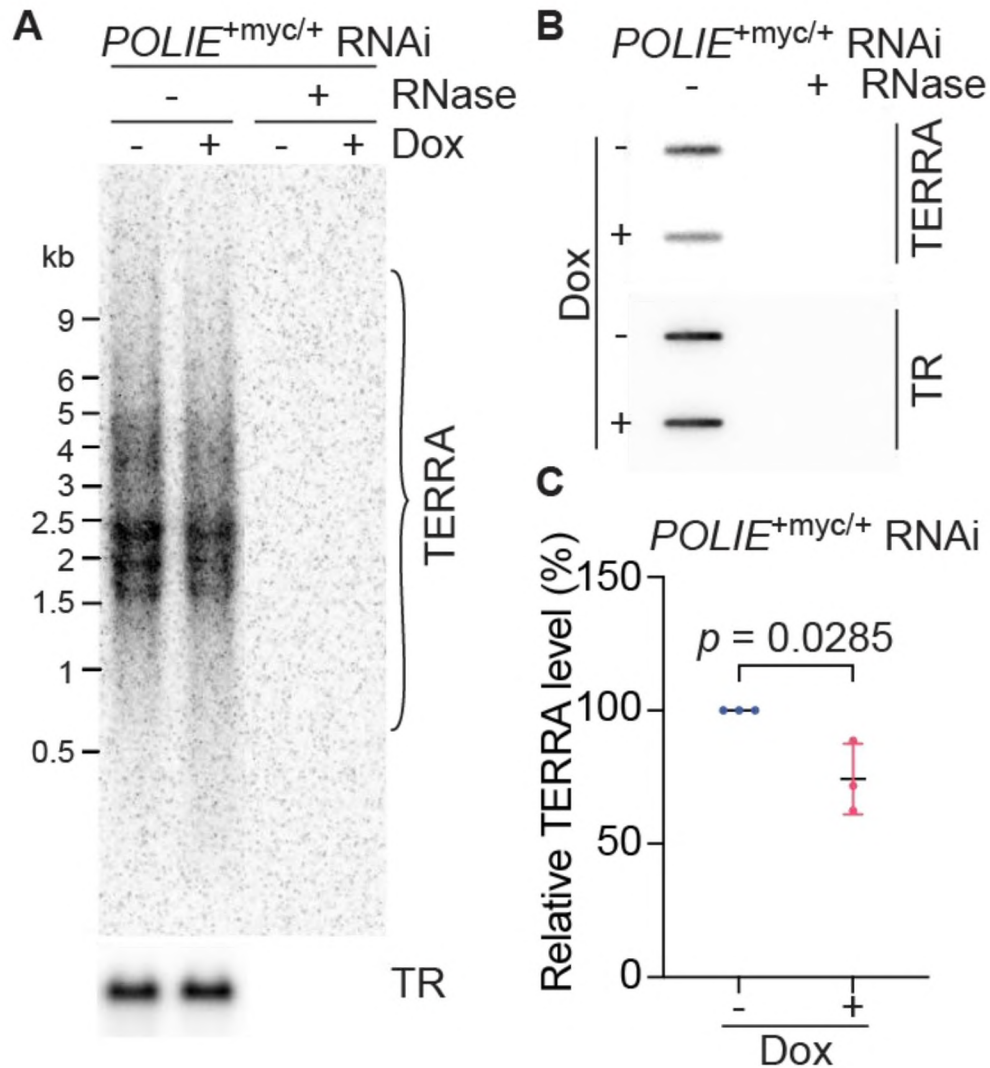
Fig. 17: TERRA may not contribute to an increase in recombination at the telomere and subtelomere. (A) Northern hybridization detecting TERRA in *POLIE*[+myc/+] RNAi cells before (-Dox) and after (+Dox) the RNAi induction. The rRNA precursors are very abundant and shown as non-specific bands (three bands between 1.6 and 2.5 kb) overlapping with the TERRA species. The telomerase RNA component, TR, was detected as a loading control. **(B)** A representative slot blot detecting TERRA in *POLIE*[+myc/+] RNAi cells. TR was detected as a loading control. **(C)** Quantification of relative TERRA levels in *POLIE*[+myc/+] RNAi cells (normalized against the TR level). The Average was calculated from three independent experiments. P values of unpaired t-tests are shown in (C).

To our surprise, I detected a lower level of TERRA after POLIE depletion in both

northern (Fig. 17A) and slot blot hybridizations (Fig. 17B, C). Therefore, it is unlikely that

the increased level of telomere and subtelomere recombination is caused by an increased

TRL level in POLIE-depleted cells.

3.2.6 POLIE is essential to coordinate telomere G- and C-strand syntheses

The single-stranded telomere 3' overhangs can invade a homologous sequence and induce HR (Haber, 2018). Therefore, I tested whether depletion of POLIE affected the telomere 3' overhang structure. Using the native in-gel hybridization analysis, I detected a very faint telomere 3' overhang signal in WT cells (Fig. 18A), confirming our previous observations (Sandhu and Li, 2011; Sandhu and Li, 2017).
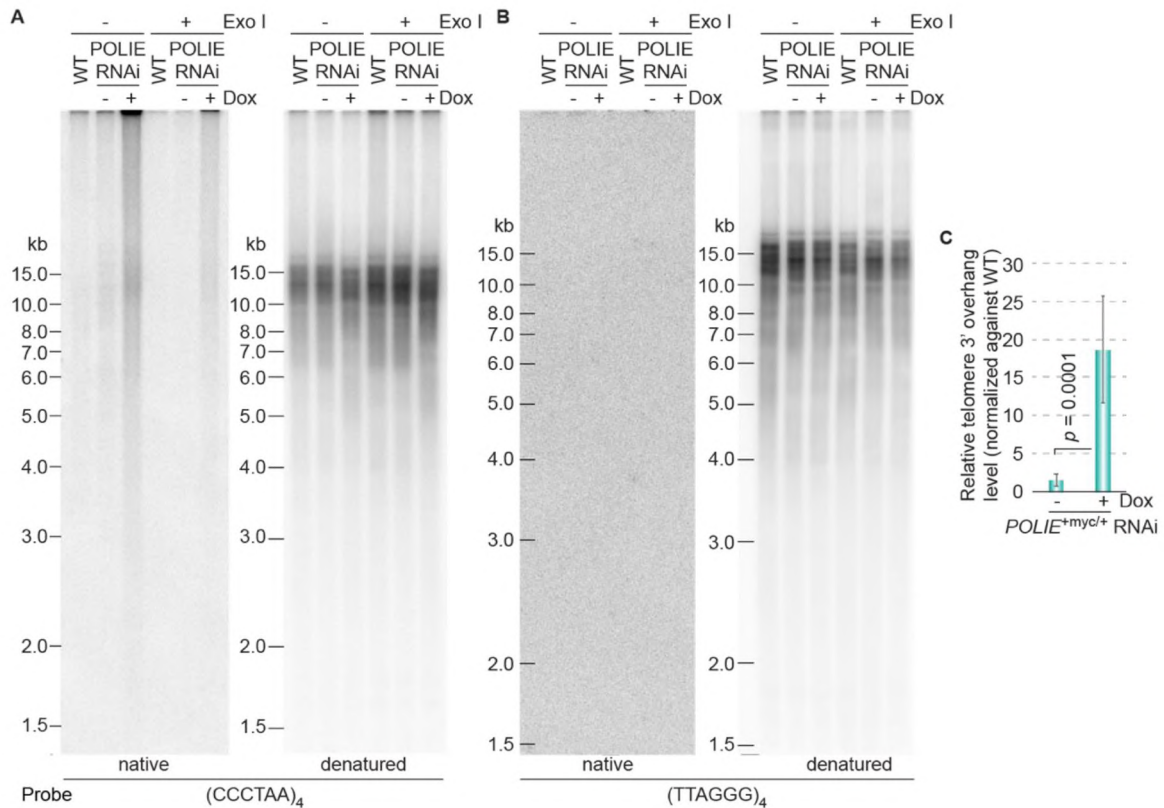
Fig. 18: POLIE depletion results in similar telomere length but more ssDNA hybridization. Genomic DNAs were isolated from WT and *POLIE*[+myc/+] RNAi (labeled as POLIE RNAi) cells **(A & B)** before (-Dox) and after (+Dox) a 24-hr induction of RNAi. The genomic DNA was treated with and without ExoI (NEB), which is a 3' to 5' single-strand DNA-specific exonuclease and digested with AluI and MboI. In-gel hybridization was performed using a (CCCTAA)4 or a (TTAGGG)4 probe first under the native condition, and then after denaturation and neutralization. **(C)** Quantification of the relative telomere 3' overhang level (using that in WT cells as a reference) in *POLIE*[+myc/+] RNAi cells before (-Dox) and after (+Dox) POLIE RNAi induction. The average telomere 3' overhang level was calculated from three to five independent experiments. P values of unpaired t-tests are shown in (C).

Depletion of POLIE led to an ~19-fold more intense telomere 3' overhang signal (Fig. 18 A, C), which was sensitive to Exo I, a 3' to 5' ssDNA specific exonuclease (Fig. 18A), indicating that the signal was detected indeed from the telomere 3' overhang. In addition, only the (CCCTAA)4 probe detected overhang signals (Fig. 18A), while the (TTAGGG)4 probe did not (Fig. 18B), confirming that the *T. brucei* telomere overhang has a G-rich sequence (Sandhu and Li, 2011; Sandhu and Li, 2017). This experiment

suggests that POLIE is necessary for C-strand synthesis, depletion of which leads to shorter C-strand which results in elongated G- overhang. This observation also suggests that POLIE helps to coordinate telomere G- and C-strand syntheses.

I also performed Pulsed- Field Gel Electrophoresis (PFGE) to separate intact *T. brucei* chromosomes and performed the same native in-gel hybridization. Only G-rich telomere overhang signals were detected, and POLIE depletion again increased the intensity of the telomere 3' overhang signal significantly (Fig. 19).
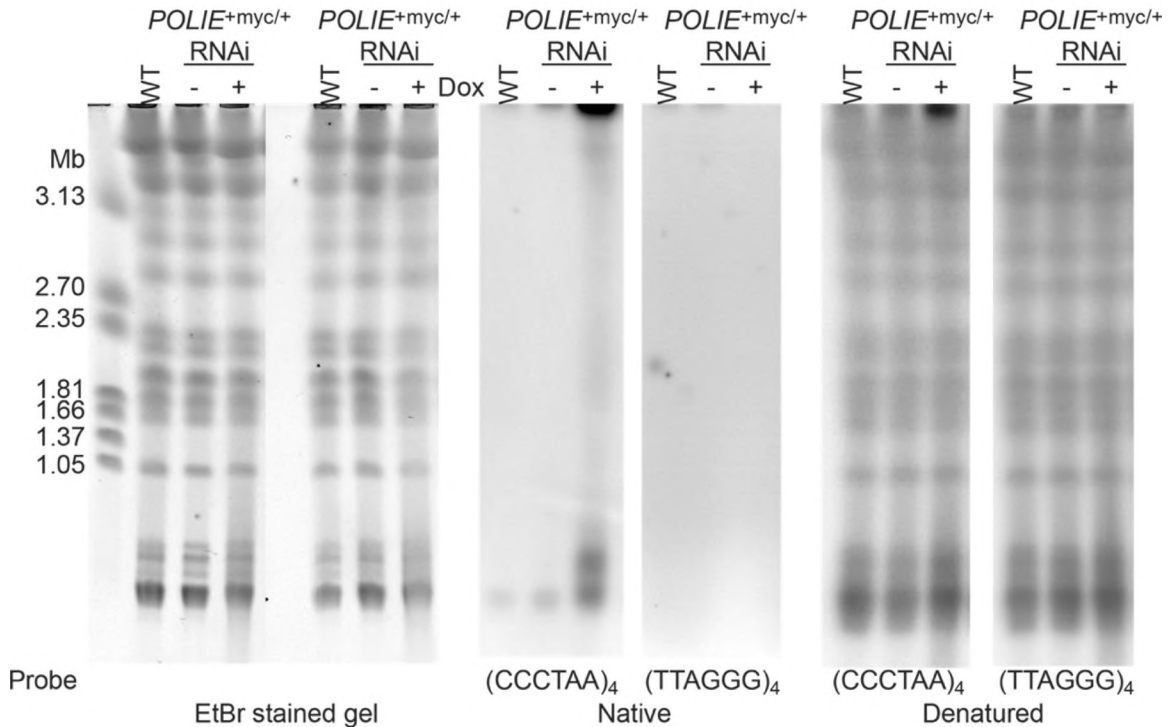
Fig. 19: Native in-gel hybridization analysis to examine the telomere 3' overhang structure. DNA plugs were prepared from *POLIE*$^{+myc/+}$ RNAi cells (A) before (-) and after (+) the RNAi induction. Undigested chromosomes were separated by Pulsed- Field Gel Electrophoresis. After electrophoresis, the gel was dried at room temperature followed by hybridization with end-labeled (CCCTAA)$_4$ or (TTAGGG)$_4$ probes under the native condition. After exposing the gel to a phosphorimager, the gel was denatured, neutralized, and again hybridized with the same (CCCTAA)$_4$ and (TTAGGG)$_4$ probes, respectively. The EtBr-stained gel is shown on the left. The native in-gel hybridization result is shown in the middle. The hybridization result after the denaturation is shown on the right.

Furthermore, the EtBr-stained gel and the post-denaturation hybridization showed more smeary DNA species in POLIE-depleted cells than in WT and uninduced POLIE RNAi cells (Fig. 19, left and right), further indicating that depletion of POLIE led to an increased amount of telomere DNA degradation. These observations suggest that POLIE normally suppresses the telomere recombination by limiting the length of the telomere 3' overhang. As a control, I have also examined the telomere 3' overhang structure in *POLIE*$^{+myc/-}$ and S/IEi + ecPOLIE-myc cells. As shown in Fig. 20, the telomere 3' overhang level in *POLIE*$^{+myc/-}$ and S/IEi + ecPOLIE-myc cells is comparable to that in WT cells, indicating that POLIE-myc retains POLIE's key telomere function and that ectopic POLIE-myc can complement phenotypes in POLIE-depleted cells.
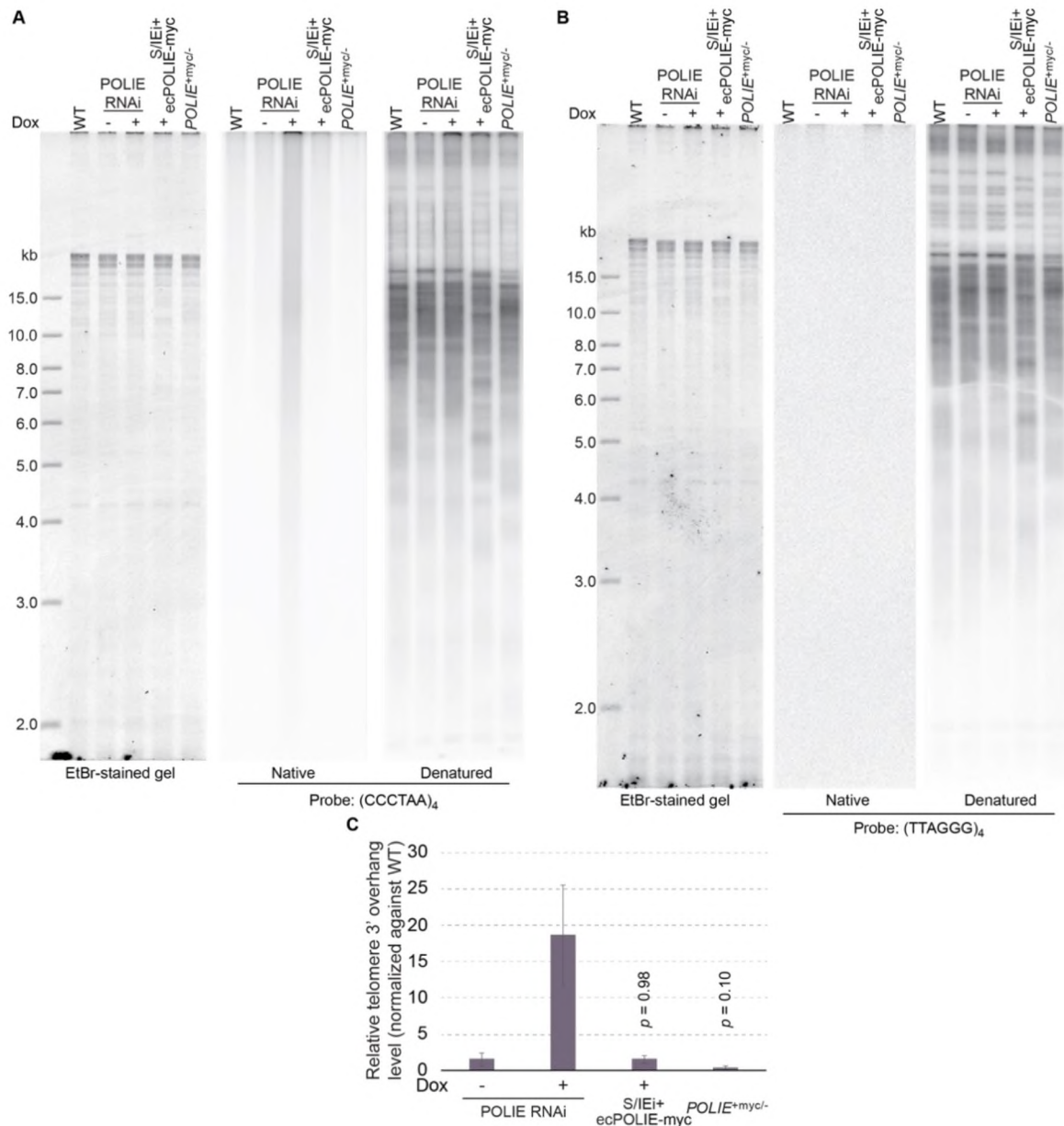
Fig. 20: Telomere 3' overhang length in $POLIE^{+myc/-}$ and S/IEi+ecPOLIE-myc cells is similar to WT length. (A) & (B) Native in-gel hybridization assays were performed for $POLIE^{+myc/+}$ RNAi cells before and after induction (+ Dox for 24 hrs, used as a control), $POLIE^{+myc/-}$, and S/IEi+ecPOLIE-myc cells the same way as described in Fig. 18. Telomeres on various chromosome ends have different sizes, and different trypanosome clones always have different telomere fragment hybridization patterns, as seen in the post-denaturation hybridization results. In-gel hybridization was performed using a $(CCCTAA)_4$ (A) or a $(TTAGGG)_4$ (B) probe. **(C)** The relative level of the telomere 3' overhang was quantified as described in Fig. 18. The average telomere 3' overhang levels in $POLIE^{+myc/-}$ and S/IEi+ecPOLIE-myc cells were calculated from three independent experiments. The result for $POLIE^{+myc/+}$ RNAi cells (labeled as POLIE RNAi) is the same as shown in Fig. 18C. P values for unpaired student t-tests are shown (compare to the unindexed POLIE RNAi sample).

The telomerase-mediated telomere G-strand synthesis is expected to elongate the telomere 3' overhang length (Bonetti *et al.,* 2014). In addition, we previously found that the telomere 3' overhang is lost in telomerase null *T. brucei* cells (Sandhu and Li, 2017). To examine whether the elongated telomere 3' overhang in POLIE-depleted cells depends on telomerase, I tested the telomere 3' overhang signal in the TR -/- POLIE RNAi strain (Table 1). Although the telomere 3' overhang signal in uninduced TR -/- POLIE RNAi cells was essentially undetectable (Fig. 21A, left), an ~17-fold higher level of the telomere 3' overhang signal was observed upon depletion of POLIE (Fig. 21A, B). The appearance of telomerase-independent long overhang in cells lacking POLIE was surprising and is likely to be contributed by either higher 5' to 3' exonuclease mediated resection of the telomere 5' end or decreased telomere C-strand fill-in synthesis (Bonetti *et al.,* 2014). In mammals, Apollo, a 5' to 3' exonuclease is involved in telomere end processing; however, the functional assessment of such exonuclease is not studied yet in *T. brucei.* On the contrary, a defective telomere C-strand fill-in synthesis is plausible since, in telomerase null cells, depletion of POLIE still increases the telomere 3 overhang length to a similar extent as that in the TR+/+ background.
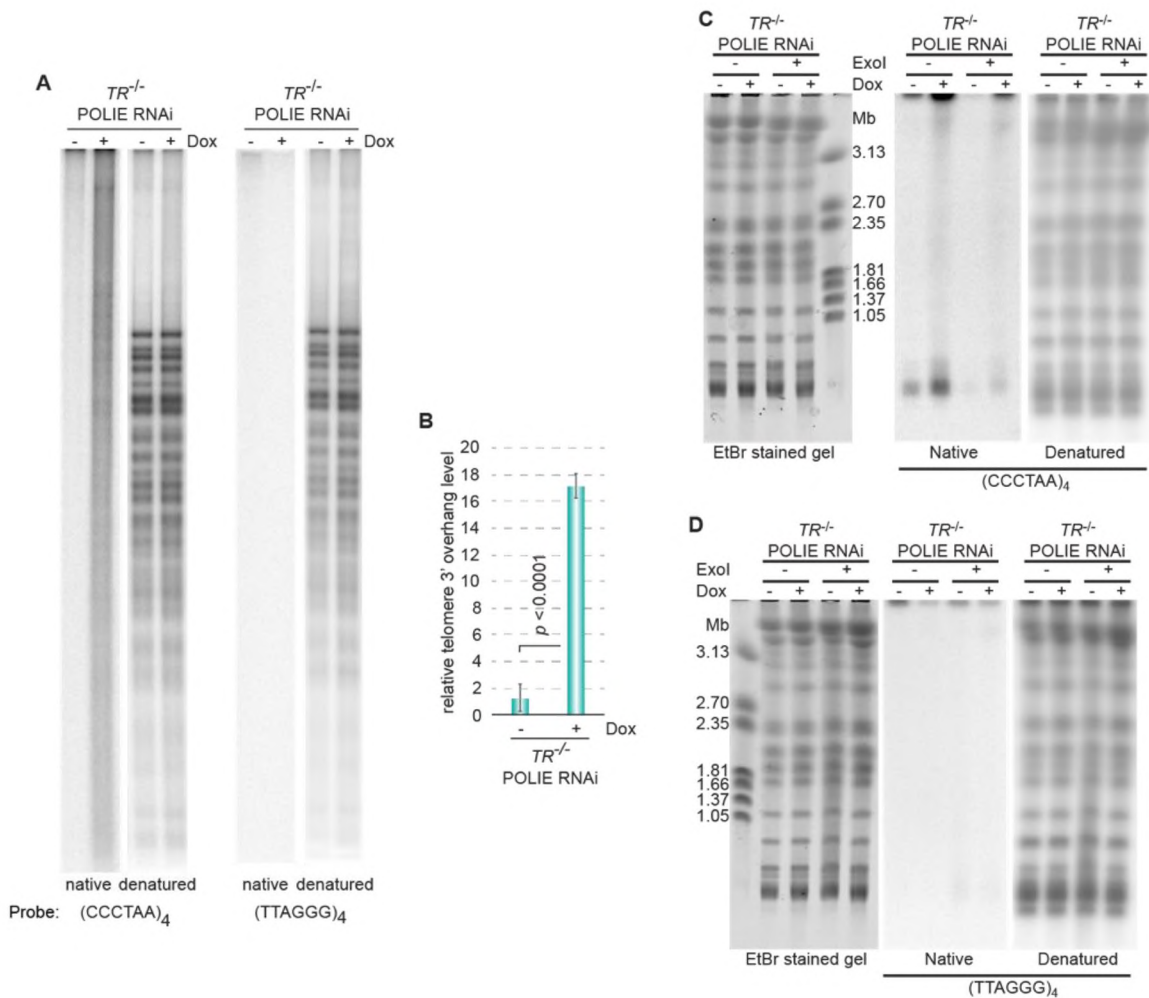
Fig. 21: Elongated telomere 3' overhang in POLIE-depleted cells is not dependent on the telomerase activity. (A) Genomic DNAs were isolated from WT and *TR*⁻/⁻ POLIE RNAi cells before (-Dox) and after (+Dox) a 24-hr induction of RNAi. The genomic DNA was treated with and without ExoI (NEB), which is a 3' to 5' single-strand DNA-specific exonuclease and digested with AluI and MboI. In-gel hybridization was performed using a (CCCTAA)₄ or a (TTAGGG)₄ probe first under the native condition, and then after denaturation and neutralization. The telomere 3' overhang level is reflected by the hybridization intensity throughout the whole lane (excluding the signal in the well) but not by the sizes of the telomere fragments. **(B)** Quantification of the relative telomere 3' overhang level (using the hybridization signal after the denaturation/neutralization as a loading control and using the telomere 3' overhang level in WT cells as a reference) in *TR*⁻/⁻ POLIE RNAi cells before (-Dox) and after (+Dox) POLIE RNAi induction. The average telomere 3' overhang level was calculated from three to six independent experiments. **(C & D)** Native in-gel hybridization analysis to examine the telomere 3' overhang structure. DNA plugs were prepared from *TR*⁻/⁻ POLIE RNAi cells before (-) and after (+) the RNAi induction. Undigested chromosomes were separated by PFGE. After electrophoresis, the gel was dried at room temperature followed by hybridization with end-labeled (CCCTAA)₄ (C) or (TTAGGG)₄ probes (D) under the native condition. After exposing the gel to a

67

phosphorimager, the gel was denatured, neutralized, and again hybridized with the same (CCCTAA)$_4$ and (TTAGGG)$_4$ probes, respectively. The EtBr-stained gel is shown on the left. The native in-gel hybridization result is shown in the middle. The hybridization result after the denaturation is shown on the right. P values of unpaired t-tests are shown in (B).

Similarly, PFGE of intact chromosomes followed by native in-gel hybridization showed the same elongated telomere 3' overhang phenotype upon POLIE depletion in the TR -/- background (Fig. 21, C, D). As expected, no (TTAGGG)4 hybridization signal was detected in the TR -/- background, either (Fig. 21, A, right; D, middle). Therefore, the elongated telomere 3' overhang phenotype in POLIE-depleted cells is not dependent on the telomerase activity.

3.2.7 POLIE inhibits telomerase-dependent telomere G-strand extension

Telomerase contains a protein catalytic subunit with a reverse transcriptase activity, TERT, and a template-harboring RNA subunit, TR (Greider and Blackburn, 1987; Greider and Blackburn, 1989). Telomerase uses a G-rich single-stranded 3' DNA end as its substrate (Blackburn and Collins, 2011; Schmidt and Cech, 2015). Hence, the telomere 3' overhang is essential for telomerase-mediated telomere extension (Bonetti *et al.*, 2014). WT *T. brucei* cells have very short telomere 3' overhangs (Sandhu and Li, 2011; Sandhu and Li, 2017), suggesting that the telomere G and C-strand synthesis need to be well-coordinated. To investigate how telomere 3' overhangs were elongated in POLIE-depleted cells, I examined the telomere DNA synthesis.

Labeling cells with BrdU for one cell cycle followed by CsCl gradient centrifugation should be able to separate the leading and lagging telomere DNA synthesis products because one telomere strand has two Ts per TTAGGG repeat and the other strand one T per CCCTAA repeat (Chai *et al.*, 2006). However, BrdU incorporation in *T. brucei* is frequently at very low efficiency (da Silva *et al.*, 2017) and appears to be toxic at a high

level (Reynolds *et al.,* 2014). In addition, although *T. brucei* cells can be arrested at the S phase by hydroxyurea (HU), they are poorly synchronized after HU release, possibly due to the atypical cell cycle control in these cells (McKean, 2003).

Therefore, I used EdU-labeling to examine the telomere DNA synthesis in asynchronous cells, and most of the incorporated EdU signal is expected to result from DNA replication in the S phase. POLIE depletion leads to cell growth arrest 24 hrs after induction, which interferes with the EdU incorporation. Hence, *POLIE*$^{+myc/+}$ RNAi cells were only induced for 12 hrs before the cells were labeled with EdU for 3 hrs. EdU-labeled DNA was conjugated to desthiobiotin by the CLICK chemistry, pulled down by streptavidin beads, and detected by hybridization with telomere and tubulin probes. Because the two telomere strands contain either G or C but not both, I used radioactive dCTP-labeled (CCCTAA)n and radioactive dGTP-labeled (TTAGGG)n probes to specifically detect the G- and C-strand telomere DNA, respectively. Depletion of POLIE did not affect tubulin DNA synthesis (Fig. 22 A, B, C). Interestingly, POLIE depletion resulted in a mild and significant increase in the telomere G strand DNA synthesis (Fig. 22 A, B). POLIE depletion appeared to also decrease the telomere C-strand synthesis (Fig. 22 A, B, C), but the decrease was significant when the experiment was performed in denatured condition with 4M Urea to separate both strands during pull-down and to reduce the background associated with an opposite strand when hybridized with a probe against a specific strand of the telomere (Fig. 22C). A decrease in C-strand synthesis suggests the role of POLIE in C-strand fill-in.
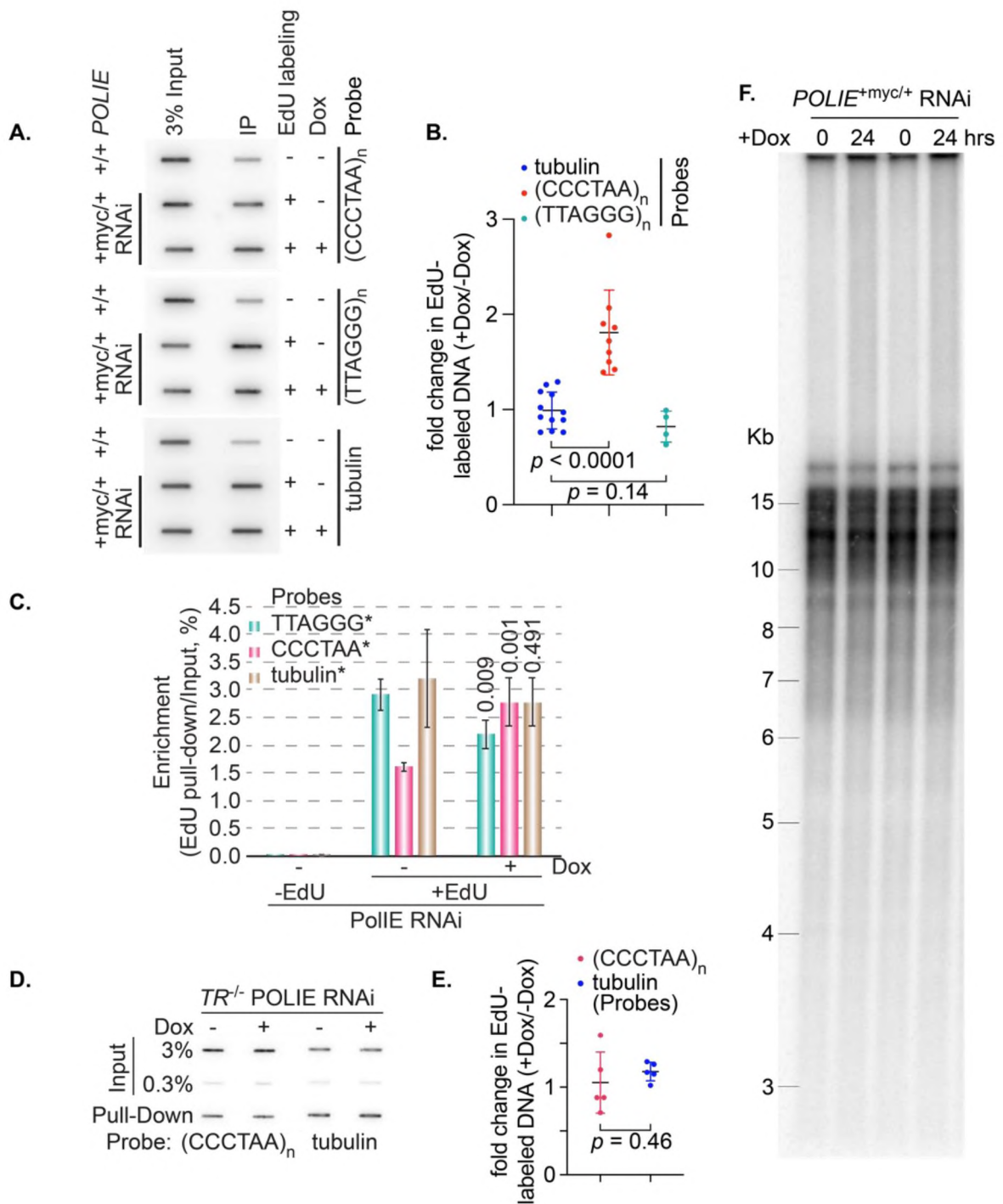
Fig. 22: POLIE depletion increases the telomerase-mediated telomere G-strand synthesis. In *POLIE*[+myc/+] RNAi cells, before (-Dox) and after 12-hr (+Dox) of POLIE RNAi induction, EdU-labeled nascent DNA was conjugated with desthiobiotin in native **(A, B)** or denatured condition (C) and pulled-down by streptavidin beads. In TR^{-/-} POLIE RNAi **(D)** cells, before (-Dox) and after 12-hr (+Dox) of POLIE RNAi induction, EdU-labeled nascent DNA was conjugated with desthiobiotin in native condition and pulled down by streptavidin beads. The pulled-down DNA was slot blotted in the Hybond nylon

membrane and hybridized using a telomere or a tubulin probe. The fold changes in the amount of EdU-labeled telomeric and tubulin DNA (+Doc/-Dox) were quantified and shown in **(B, C) & (E)**, respectively. The average change was calculated from four to twelve independent experiments. **(F)** Depletion of POLIE did not affect the bulk telomere length within a short time frame. Genomic DNA isolated from $POLIE^{+myc/+}$ RNAi cells before (0 hr) and after (24 hr) POLIE RNAi induction were digested with AluI and MboI and separated by agarose gel electrophoresis. Southern blotting was performed using a telomere probe. P values of unpaired t-tests are shown in B, C, and E.

Telomerase can synthesize the telomere G-strand DNA de novo. To examine whether the increased level of telomere G-strand synthesis in POLIE-depleted cells is telomerase-dependent, I performed the EdU-labeling in TR-/- POLIE RNAi cells. I found that POLIE depletion no longer increased the telomere G-strand synthesis in the TR null background (Fig. 22D, E), indicating that the higher level of the telomere G-strand synthesis was due to excessive telomerase-mediated telomere G-strand extension in POLIE-depleted cells. Therefore, POLIE is the first telomere protein in *T. brucei* that has been identified to suppress telomerase.

Additionally, I further performed telomere southern analysis in POLIE$^{+myc/+}$ RNAi cells to see whether depletion of POLIE for 24 hrs affects telomere length due to a higher level of the telomere G-strand synthesis. However, within 24 hrs of POLIE RNAi induction, no significant telomere length change was observed (Fig. 22F).

3.2.8 POLIE promotes the telomere C-strand synthesis

POLIE depletion may affect the telomere C-strand fill-in, as EdU-labeling experiment in denatured condition shows a significant decrease the telomere C-strand synthesis (Fig. 22C). Therefore, I examined whether POLIE depletion affected the telomeric C-circle level, as defects in telomere C-strand replication can lead to an increased amount of telomeric C-circles (Fig. 23A) (Zhang *et al.,* 2019). I performed the φ29 DNA

polymerase-mediated telomeric C-circle assay (Fig. 23B), which does not amplify T-circles because both strands of T-circles have nicks (Henson *et al.,* 2009).
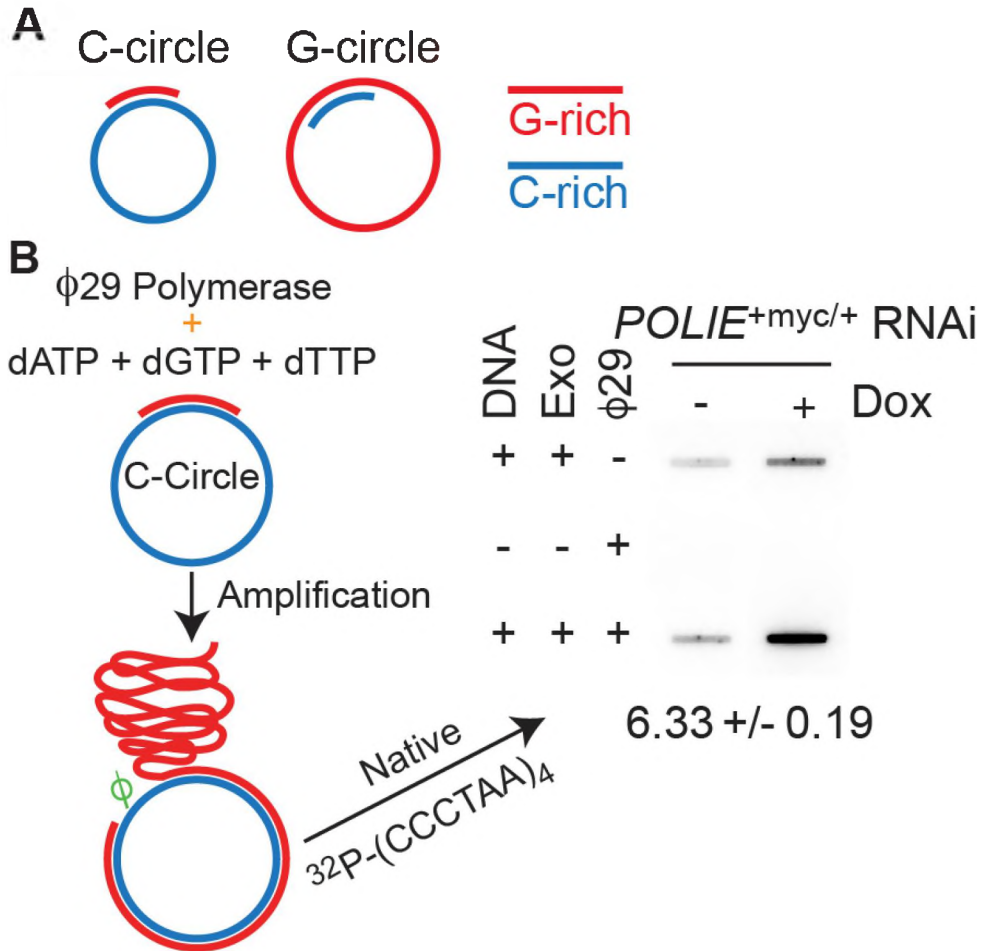
Fig. 23: Principle of the C-circle amplification assay. (A) Diagrams of telomeric C and G-circles. **(B)** Left, is a schematic diagram showing the principle of the C-circle amplification assay. Right, depletion of POLIE leads to an increased amount of telomeric C-circles. The C-circle amplification products were analyzed by slot blot hybridization using a $(CCCTAA)_4$ probe. The average fold difference in C-circle amount (+Dox/-Dox) (+/- standard deviation) is calculated from three independent experiments and shown beneath the slot blot.

I found that POLIE depletion led to a 6.7-fold increase in the amount of telomeric C-circles but did not affect the telomeric G-circle level (Fig. 24). Telomeric C-circles are a hallmark of telomerase-negative cancer ALT cells (Henson *et al.,* 2009). Therefore, I

examined whether deleting the telomerase further increased the telomeric C circle level in

POLIE-depleted cells.
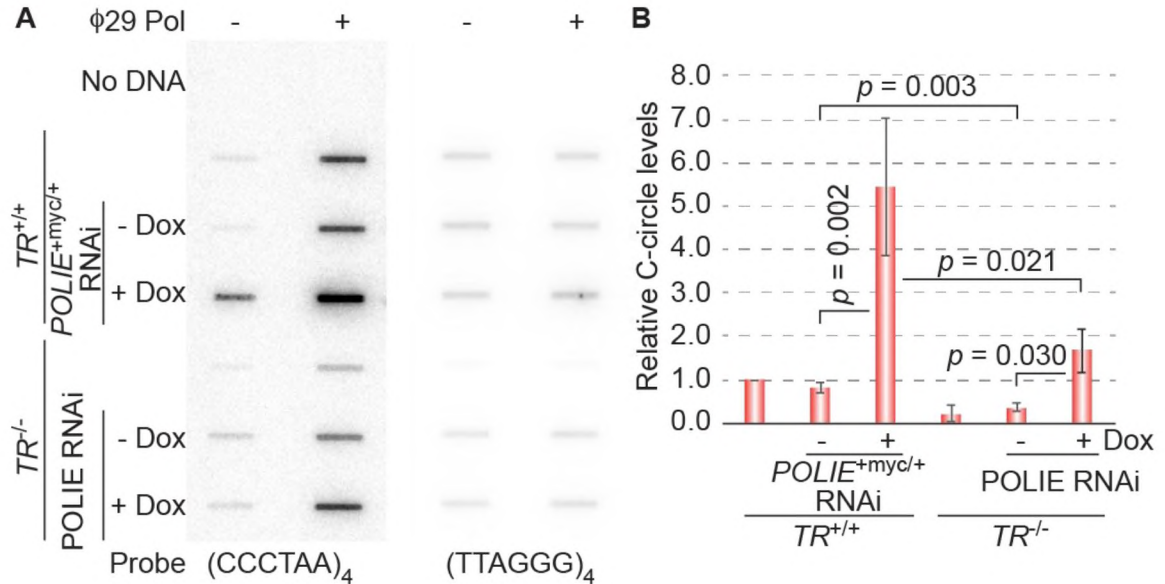
Fig. 24: POLIE depletion increases the amount of telomeric C-circles, which is telomerase-independent. (A) The C-circle and G-circle products from indicated cells were detected in slot blot hybridization using a $(CCCTAA)_4$ and a $(TTAGGG)_4$ probe, respectively. **(B)** Quantification of the telomeric C-circle amount in the C-circle assay. The C-circle level in WT cells was arbitrarily set to 1, and relative C-circle levels in other cells were quantified using the WT level as a reference. The average C-circle signal level was calculated from three to four independent experiments. *P* values of unpaired *t*-tests are shown.

Unexpectedly, TR-/- cells had a lower level of telomeric C circles than WT cells

(Fig. 24A, B), and uninduced TR -/- POLIE RNAi cells also had a lower level of telomeric

C-circles than uninduced POLIE RNAi cells (Fig. 24B). Therefore, deleting telomerase is

not sufficient to make *T. brucei* more ALT-like. Importantly, depletion of POLIE induced

a 4.8- fold increase in the telomeric C-circle level in the TR-/- background (Fig. 24A, B),

indicating that the POLIE depletion-induced increase in the telomeric C-circle level is

telomerase-independent.

3.3 Discussion

While many telomere chromatin components have been identified in *T. brucei* (Li *et al.*, 2005; Yang *et al.*, 2009; Jehi *et al.*, 2014b; Rabbani *et al.*, 2022), we still have not identified any OB-fold containing telomere-specific proteins, suggesting that *T. brucei* telomere complex has quite different protein components than those in higher eukaryotes and telomere end processes are poorly understood in this organism. In mammals, yeasts, and plants, OB-fold containing telomere ssDNA binding proteins play critical roles in the coordination of the telomere G- and C- strand syntheses. *T. brucei* appear to lack these OB-fold containing telomere-specific ssDNA binding factors, suggesting that *T. brucei* uses a different mechanism to coordinate DNA syntheses of the two telomere strands and to regulate telomerase action at the telomere end. Indeed, our observations strongly suggest that POLIE is a novel telomere protein that suppresses telomerase-mediated telomere G-strand elongation and helps ensure proper telomere C-strand synthesis.

POLIE depletion increased the VSG switching rate and the amount of T-circles, indicating that POLIE suppresses DNA recombination at the telomere and subtelomere. POLIE-depleted cells have much longer telomere 3' overhangs than WT cells, which likely contributes to the increased level of telomere recombination, as the long single-stranded 3' overhang is prone to invade duplex DNA with a homologous sequence (Haber, 2018). The telomere 3' overhang length depends on several factors (Fig. 25), including the exonuclease-mediated resection of the telomere 5' end, the telomerase-mediated telomere G-strand extension, and the telomere C strand fill-in (Bonetti *et al.*, 2014).
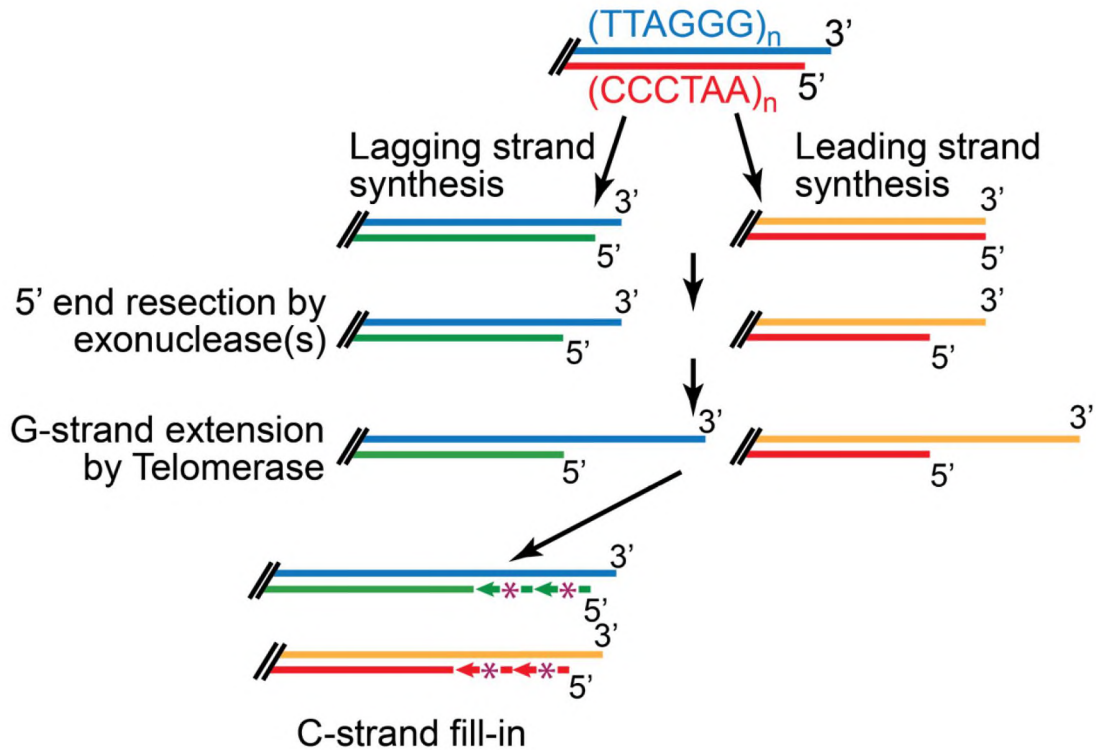
Fig. 25: Telomere end processing involve progression through several steps. Multiple processes are involved in the generation of a proper telomere 3' overhang structure. The exonuclease that process the telomere 5' end has not been identified in *T. brucei*.

Our results suggest that POLIE maintains a normal length of telomere 3' overhang at least two steps (Fig. 25): EdU-labeling showed that POLIE-depleted cells have a significantly elevated level of telomere G-strand synthesis, which is telomerase-dependent, indicating that POLIE suppresses telomerase-mediated telomere G-strand extension. Considering that *T. brucei* telomeres are ~15 kb on average (Fig. 22E) and the conventional DNA replication in the S phase contributes to the EdU-labeling signal considerably, even a mild increase in the telomere G-strand synthesis reflects a dramatically enhanced telomerase action at the telomere.

POLIE is also likely required for telomere C-strand fill-in, which is supported by several observations (Fig. 26). First, in telomerase null cells, depletion of POLIE still

increases the telomere 3' overhang length to a similar extent as that in the TR+/+ background (Fig. 21B), suggesting that in addition to suppressing telomerase, POLIE also promotes the telomere C-strand fill-in. Second, I observed a mild but significant decrease in telomere C-strand DNA synthesis upon POLIE depletion using the EdU-labeling assay (Fig. 22C). This a mild decrease could be because the EdU-labeling technique is not sensitive enough as asynchronous *T. brucei* cells were used. In addition, telomeres in the *T. brucei* cells used in this study are ~15 kb long (Fig. 22E). Hence, the telomere C-strand fill-in is expected to have a limited contribution to the EdU incorporation. Third, POLIE depletion dramatically increases the telomeric C-circle level in a telomerase-independent manner, while telomeric C-circles can arise from telomere C-strand replication stress (Zhang *et al.*, 2019), further suggesting that POLIE is important for the telomere C-strand fill-in and helps to ensure telomere C-strand synthesis (Fig. 26).
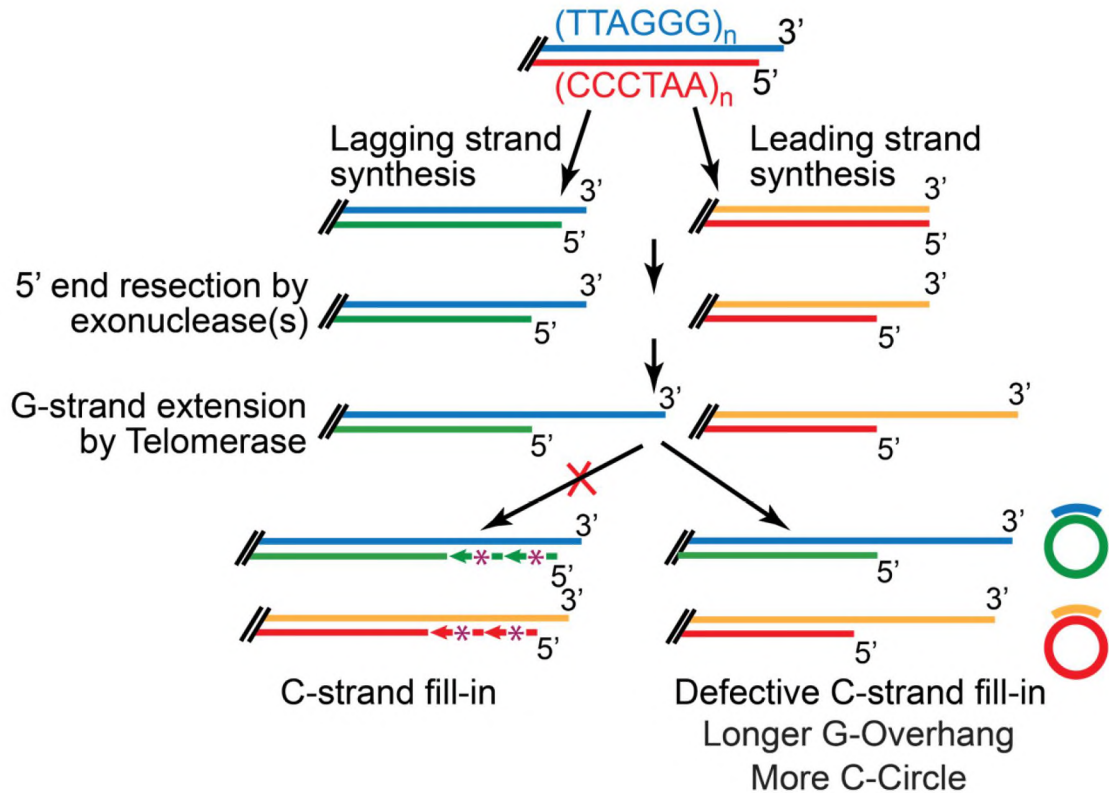
Fig. 26: POLIE suppresses telomerase-mediated telomere G-strand extension and is involved in telomere C-strand fill-in. Our observations suggest that POLIE suppresses the telomerase-mediated telomere G-strand elongation and is important for telomere C-strand fill-in.

Interestingly, I detected a higher level of telomerase-dependent telomere G-strand extension in POLIE-depleted cells, identifying POLIE as the first telomere protein that suppresses telomerase in *T. brucei*. The inhibitory effects of POLIE on telomerase-mediated telomere G-strand extension and the positive effect of POLIE on telomere C-strand fill-in are unexpected (Fig. 27).
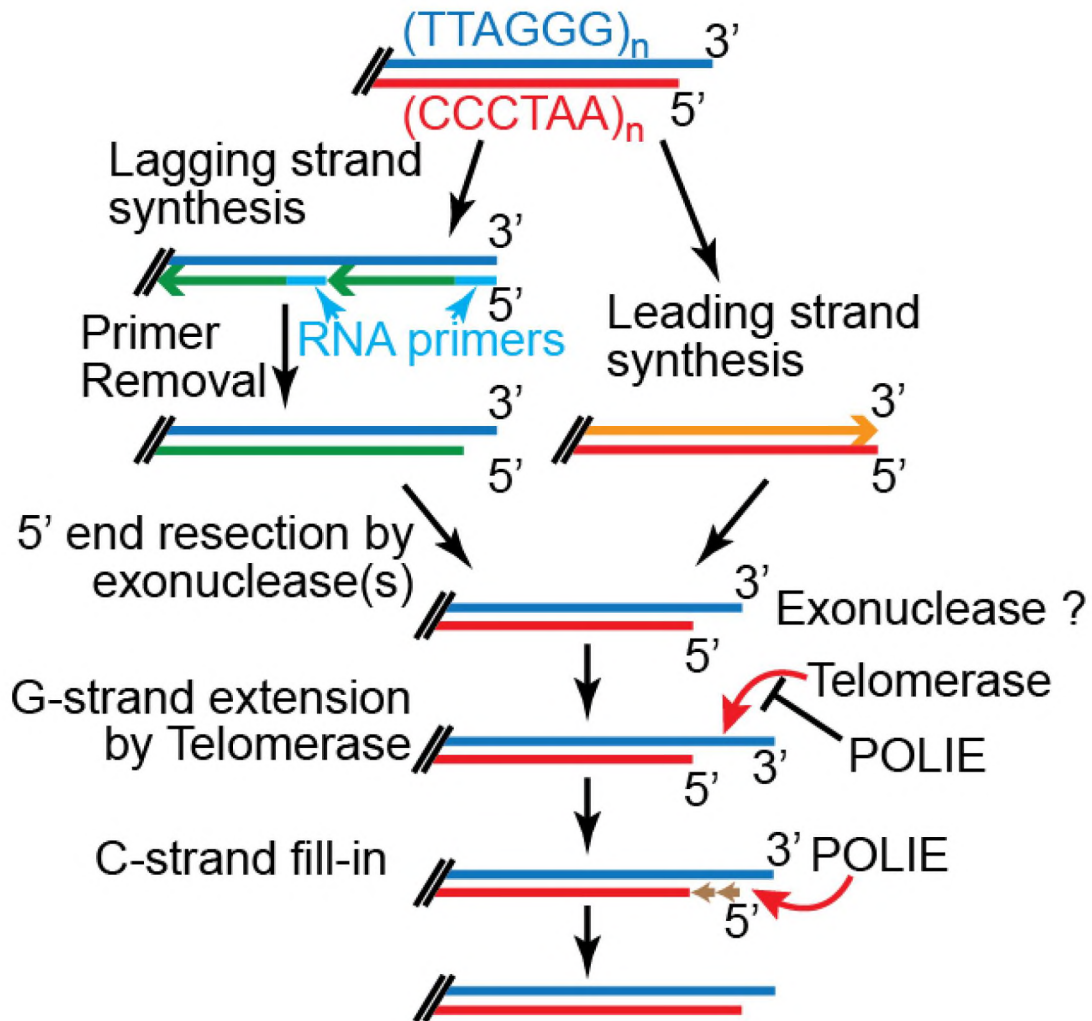
Fig. 27: Model of POLIE functions in telomere end processing.

In mammalian, yeast, and plant cells, OB fold-containing proteins that bind the single-stranded telomere 3' overhang play important roles in coordinating the telomere G- and C-strand syntheses (Lue, 2018). Specifically, human TPP1 recruits telomerase to the telomere and stimulates telomerase activity through TPP1 (Nandakumar *et al.,* 2012; Zhong *et al.,* 2012; Sandhu *et al.,* 2021), while binding of the CST complex on the telomere 3' overhang effectively inhibits telomerase-mediated telomere extension (Chen *et al.,* 2012). CST action is needed for DNA polymerase to initiate the C-strand fill-in reaction (Feng *et al.,* 2017; Wang *et al.,* 2012; Huang *et al.,* 2012). CST depletion leads to a delay

in C-strand synthesis which results in the maintenance of extended G-overhangs throughout G2 of the cell cycle (Wang *et al.,* 2012). CST also appears to participate in several aspects of G-overhang maturation (Feng *et al.,* 2017) and appears to limit G-strand extension by telomerase (Chen *et al.,* 2012). In budding yeasts, CDC13, the single-stranded telomere DNA binding factor, both positively and negatively regulates telomerase-mediated telomere extension (Wu and Zakian, 2011; Mersaoui and Wellinger, 2019). Importantly, both vertebrate and yeast CST complexes promote the telomere C-strand fill-in by directly interacting with and recruiting DNA polymerase alpha-primase to the telomere (Wu *et al.,* 2012; Amir *et al.,* 2020; Casteel *et al.,* 2009; Huang *et al.,* 2012; Qi and Zakian, 2000). Therefore, single-stranded telomere DNA binding factors are major players to coordinate the synthesis of the two telomere strands.

However, the *T. brucei* genome appears to lack these OB fold-containing telomere-specific ssDNA binding factors. On the other hand, our study identifies POLIE as an essential telomere maintenance factor that plays a critical role in coordinating the telomerase-mediated G-strand synthesis and C-strand fill-in. *T. brucei* POLIE is not only a novel telomerase regulator but also represents a completely new mechanism of telomere maintenance. Since POLIE is essential for *T. brucei* proliferation and regulates antigenic variation, our findings can also be applied to the future development of anti-parasite agents.

CHAPTER IV

FUTURE PERSPECTIVE

Telomeres help to protect the natural chromosome ends of eukaryotic cells from nucleolytic degradations, improper damage repair processes, and DNA recombination. Hence telomere maintenance mechanism is crucial for chromosome end protection, genome maintenance, and organism survival. Telomere maintenance involves many processes, including telomerase extension and the timely progression of DNA replication (Pickett and Reddel, 2012). The molecular pathogenesis of *T. brucei* was studied throughout history to develop safer and more effective safer treatments due to toxicity related to existing treatment. *T. brucei* evolved to escape the host immune response by using the antigenic variation mechanism. Therefore, it is essential to dissect the consequences of deletion or depletion of essential genes to elucidate the most effective drug targets. Additionally, telomere length maintenance mechanisms are crucial for *T. brucei* cell survival in the host.

A previous study identified that POLIE is associated with telomeric sequences and important for DNA damage repair with potential translesion polymerase activity (Leal *et al.*, 2020). Our study further confirms POLIE as an intrinsic component of telomere that is

essential in maintaining telomere integrity in *T. brucei*. In this study, we used 13 x myc-tagged POLIE for easier identification of POLIE in different experiments with an anti-myc antibody. However, POLIE$^{+myc/-}$ strains show slightly reduced growth than *POLIE*$^{+myc/+}$ and *POLIE*$^{+/-}$. Although we used POLIE-13 x myc as a negative control for all experiments to consider mild growth defect, but there may be a mild defect due to the tagged allele. We need to develop an endogenous antibody to validate the results of this study and replicate individual experiment to prove that tagged alleles was indeed functional.

POLIE is involved in the regulation of VSG, depletion of which leads to ~3-fold higher VSG switching rate when compared to the control strain. *T. brucei* regularly VSG to effectively evade the host immune response. POLIE appears to suppress DNA recombination at the telomere and the subtelomere as depletion of POLIE increased the frequency of gene conversion-mediated VSG switching and an increased amount of the telomeric circles (T-circles). Recombination is a key mechanism for VSG switching. However, it is interesting that telomeric and subtelomeric DNA recombination in POLIE depleted cells is unlikely to be mediated by the increased telomeric R-loop level as POLIE depletion did not significantly increase the telomeric repeat-containing RNA (TERRA) level. Further studies are required to understand how depletion of POLIE mediates telomeric and subtelomeric DNA recombination without an R-loop. Studying the POLIE-mediated VSG regulation could help us to better understand *T. brucei* pathogenesis and to develop better anti-parasite agents to treat trypanosomiasis.

POLIE is essential to coordinate telomere G- and C-strand syntheses as transient depletion of POLIE dramatically elongates telomere G-rich 3' overhangs. These long telomeres 3' overhang could act as a potential inducer of telomeric and subtelomeric

recombination. Additionally, this study identified POLIE as a regulator of telomerase as it inhibits telomerase-dependent telomere G-strand extension. This implies POLIE is the first telomere protein that suppresses telomerase in *T. brucei* as no other telomerase regulator has been identified in *T. Brucei*. However, how POLIE inhibits telomerase-dependent telomere G-strand extension is need studied further. Does it directly affect telomerase recruitment? Or does it interact with another telomerase regulator to inhibit telomerase-dependent telomere G-strand extension? In mammalian, yeast, and plant cells, the OB-fold domain bind ssDNA to coordinating telomere G- and C-strand syntheses. We still need to explore whether POLIE directly binds to ssDNA similar to OB-fold domain containing protein or it interact with other protein to inhibit telomerase-dependent telomere G-strand extension.

Depletion of POLIE greatly increases the amount of telomeric C-circle which may be derived from C stand stress. However, how POLIE suppresses telomeric C-circle to maintain telomere integrity is yet unexplored. Is it directly involved in C strand fill-in? or does it work with another polymerase such as PrimPol-like (PPL) proteins to support proper C-strand synthesis? The elongated telomere 3' overhang phenotype and elevated telomeric C-circle level phenotypes are independent of the telomerase, which suggests that POLIE promotes the telomere C-strand synthesis. Overall, POLIE is likely required for telomere C strand fill-in, which is supported by several observations in our study. However, further study is required to establish its role in C strand fill-in. We would also like to study whether POLIE is the only polymerase involved in C-strand fill-in in *T. brucei* or if it helps other polymerases in C-strand replication. Studies of C-strand replication in *T. brucei* will provide further evidence of unique telomere C-strand synthesis in *T. brucei*.

Overall, this study identified a unique pathway by which POLIE regulates antigenic variation and maintains telomere integrity in *T. brucei* which may be applied to trypanocidal therapies in the future. Since many aspects of telomere maintenance are conserved among eukaryotes, our study in *T. brucei* has an additional impact on other eukaryotes. Understanding the mechanisms of telomere length regulation in lower eukaryotes will shed light on telomere regulation in humans, where telomere length has been linked to organismal life span.

BIBLIOGRAPHY

Afrin M., Gaurav A.K., Yang X., Pan X., Zhao Y., Li B.. TbRAP1 has an unusual duplex DNA binding activity required for its telomere localization and VSG silencing. *Sci Adv*. 2020; **6**:eabc4065.

Alexandre S., Guyaux M., Murphy N.B., Coquelet H., Pays A., Steinert M., Pays E.. Putative genes of a variant-specific antigen gene transcription unit in *Trypanosoma brucei*. *Mol Cell Biol*. 1988; **8(6)**:2367-78.

Alarcon C.M., Son H.J., Hall T., Donelson J.E.. A monocistronic transcript for a trypanosome variant surface glycoprotein. *Mol Cell Biol*. 1994; **14(8)**:5579-91.

Alirol E., Schrumpf D., Amici Heradi J., Riedel A., de Patoul C., Quere M., Chappuis F.. Nifurtimox-eflornithine combination therapy for second-stage gambiense human African trypanosomiasis: Médecins Sans Frontières experience in the Democratic Republic of the Congo. *Clin Infect Dis*. 2013; **56(2)**:195-203.

Alsford S., Wickstead B., Ersfeld K., Gull K.. Diversity and dynamics of the minichromosomal karyotype in *Trypanosoma brucei*. *Mol Biochem Parasitol*. 2001; **113(1)**:79-88.

Amir,M., Khan,P., Queen,A., Dohare,R., Alajmi,M.F., Hussain,A., Islam,A., Ahmad,F. and Hassan,I. Structural Features of Nucleoprotein CST/Shelterin Complex Involved in the Telomere Maintenance and Its Association with Disease Mutations. *Cells*, 2020; **9**.

Andersen P.L., Xu F., Xiao W.. Eukaryotic DNA damage tolerance and translesion synthesis through covalent modifications of PCNA. *Cell Res*. 2008; **18**:162–173.

Aramburu,T., Plucinsky,S. and Skordalakes,E. POT1-TPP1 telomere length regulation and disease. *Comput Struct Biotechnol J*, 2020; **18**:1939-1946.

Aresta-Branco F., Sanches-Vaz M., Bento F., Rodrigues J.A., Figueiredo L.M.. African trypanosomes expressing multiple VSGs are rapidly eliminated by the host immune system. *Proc Natl Acad Sci U S A*. 2019;n**116(41)**:20725-20735.

Arnoult,N., Saintome,C., Ourliac-Garnier,I., Riou,J.F. and Londoño-Vallejo,A. Human POT1 is required for efficient telomere C-rich strand replication in the absence of WRN. *Genes Dev*. 2009; **23**:2915-2924.

Arnoult N., Karlseder J.. Complex interactions between the DNA-damage response and mammalian telomeres. *Nat Struct Mol Biol*. 2015; **22**:859–866.

Atouguia, J.L.M., and Kennedy, P.G.E.. Neurological aspects of human African trypanosomiasis. In Infectious diseases of the nervous system. L.E. Davis and P.G.E. Kennedy, editors. Butterworth-Heinemann. Oxford, United Kingdom. 2000:321–372.

Aksoy, S.. Control of tsetse flies and trypanosomes using molecular genetics. *Vet Parasitol*. 2003; **115**:125–145.

Avilion A.A., Piatyszek M.A., Gupta J., Shay J.W., Bacchetti S., Greider C.W.. Human telomerase RNA and telomerase activity in immortal cell lines and tumor tissues. *Cancer Res*. 1996; **56(3)**:645-50.

Bacchi C.J.. Chemotherapy of human african trypanosomiasis. *Interdiscip Perspect Infect Dis*. 2009:195040.

Barry, J.D. The biology of antigenic variation in African trypanosomes. In Trypanosomiasis and leishmaniasis. G. Hide, J.C. Mottram, G.H. Coombs, and P.H. Holmes, editors. Cab International. Oxford, United Kingdom. 1997:89–107.

Benmerzouga I., Concepcion-Acevedo J., Kim H.S., Vandoros A.V., Cross G.A., Klingbeil M.M., Li B.. *Trypanosoma brucei* Orc1 is essential for nuclear DNA replication and affects both VSG silencing and VSG switching. *Mol Microbiol.* 2013; **87**:196–210.

Berriman M., Ghedin E., Hertz-Fowler C., Blandin G., Renauld H., Bartholomeu D.C., Lennard N.J., Caler E., Hamlin N.E., Haas B. *et al*. The genome of the African trypanosome *Trypanosoma brucei. Science.* 2005; **309**:416–422.

Bhattacharjee A., Stewart J., Chaiken M. and Price C. M.. (2016) STN1 OB fold mutation alters DNA binding and affects selective aspects of CST function. *PLoS Genet.* 2016; **12**:e1006342.

Blackburn E.H.. Structure and function of telomeres. *Nature.* 1991; **350**:569-573.

Blackburn E.H.. Switching and signaling at the telomere. *Cell,* 2001; **106**:661-673.

Blackburn E.H. and Collins K.. Telomerase: an RNP enzyme synthesizes DNA. *Cold Spring Harb Perspect Biol,* 2011; **3**:a003558.

Blum J.A., Neumayr A.L., Hatz C.F.. Human African trypanosomiasis in endemic populations and travellers. *Eur J Clin Microbiol Infect Dis.* 2012; **31(6)**:905-13.

Boehm E.M., Spies M., Washington M.T.. PCNA tool belts and polymerase bridges form during translesion synthesis. *Nucleic Acids Res.* 2016; **44**:8250–8260.

Bonetti D., Martina M., Falcettoni M. and Longhese M.P.. Telomere-end processing: mechanisms and regulation. *Chromosoma.* 2014; **123**:57-66.

Bonnell E., Pasquier E. and Wellinger R.J.. Telomere Replication: Solving Multiple End Replication Problems. *Front Cell Dev Biol*. 2014; **9**:668171.

Boothroyd C.E., Dreesen O., Leonova T., Ly K.I., Figueiredo L.M., Cross G.A.M.. and Papavasiliou,F.N. A yeast-endonuclease-generated DNA break induces antigenic switching in *Trypanosoma brucei*. *Nature*. 2009; **459**:278-281.

Brachmann C.B., Davies A., Cost G.J., Caputo E., Li J., Hieter P., Boeke J.D.. Designer deletion strains derived from *Saccharomyces cerevisiae* S288C: a useful set of strains and plasmids for PCR-mediated gene disruption and other applications. *Yeast*. 1998; **14(2)**:115-32.

Bray P.G., Barrett M.P., Ward S.A., de Koning H.P.. Pentamidine uptake and resistance in pathogenic protozoa: past, present and future. *Trends Parasitol*. 2003; **19**:232-239.

Broccoli D., Smogorzewska A., Chong L., de Lange T.. Human telomeres contain two distinct Myb-related proteins, TRF1 and TRF2. *Nat Genet*. 1997;**17(2)**:231-5.

Bruce D.. Preliminary report on the tsetse fly disease or nagana in Zululand Durban: Bennett and Davis; 1895.

Bryan C., Rice C., Harkisheimer M., Schultz D.C. and Skordalakes E.. (Structure of the human telomeric Stn1-Ten1 capping complex. *PLoS One*, 2013; **8**:e66756.

Buguet A., Mpanzou G., Bentivoglio M. Human African Trypanosomiasis: A Highly Neglected Neurological Disease. In: Bentivoglio M., Cavalheiro E., Kristensson K., Patel N. (eds) Neglected Tropical Diseases and Conditions of the Nervous System. Springer, New York, NY, 2014.

Cano M.I., Blake J.J., Blackburn E.H., Agabian N.. A Trypanosoma brucei protein complex that binds G-overhangs and co-purifies with telomerase activity. *J Biol Chem.* 2002; **277(2)**:896-906.

Carrington M., Miller N., Blum M., Roditi I., Wiley D., Turner M.. Variant specific glycoprotein of *Trypanosoma brucei* consists of two domains each having an independently conserved pattern of cysteine residues. *J Mol Biol.* 1991; **221(3)**:823-35.

Casteel D.E., Zhuang S., Zeng Y., Perrino F.W., Boss G.R., Goulian M. and Pilz R.B. A DNA polymerase-{alpha}•primase cofactor with homology to replication protein A-32 regulates DNA replication in mammalian cells. *J Biol Chem*, 2009; **284**:5807-5818.

CDC (Centers for Disease Control and Prevention), 2021 https://www.cdc.gov/parasites/sleepingsickness /biology.html, last accessed on 09-29-21.

Cestari I., Stuart K.. Transcriptional Regulation of Telomeric Expression Sites and Antigenic Variation in Trypanosomes. *Curr Genomics.* 2018; **19(2)**:119-132.

Chai W., Du Q., Shay J.W. and Wright W.E.. Human telomeres have different overhang sizes at leading versus lagging strands. *Mol Cell*, 2006; **21**:427-435.

Chang D.J., Cimprich K.A.. DNA damage tolerance: when it's OK to make mistakes. *Nat Chem Biol.* 2009; **5(2)**:82-90.

Chen L.Y., Redon S. and Lingner J.. The human CST complex is a terminator of telomerase activity. *Nature*, 2012; **488**:540–544.

Chow T.T., Zhao Y., Mak S.S., Shay J.W. and Wright W.E.. Early and late steps in telomere overhang processing in normal human cells: the position of the final RNA primer drives telomere shortening. *Genes Dev.* 2012; **26**:1167–1178.

Cohen S., Méchali M.. Formation of extrachromosomal circles from telomeric DNA in Xenopus laevis. *EMBO Rep.* 2002; **3(12)**:1168-74.

Cooper J.P., Nimmo E.R., Allshire R.C., Cech T.R.. Regulation of telomere length and function by a Myb-domain protein in fission yeast. Nature 1997; **385**:744–747.

Cotterill S. and Kearsey S. Eukaryotic DNA polymerases. In: Encyclopedia of Life Sciences (ELS). John Wiley & Sons, Ltd., Chichester, 2009, pp. 1–6.

Cox F.E.G.. History of sleeping sickness (African trypanosomiasis*). Infect Dis Clin N Am*, 2004; **18**:231-245.

Cross G.A.M.. Identification, purification and properties of clone-specific glycoprotein antigens constituting the surface coat of *Trypanosoma brucei. Parasitology.* 1975; **71**:393–417.

Cross G.A., Kim H.S., Wickstead B.. Capturing the variant surface glycoprotein repertoire (the VSGnome) of *Trypanosoma brucei* Lister 427. *Mol. Biochem. Parasitol.* 2014; **195**:59–73.

da Silva M.S., Muñoz P.A.M., Armelin H.A. and Elias M.C.. Differences in the Detection of BrdU/EdU Incorporation Assays Alter the Calculation for G1, S, and G2 Phases of the Cell Cycle in Trypanosomatids. *J Eukaryot Microbiol*, 2017; **64**:756-770.

Daniels J.P., Gull K., Wickstead B.. Cell biology of the trypanosome genome. *Microbiol Mol Biol Rev.* 2010; **74(4)**:552-69.

De Greef C., Imberechts H., Matthyssens G., Van Meirvenne N., & Hamers R.. A gene expressed only in serum-resistant variants of *Trypanosoma brucei* rhodesiense. *Molecular and Biochemical Parasitology*, 1989; **36**:169-176.

de Lange T.. Shelterin: the protein complex that shapes and safeguards human telomeres. *Genes Dev*. 2005; **19(18)**:2100-10.

de Lange T.. Shelterin-Mediated Telomere Protection. *Annu Rev Genet*. 2018; **52**:223-247.

de Lange T. and Borst P.. Genomic environment of the expression-linked extra copies of genes for surface antigens of *Trypanosoma brucei* resembles the end of a chromosome. *Nature*. 1982; **299**:451-453.

de Raadt P.. The history of sleeping sickness.[http://www.who.int/trypanosomiasis_african /country /history/en/print.html]. World Health Org, 2005.

Dejardin J. and Kingston R.E.. Purification of proteins associated with specific genomic Loci. *Cell*, 2009; **136**:175-186.

Devlin R., Marques C.A., Paape D., Prorocic M., Zurita-Leal A.C., Campbell S.J., Lapsley C., Dickens N., McCulloch R.. Mapping replication dynamics in *Trypanosoma brucei* reveals a link with telomere transcription and antigenic variation. *Elife*. 2016; **5**:e12765.

Donelson, J.E.. Antigenic variation and the African trypanosome genome. Acta Tropica. 2002; **85**:391–404.

Dreesen O., Li B. and Cross G.A.M.. Telomere structure and shortening in telomerase-deficient *Trypanosoma brucei*. *Nuc Acids Res*, 2005; **33**:4536-4543.

Dubois M.E., Demick K.P., Mansfield J.M.. Trypanosomes expressing a mosaic variant surface glycoprotein coat escape early detection by the immune system. *Infect Immun*. 2005; **73(5)**:2690-7.

Duraisingh M.T., Horn D.. Epigenetic regulation of virulence gene expression in parasitic protozoa. *Cell Host Microbe*. 2016; **19**:629–640.

Dutton J.E.. Preliminary note upon a trypanosome occurring in the blood of man. *Thompson Yates Lab Rep*, 1902; **4**:455-468.

El-Sayed N.M.A., and Donelson J.E.. Sequencing and mapping the African trypanosome Genome. In Trypanosomiasis and leishmaniasis. G. Hide, J.C. Mottram, G.H. Coombs, and P.H. Holmes, editors. Cab International. Oxford, United Kingdom, 1997; **51–55**:9.

Feng X., Hsu S.J., Kasbek C., Chaiken M., Price C.M.. CTC1-mediated C-strand fill-in is an essential step in telomere length maintenance. *Nucleic Acids Res*. 2017; **45**:4281–4293.

Feng X., Hsu S.J., Bhattacharjee A., Wang Y., Diao J. and Price C.M.. CTC1-STN1 terminates telomerase while STN1-TEN1 enables C-strand synthesis during telomere replication in colon cancer cells. *Nat Commun*, 2018; **9**:2827.

Field H., Field M.C.. Leptomonas seymouri, Trypanosoma brucei: a method for isolating trypanosomatid nuclear factors which bind T. brucei single-stranded g-rich telomere sequence. *Exp Parasitol*. 1996; **83(1)**:155-8.

Ganduri S. & Lue N.F.. STN1-POLA2 interaction provides a basis for primase-pol alpha stimulation by human STN1. *Nucleic Acids Res*. 2017; **45**:9455–9466.

Gao Y., Mutter-Rottmayer E., Zlatanou A., Vaziri C. and Yang Y. Mechanisms of post-replication DNA repair. *Genes (Basel)*. 2017; **8**:64.

Ge Y., Wu Z., Chen H., Zhong Q., Shi S., Li G., Wu J., Lei M.. Structural insights into telomere protection and homeostasis regulation by yeast CST complex. *Nat Struct Mol Biol*. 2020; **27(8)**:752-762.

Glover L., Alsford S. and Horn D.. DNA break site at fragile subtelomeres determines probability and mechanism of antigenic variation in African trypanosomes. *PLoS Pathog*. 2013; **9**:e1003260.

Glover L. and Horn D.. Trypanosomal histone gammaH2A and the DNA damage response. *Mol Biochem Parasitol*. 2012; **183**:78-83.

Goodman M.F. and Woodgate R.. Translesion DNA polymerases. *Cold Spring Harb Perspect Biol*. 2013; **5**:a010363.

Gottschling D.E., Aparicio O.M., Billington B.L., Zakian V.A.. Position effect at *S. cerevisiae* telomeres: reversible repression of Pol II transcription. *Cell*. 1990; **63(4)**:751-62.

Graham S.V., Barry J.D.. Transcriptional regulation of metacyclic variant surface glycoprotein gene expression during the life cycle of *Trypanosoma brucei. Mol Cell Biol*. 1995; **15(11)**:5945-56.

Greider C.W., Blackburn E.H.. The telomere terminal transferase of Tetrahymena is a ribonucleoprotein enzyme with two kinds of primer specificity. *Cell*. 1987; **51(6)**:887-98.

Greider C.W., Blackburn E.H.. A telomeric sequence in the RNA of Tetrahymena telomerase required for telomere repeat synthesis. *Nature*. 1989; **337(6205)**:331-7.

Griffith F.L.. The Petrie Papyri: Hieratic Papyri from Kahun and Gurob (Principally of the Middle Kingdom). (Text + Plates) London: Bernard Quaritch; 1898.

Gruszynski A.E., van Deursen F.J., Albareda M.C., Best A., Chaudhary K., Cliffe L.J., del Rio L., Dunn J.D., Ellis L., Evans K.J., Figueiredo J.M., Malmquist N.A., Omosun Y., Palenchar J.B., Prickett S., Punkosdy G.A., van Dooren G., Wang Q., Menon A.K., Matthews K.R., Bangs J.D.. Regulation of surface coat exchange by differentiating African trypanosomes. *Mol Biochem Parasitol.* 2006; **147(2)**:211-23.

Gu P., Min J.N., Wang Y., Huang C., Peng T., Chai W., Chang S.. CTC1 deletion results in defective telomere replication, leading to catastrophic telomere loss and stem cell exhaustion. *EMBO J.* 2012; **31**:2309–2321

Gu P., Jia S., Takasugi T., Smith E., Nandakumar J., Hendrickson E. and Chang S.. CTC1-STN1 coordinates G- and C-strand synthesis to regulate telomere length. Aging Cell, 2018; **17**:e12783.

Gupta S.K., Kolet L., Doniger T., Biswas V.K., Unger R., Tzfati Y. and Michaeli S.. The *Trypanosoma brucei* telomerase RNA (TER) homologue binds core proteins of the C/D snoRNA family. *FEBS Lett.* 2013; **587**:1399-1404.

Haag J., O'hUigin C., Overath P.. The molecular phylogeny of trypanosomes: evidence for an early divergence of the Salivaria. *Mol Biochem Parasitol.* 1998; **91**:37-49.

Haber J.E.. DNA Repair: The Search for Homology. *Bioessays.* 2018; **40**:e1700229.

Harland J. L., Chang Y.T., Moser B.A., Nakamura T.M.. Tpz1-Ccq1 and Tpz1-Poz1 interactions within fission yeast shelterin modulate Ccq1 Thr93 phosphorylation and telomerase recruitment. *PLoS Genet.* 2014; **10**:e1004708.

Henson J.D., Cao Y., Huschtscha L.I., Chang A.C., Au A.Y., Pickett H.A. and Reddel R.R. DNA C-circles are specific and quantifiable markers of alternative-lengthening-of telomeres activity. *Nat Biotechnol*, 2009; **27**;1181-1185.

Hertz-Fowler C., Figueiredo L.M., Quail M.A., Becker M., Jackson A., Bason N., Brooks K., Churcher C., Fahkro S., Goodhead I. et al. .. Telomeric expression sites are highly conserved in *Trypanosoma brucei*. *PLoS One*. 2008; **3**:e3527.

Hide G. History of sleeping sickness in East Africa. Clin Microbiol Rev 1999, 12:112-125.

Hockemeyer D., Collins K.. Control of telomerase action at human telomeres. *Nat Struct Mol Biol*. 2015; **22**:848–852.

Hong Y., Kinoshita T.. Trypanosome glycosylphosphatidylinositol biosynthesis. *Korean J Parasitol*. 2009; **47(3)**:197-204.

Horn D.. Antigenic variation in African trypanosomes. *Mol Biochem Parasitol*. 2014; **195(2)**:123-9.

Hovel-Miner G.A., Boothroyd C.E., Mugnier M., Dreesen O., Cross G.A.M. and Papavasiliou F.N.. Telomere length affects the frequency and mechanism of antigenic variation in *Trypanosoma brucei*. *PLoS Pathog*, 2012; **8**:e1002900.

Huang C., Dai X. and Chai W. Human Stn1 protects telomere integrity by promoting efficient lagging-strand synthesis at telomeres and mediating C-strand fill-in. *Cell Res*. 2012; **22**:1681–1695.

Ishikawa F. Portrait of replication stress viewed from telomeres. *Cancer Sci*. 2013; **104**:790–794.

Iyama T. and Wilson D.M. 3rd DNA repair mechanisms in dividing and non-dividing cells. DNA Repair (Amst.), 2013; **12**;620–636.

Jehi S.E., Li X., Sandhu R., Ye F., Benmerzouga I., Zhang M., Zhao Y., Li B.. Suppression of subtelomeric VSG switching by *Trypanosoma brucei* TRF requires its TTAGGG repeat-binding activity. *Nucleic Acids Res.* 2014a; **42**:12899–12911.

Jehi S.E., Wu F., Li B.. *Trypanosoma brucei* TIF2 suppresses VSG switching by maintaining subtelomere integrity. *Cell Res.* 2014b; **24**:870–885.

Jehi S.E., Nanavaty V., Li B.. *Trypanosoma brucei* TIF2 and TRF suppress VSG switching using overlapping and independent mechanisms. *PLoS One.* 2016; **11**:e0156746.

Kaiser C.S., S. Michaelis, and Mitchell A.. Methods in yeast genetics. Cold Spring Harbor Laboratory Press, Cold Spring Harbor, NY, 1994.

Kasbek C., Wang F., Price C.M.. Human TEN1 maintains telomere integrity and functions in genome-wide replication restart. *J Biol Chem.* 2013; **288**:30139–30150.

Keijzers G., Liu D. and Rasmussen L.J. Exonuclease 1 and its versatile roles in DNA repair. *Crit Rev Biochem Mol Biol.* 2016; **51**;440-451.

Kennedy P.G.E.. Human African trypanosomiasis of the CNS: current issues and challenges. *The Journal of Clinical Investigation.* 2004; **113(4)**:496–504.

Kennedy P.G.E., Rodgers J.. Clinical and Neuropathogenetic Aspects of Human African Trypanosomiasis. *Front Immunol.* 2019; **10**:39.

Kieft R., Capewell P., Turner C.M., Veitch N.J., MacLeod A., Hajduk S.. Mechanism of *Trypanosoma brucei gambiense* (group 1) resistance to human trypanosome lytic factor. *Proc Natl Acad Sci U S A.* 2010; **107(37)**:16137-41.

Kim H.S. and Cross G.A.M.. TOPO3alpha influences antigenic variation by monitoring expression-site-associated VSG switching in *Trypanosoma brucei. PLoS Pathog.* 2010; **6**:e1000992.

Kim H.S.. Genome-wide function of MCM-BP in *Trypanosoma brucei* DNA replication and transcription. *Nucleic Acids Res.* 2019; **47**:634–647.

Klebanov-Akopyan O., Mishra A., Glousker G., Tzfati,Y. and Shlomai J.. *Trypanosoma brucei* UMSBP2 is a single-stranded telomeric DNA binding protein essential for chromosome end protection. *Nucleic Acids Res.* 2018; **46**:7757-7771.

Kruzel E.K., Zimmett G.P. 3rd, Bangs J.D.. Life Stage-Specific Cargo Receptors Facilitate Glycosylphosphatidylinositol-Anchored Surface Coat Protein Transport in Trypanosoma brucei. *mSphere.* 2017; **2(4)**:e00282-17.

Kunkel T.A.. DNA replication fidelity. *J Biol Chem.* 2004; **279**:16895–16898.

Kyrion G., Liu K., Liu C., Lustig A.J.. RAP1 and telomere structure regulate telomere position effects in *Saccharomyces cerevisiae. Genes Dev.* 1993; **7(7A)**:1146-59.

Leal A.Z., Schwebs M., Briggs E., Weisert N., Reis H., Lemgruber L., Luko K., Wilkes J., Butter F., McCulloch R and Janzen C.Z.. Genome maintenance functions of a putative *Trypanosoma brucei t*ranslesion DNA polymerase include telomere association and a role in antigenic variation. *Nucleic Acids Res.* 2020; **48**:9660–9680.

Lei M., Podell E.R. and Cech T.R.. Structure of human POT1 bound to telomeric single-stranded DNA provides a model for chromosome end-protection. *Nat Struct Mol Biol.* 2004; **11**:1223-1229.

Li B.. Telomere components as potential therapeutic targets for treating microbial pathogen infections. *Front Oncol.* 2012; **2**:156.

Li B.. Keeping Balance Between Genetic Stability and Plasticity at the Telomere and Subtelomere of *Trypanosoma brucei. Frontiers in Cell and Developmental Biology*. 2021; **9**:1722.

Li B. and Zhao Y.. Regulation of Antigenic Variation by *Trypanosoma brucei* Telomere Proteins Depends on Their Unique DNA Binding Activities. *Pathogens*. 2021; **10(8)**:967

Li B., Espinal A. and Cross G.A.M.. Trypanosome telomeres are protected by a homologue of mammalian TRF2. *Mol Cell Biol*. 2005; **25**:5011-5021.

Lim C.J. & Cech T.R.. Shaping human telomeres: from shelterin and CST complexes to telomeric chromatin organization. *Nat Rev Mol Cell Biol*. 2021; **22**:283–298.

Loayza D. and de Lange T.. POT1 as a terminal transducer of TRF1 telomere length control *Nature*. 2003; **424**:1013-1018.

Lu J., Vallabhaneni H., Yin J., Liu Y.. Deletion of the major peroxiredoxin Tsa1 alters telomere length homeostasis. *Aging Cell*. 2013; **12(4)**:635-44.

Lue N.F.. Evolving linear chromosomes and telomeres: a C-strand-centric view. *Trends in biochemical sciences*, 2018; **43**:314-326.

Mailand N., Gibbs-Seymour I., Bekker-Jensen S.. Regulation of PCNA-protein interactions for genome stability. *Nat Rev Mol Cell Biol*. 2013; **14**:269–282.

Manna P.T., Boehm C., Leung K.F., Natesan S.K., Field M.C. Life and times: synthesis, trafficking, and evolution of VSG. *Trends Parasitol*. 2014; **30(5)**:251-8.

Martín V., Du L.L., Rozenzhak S., Russell P.. Protection of telomeres by a conserved Stn1-Ten1 complex. *Proc Natl Acad Sci U S A*, 2007; **104(35)**:14038-43.

Martinez P., Blasco M.A. Replicating through telomeres: a means to an end. *Trends Biochem. Sci.* 2015; **40**:504–515.

McCulloch R., Morrison L.J., Hall J.P.J.. DNA recombination strategies during antigenic variation in the African Trypanosome. *Microbiol. Spectr.* 2015; **3**:MDNA3-0016-2014.

McKean P.G.. Coordination of cell cycle and cytokinesis in *Trypanosoma brucei. Curr Opin Microbiol.* 2003; **6**:600-607.

Melville S.E., Leech V., Gerrard C.S., Tait A., Blackwell J.M.. The molecular karyotype of the megabase chromosomes of *Trypanosoma brucei* and the assignment of chromosome markers. *Mol Biochem Parasitol.* 1998; **94(2)**:155-73.

Mersaoui S.Y. and Wellinger R.J.. Fine tuning the level of the Cdc13 telomere capping protein for maximal chromosome stability performance. *Curr Genet.* 2019; **65**:109-118.

Metcalf P., Blum M., Freymann D., Turner M., Wiley D.C.. Two variant surface glycoproteins of *Trypanosoma brucei* of different sequence classes have similar 6 A resolution X-ray structures. *Nature.* 1987; **325(6099)**:84-6.

Meyskens F.L.J., Gerner E.W.. Development of difluoromethylornithine (DFMO) as a chemoprevention agent. *Clin Cancer Res.* 1999; **5**:945-951.

Milman N., Motyka S.A., Englund P.T., Robinson D. and Shlomai J., Mitochondrial origin-binding protein UMSBP mediates DNA replication and segregation in trypanosomes. *Proc Natl Acad Sci U S A.* 2007; **104**:19250-19255.

Miyake Y., Nakamura M., Nabetani A., Shimamura S., Tamura M., Yonehara S., Saito M. and Ishikawa F.. RPA-like mammalian Ctc1-Stn1-Ten1 complex binds to single-

stranded DNA and protects telomeres independently of the Pot1 pathway. *Mol Cell.* 2009; **36**:193–206.

Miyoshi T., Kanoh J., Saito M., Ishikawa F.. Fission yeast Pot1-Tpp1 protects telomeres and regulates telomere length. *Science.* 2008; **320**:1341–1344.

Moldovan G.L., Madhavan M.V., Mirchandani K.D., McCaffrey R.M., Vinciguerra P. and D'Andrea A.D.. DNA polymerase POLN participates in cross-link repair and homologous recombination. *Mol Cell Biol.* 2010; **30**:1088-1096.

Morrison L.J., Marcello L., and McCulloch R.. Antigenic variation in the African trypanosome: molecular mechanisms and phenotypic complexity. *Cell Microbiol.* 2009; **11**:1724–1734.

Morrison L.J.. Parasite-driven pathogenesis in *Trypanosoma brucei* infections. Parasite *Immunol.* 2011; **33(8)**:448-55.

Moser B.A., Nakamura T.M.. Protection and replication of telomeres in fission yeast. Biochem *Cell Biol.* 2009; **87(5)**:747-58.

Moser B.A., Chang Y.T., Kosti J., Nakamura T.M.. Tel1ATM and Rad3ATR kinases promote Ccq1-Est1 interaction to maintain telomeres in fission yeast. *Nat Struct Mol Biol.* 2011; **18**:1408–1413.

Mukherjee S., Wright W.D., Ehmsen K.T., Heyer W.D.. The Mus81-Mms4 structure-selective endonuclease requires nicked DNA junctions to undergo conformational changes and bend its DNA substrates for cleavage. *Nucleic Acids Res.* 2014; **42(10)**:6511-6522.

Munoz-Jordan J.L., Cross G.A.M., de Lange T. and Griffith J.D.. t-loops at trypanosome telomeres. *EMBO J.* 2001; **20**:579-588.

Myler L.R., Kinzig C.G., Sasi N.K., Zakusilo G., Cai S.W., de Lange T.. The evolution of metazoan shelterin. *Genes Dev*. 2021; **35(23-24)**:1625-1641.

Nanavaty V., Sandhu R., Jehi S.E., Pandya U.M. and Li B.. *Trypanosoma brucei* RAP1 maintains telomere and subtelomere integrity by suppressing TERRA and telomeric RNA: DNA hybrids. *Nucleic Acids Res*. 2017; **45**:5785-5796.

Nandakumar J., Bell C.F., Weidenfeld I., Zaug A.J., Leinwand L.A. and Cech T.R.. The TEL patch of telomere protein TPP1 mediates telomerase recruitment and processivity. *Nature*, 2012; **492**:285-289.

Navarro M., Cross G.A.. DNA rearrangements associated with multiple consecutive directed antigenic switches in *Trypanosoma brucei*. *Mol Cell Biol*. 1996; **16(7)**:3615-25.

Ohki R., Tsurimoto T. and Ishikawa F. *In vitro* reconstitution of the end replication problem. *Mol Cell Biol*. 2001; **21**:5753-5766.

Olovnikov A.M.. A theory of marginotomy. The incomplete copying of template margin in enzymic synthesis of polynucleotides and biological significance of the phenomenon. *J Theor Biol*. 1973; **41**:181-190.

Pandya U.M., Sandhu R. and Li B.. Silencing subtelomeric VSGs by *Trypanosoma brucei* RAP1 at the insect stage involves chromatin structure changes. *Nucleic Acids Res*, 2013; **41**:7673-7682.

Pays E., Tebabi P., Pays A., Coquelet H., Revelard P., Salmon D., Steinert M.. The genes and transcripts of an antigen gene expression site from *T. brucei*. *Cell*. 1989; **57(5)**:835-45.

Pickett H.A., Reddel R.R.. The role of telomere trimming in normal telomere length dynamics. *Cell Cycle*. 2012; **11(7)**:1309-15.

Pickett H.A., Reddel R.R.. Molecular mechanisms of activity and derepression of alternative lengthening of telomeres. *Nat Struct Mol Biol*. 2015; **22(11)**:875-80.

Podlevsky J.D., Bley C.J., Omana R.V., Qi X. and Chen J.J.. The telomerase database. *Nucleic Acids Res*. 2008; **36**:D339-43.

Powers K.T. and Washington M.T.. Eukaryotic translesion synthesis: choosing the right tool for the job. *DNA Repair (Amst.)*, 2018; **71**:127–134.

Procházková Schrumpfová P., Schořová Š., Fajkus J.. Telomere- and Telomerase-Associated Proteins and Their Functions in the Plant Cell. *Front Plant Sci*. 2016; **7**:851.

Price C.M., Boltz K.A., Chaiken M.F., Stewart J.A., Beilstein M.A., Shippen D.E.. Evolution of CST function in telomere maintenance. *Cell Cycle*. 2010; **9(16)**:3157-65.

Pustovalova Y., Magalhães M.T., D'Souza S., Rizzo A.A., Korza G., Walker G.C., Korzhnev D.M.. Interaction between the Rev1 C-Terminal Domain and the PolD3 Subunit of Polζ Suggests a Mechanism of Polymerase Exchange upon Rev1/Polζ-Dependent Translesion Synthesis. *Biochemistry*. 2016; **55(13)**:2043-53.

Qi H., Zakian V.A.. The Saccharomyces telomere-binding protein Cdc13p interacts with both the catalytic subunit of DNA polymerase alpha and the telomerase-associated est1 protein. *Genes Dev*. 2000; **14(14)**:1777-88.

Rabbani M.A.G., Tonini ML, Afrin M., Li B.. POLIE suppresses telomerase-mediated telomere G-strand extension and helps ensure proper telomere C-strand synthesis in trypanosomes. *Nucleic Acids Res*. 2022; **50(4)**:2036-2050.

Raia P., Delarue M. and Sauguet L.. An updated structural classification of replicative DNA polymerases. *Biochem Soc Trans.*, 2019; **47**:239–249.

Rajavel M., Mullins M.R. and Taylor D.J.. Multiple facets of TPP1 in telomere maintenance. *Biochim Biophys Acta*. 2014: **1844**:1550-1559.

Reis H., Schwebs M., Dietz S., Janzen C.J., Butter F.. TelAP1 links telomere complexes with developmental expression site silencing in African trypanosomes. *Nucleic Acids Res*. 2018; **46**:2820–2833.

Reynolds D., Cliffe L., Forstner K.U., Hon C.C., Siegel T.N. and Sabatini R.. Regulation of transcription termination by glucosylated hydroxymethyluracil, base J, in Leishmania major and *Trypanosoma brucei. Nucleic Acids Res*. 2014; **42**:9717-9729.

Rice C., Skordalakes E.. Structure and function of the telomeric CST complex. Comput Struct *Biotechnol J*. 2016; **14**:161-7.

Robinson N.P., Burman N., Melville S.E., and Barry J.D.. Predominance of duplicative VSG gene conversion in antigenic variation in African trypanosomes. *Mol Cell Biol*. 1999; **19**:5839–5846.

Rudd S.G., Glover L., Jozwiakowski S.K., Horn D., Doherty A.J.. PPL2 translesion polymerase is essential for the completion of chromosomal DNA replication in the African trypanosome. *Mol. Cell*. 2013; **52**:554–565.

Rudenko G., McCulloch R., Dirksmulder A., and Borst P.. Telomere exchange can be an important mechanism of variant surface glycoprotein gene switching in *Trypanosoma brucei. Mol Biochem. Parasitol.* 1996; **80**:65–75.

Rudenko G., Cross M., Borst P.. Changing the end: antigenic variation orchestrated at the telomeres of African trypanosomes. *Trends Microbiol.* 1998; **6(3)**:113-6.

Saha A., Gaurav A.K., Pandya U.M., Afrin M., Sandhu R., Nanavaty V., Schnur B. and Li B.. TbTRF suppresses the TERRA level and regulates the cell cycle-dependent TERRA foci number with a TERRA binding activity in its C-terminal Myb domain. *Nucleic Acids Res.* 2021; **49(10)**:5637-5653.

Saha A., Nanavaty V.P. and Li B.. Telomere and Subtelomere R-loops and Antigenic Variation in Trypanosomes. *J Mol Biol.* 2019: **432**;4167-4185.

Sale J.E.. Translesion DNA synthesis and mutagenesis in eukaryotes. *Cold Spring Harb Perspect Biol,* 2013: **5**:a012708.

Sandhu R. and Li B.. Examination of the telomere G-overhang structure in *Trypanosoma brucei. J Vis Exp.* 2011; **47**:1959.

Sandhu R., Sanford S., Basu S., Park M., Pandya U.M., Li B. and Chakrabarti K.. A trans-spliced telomerase RNA dictates telomere synthesis in *Trypanosoma brucei. Cell Res.* 2013; **23**:537-551.

Sandhu R. and Li B.. Telomerase activity is required for the telomere G-overhang structure in *Trypanosoma brucei. Sci Rep.* 2017; **7**:15983.

Sandhu R., Sharma M., Wei D. and Xu L.. The structurally conserved TELR region on shelterin protein TPP1 is essential for telomerase processivity but not recruitment. *Proc Natl Acad Sci U S A.* 2021; **118**:e2024889118.

Scahill M.D., Pastar I. and Cross G.A.M.. CRE recombinase-based positive-negative selection systems for genetic manipulation in *Trypanosoma brucei*. *Mol Biochem Parasitol*. 2008; **157**:73-82.

Schmidt J.C. and Cech T.R.. Human telomerase: biogenesis, trafficking, recruitment, and activation. *Genes Dev*. 2015; **29**:1095-1105.

Schmidt J.C., Zaug A.J. and Cech T.R.. Live cell imaging reveals the dynamics of telomerase recruitment to telomeres. *Cell*. 2016; **166**:1188–1197.

Schulz D., Zaringhalam M., Papavasiliou F.N., Kim H.S.. Base J and H3.V Regulate Transcriptional Termination in *Trypanosoma brucei*. *PLoS Genet*. 2016; 12:e1005762.

Sexton A.N., Regalado S.G., Lai C.S., Cost G.J., O'Neil C.M., Urnov F.D., Gregory P.D., Jaenisch R., Collins K. and Hockemeyer D.. Genetic and molecular identification of three human TPP1 functions in telomerase action: recruitment, activation, and homeostasis set point regulation. *Genes Dev*. 2014; 28:1885–1899.

Seyfang A., Mecke D., Duszenko M.. Degradation, recycling, and shedding of Trypanosoma brucei variant surface glycoprotein. *J Protozool*. 1990; **37(6)**:546-52.

Simarro P.P., Jannin J., Cattand P.. Eliminating human African trypanosomiasis: where do we stand and what comes next? *PLoS Med*. 2008; **5(2)**:e55.

Song X., Leehy K., Warrington R.T., Lamb J.C., Surovtseva Y.V., Shippen D.E.. STN1 protects chromosome ends in Arabidopsis thaliana. *Proc Natl Acad Sci USA*. 2008; **105**:19815–19820.

Steverding D.. The history of African trypanosomiasis. *Parasit Vectors*. 2008; **1**:3.

Stewart J.A., Wang F., Chaiken M.F., Kasbek C., Chastain P.D. 2nd, Wright W.E., Price

C.M.. Human CST promotes telomere duplex replication and general replication restart after fork stalling. *EMBO J.* 2012; **31**:3537–3549.

Sugiyama T., Kowalczykowski S.C.. Rad52 protein associates with replication protein A (RPA)-single-stranded DNA to accelerate Rad51-mediated displacement of RPA and presynaptic complex formation. *J Biol Chem.* 2002; **277(35)**:31663–72.

Surovtseva Y.V., Churikov D., Boltz K.A., Song X., Lamb J.C., Warrington R., Leehy K., Heacock M., Price C.M. and Shippen D.E.. Conserved telomere maintenance component 1 interacts with STN1 and maintains chromosome ends in higher eukaryotes. *Mol Cell.* 2009; **36**:207–218.

Takai H., Jenkinson E., Kabir S., Babul-Hirji R., Najm-Tehrani N., Chitayat D.A., Crow Y.J. and de Lange T.. A POT1 mutation implicates defective telomere end fill-in and telomere truncations in Coats plus. *Genes Dev.* 2016;**30**:812-826.

Taylor J.E., Rudenko G.. Switching trypanosome coats: what's in the wardrobe? Trends Genet. 2006; **22(11)**:614-20.

Thomson R., Samanovic M., Raper J.. Activity of Trypanosome Lytic Factor: A Novel Component of Innate Immunity. *Future Microbiol.* 2009;**4**:789–796.

Tiengwe C., Marcello L., Farr H., Dickens N., Kelly S., Swiderski M., Vaughan D., Gull K., Barry J.D., Bell S.D. *et al.* Genome-wide analysis reveals extensive functional interaction between DNA replicaion initiation and transcription in the genome of *Trypanosoma brucei. Cell Rep.* 2012; **2**:185–197.

Tomaska L., Nosek J., Kramara J. and Griffith J.D.. Telomeric circles: universal players in telomere maintenance. *Nat Struct Mol Biol.* 2009; **16**:1010-1015.

Toubiana S. and Selig S.. DNA:RNA hybrids at telomeres - when it is better to be out of the (R) loop. *FEBS J.* 2018;**285**:2552-2566.

Vaisman A. and Woodgate R. Translesion DNA polymerases in eukaryotes: what makes them tick? *Crit Rev Biochem Mol Biol.* 2017; **52**:274–303.

Vickerman K.. Landmarks in trypanosome research. In Trypanosomiasis and Leishmaniasis. Biology and Control Edited by: Hide G., Mottram J.C., Coombs G.H., Holmes P.H.. Wallingford, Oxon: Cab International; 1997:1-37.

Wang C.C.. Molecular mechanisms and therapeutic approaches to the treatment of African trypanosomiasis. *Annu Rev Pharmacol Toxicol.* 1995; **35**:93-127.

Wang F., Stewart J.A., Kasbek C., Zhao Y., Wright W.E. and Price C.M. Human CST has independent functions during telomere duplex replication and C-strand fill-in. *Cell Rep.* 2012; **2**:1096–1103.

Wei C. and Price M. Protecting the terminus: t-loops and telomere end-binding proteins. *Cell Mol Life Sci.* 2003; **60**:2283-2294.

Welburn S.C., Maudlin I.. Priorities for the elimination of sleeping sickness. *Adv Parasitol.* 2012; **79**:299-337.

Williams B.I.. African trypanosomiasis. In The Wellcome Trust Illustrated History of Tropical Diseases Edited by: Cox FEG. London: *The Wellcome Trust.* 1996:178-191.

Winkle S.. Geißeln der Menschheit. Kulturgeschichte der Seuchen Düsseldorf: Artemis & Winkler. 2005.

Wirtz E., Leal S., Ochatt C. and Cross G.A.M. A tightly regulated inducible expression system for dominant negative approaches in *Trypanosoma brucei*. *Mol Biochem Parasitol*, 1999; **99**:89-101.

WHO (World Health Organization): African trypanosomiasis (sleepingsickness), [http://www.who.int/mediacentre/factsheets/fs259/en/]. World Health Organ Fact Sheet, 2006.

Wojtaszek J., Lee C.J., D'Souza S., Minesinger B., Kim H., D'Andrea A.D., Walker G.C., Zhou P.. Structural basis of Rev1-mediated assembly of a quaternary vertebrate translesion polymerase complex consisting of Rev1, heterodimeric polymerase (Pol) zeta, and Pol kappa. *J. Biol. Chem.* 2012; **287**:33836–33846.

Wood R.D. and Doublié S.. DNA polymerase θ (POLQ), double-strand break repair, and cancer. *DNA Repair (Amst)*, 2016; **44**:22-32.

Wu P., van Overbeek M., Rooney S. and de Lange T.. Apollo contributes to G overhang maintenance and protects leading-end telomeres. *Mol Cell.* 2010; **39**:606-617.

Wu P., Takai H. and de Lange T.. Telomeric 3' overhangs derive from resection by Exo1 and Apollo and fill-in by POT1b-associated CST. *Cell.* 2012; **150**:39–52.

Wu Y. and Zakian V.A.. The telomeric Cdc13 protein interacts directly with the telomerase subunit Est1 to bring it to telomeric DNA ends *in vitro*. *Proc Natl Acad Sci U S A*, 2011; **108**:20362-20369.

Yang X., Figueiredo L.M., Espinal A., Okubo E., Li B.. RAP1 is essential for silencing telomeric variant surface glycoprotein genes in *Trypanosoma brucei*. *Cell.* 2009; **137**:99–109.

Zhang T., Zhang Z., Shengzhao G., Li X., Liu H. and Zhao Y.. Strand break-induced replication fork collapse leads to C-circles, C-overhangs and telomeric recombination. *PLoS Genet*. 2019; **15**:e1007925.

Zhao Y., Sfeir A.J., Zou Y., Buseman C.M., Chow T.T., Shay J.W. and Wright W.E.. Telomere extension occurs at most chromosome ends and is uncoupled from fill-in in human cancer cells. *Cell*. 2009; **138**:463–475.

Zhong F.L., Batista L.F., Freund A., Pech M.F., Venteicher A.S. and Artandi S.E.. TPP1 OB-fold domain controls telomere maintenance by recruiting telomerase to chromosome ends. *Cell*. 2012; **150**:481-494.

Zhuang Z., Ai Y.. Processivity factor of DNA polymerase and its expanding role in normal and translesion DNA synthesis. *Biochim. Biophys. Acta*. 2010; **1804**:1081–1093.